
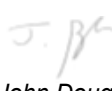


PSHA testing on observed risk European Seismic Hazard Model

Work Package #5 "PSHA"



AUTHORS		REVIEW		APPROVAL	
Name	Date	Name	Date	Name	Date
Charles Droszcz	2021/08/13	<i>Roger Musson</i> Roger Musson	16 August 2022	 Emmanuel Viallet	2023-02-15
Charisis Chatzigogos		 John Douglas	24 April 2022	Public access <input checked="" type="radio"/> SIGMA-2 restricted <input type="radio"/>	

Document history

DATE	VERSION	COMMENTS
2021/04/09	1	
2021/06/18	2	

Executive summary

Document history.....	2
Executive summary	2
1. Introduction.....	4
2. Methodology for the risk calculation.....	4
2.1. General methodology	4
2.2. Seismic risk - Numerical computations	5
2.3. Hazard curves – European Seismic Hazard Model - ESHM20.....	7
2.4. Fragility curves.....	7
2.5. Geographic domains	9
3. Risk calculations.....	10
3.1. Seismic risk derived from historical seismicity	10
3.1.1. Results inherited from the work by Drif et al. 2020.....	10
3.1.2. Summary of the method implemented in Drif et al. (2020).....	11
3.2. Comparison between ESHM20 risk and historical risk.....	13
3.2.1. Methodology	13
3.2.2. Results by geographic domains, for each percentile (5%, 16%, 50%, 84%, 95%) of hazard curves.....	14
3.2.3. Results by damage degree and vulnerability class, for each percentile (5%, 16%, 50%, 84%, 95%) of hazard curves	24
3.2.4. Discussion on the obtained results.....	28
4. Conclusions and perspectives	32
5. References	33
APPENDIX 1 Grid of points selected for risk calculation within each domain	34
APPENDIX 2 Hazard curves from ESHM20	39
APPENDIX 3 Comparison between ESHM20 risk and historical risk	44

Results by geographic domains, 50% percentile of hazard curves, variability among the different points in each domain	44
APPENDIX 4 Comparison between ESHM20 risk and historical risk	49
Results by damage degree and vulnerability class, 50% percentile of hazard curves, variability among the different points in each domain	49
APPENDIX 5 Seismic risk for each geographic domain	52
APPENDIX 6 Seismic risk for each point – ESHM20.....	55
APPENDIX 7 Seismic risk for conversion equations M&O (1977) vs. F&C (2006).....	58
APPENDIX 8 Seismic risk for fragility curves from Rosti et al. (2020).....	62

1. Introduction

As a part of the SIGMA-2 Research and Development project on seismic hazard and ground motion, Work Package #5 is dedicated to developing and implementing new and more realistic approaches for Probabilistic Seismic Hazard Analysis (PSHA) computations. In particular, one of the aims of WP #5 is testing and updating PSHA results against observations.

In this context, a previous SIGMA-2 deliverable (Drif et al. (2020)) evaluated the consistency of three hazard maps of the French metropolitan territory (MEDD, SHARE and GEOTER maps established respectively in 2002, 2012 and 2017) with respect to historical seismicity. This was performed by comparing the seismic risk derived from historical seismicity with the seismic risk calculated by convolution of the aforementioned hazard maps with relevant fragility curves.

The objective of the present report is to use the same methodology as in (Drif et al. (2020)) to compare the seismic risk derived from historical seismicity to the one calculated by convolution of hazard maps and fragility curves, using the new hazard map from the European Seismic Hazard Model - ESHM20.

This hazard map is developed for the SERA Project (Seismology and Earthquake Engineering Research Infrastructure Alliance for Europe), within the JRA3 activities (Updating and extending the European Seismic Hazard Model). Several updates of the ESHM20 hazard maps have been performed recently, the herein presented calculations have been performed using the latest version of the ESHM hazard maps (version V12d) which is available on <http://efehr-dev.ethz.ch/> (ESHM20 Community Preview).

2. Methodology for the risk calculation

2.1. General methodology

Seismic risk R_D is obtained by the following convolution integral:

$$R_D = \int_0^{\infty} -P'_{1y}(a) F_D(a) da \quad [1]$$

Where:

- $F_D(a)$ is the fragility curve, which expresses the probability that a given acceleration a induces a level of damage greater than a given level D ,
- $P_{1y}(a)$ is the annual probability of exceedance of this acceleration level a .

It's worth noting that it is strictly equivalent to convolve the derivative of the fragility curve with seismic hazard curve rather than the fragility curve with the derivative of the seismic hazard curve in equation [1]. This is a consequence of the integration by parts theorem. The former way to calculate the risk has the advantage of using the derivative of the lognormal fragility curve which is can be defined analytically, whereas the derivative of the hazard curve cannot.

The way of writing the convolution integral R_D using the derivative of the hazard curve has the advantage of being physically interpretable: P_{1y} can be interpreted as the cumulative distribution function of the acceleration, and then P'_{1y} is the probability density function (or density) of the acceleration. $-P'_{1y}(a)da$ is the probability that the acceleration is within the infinitesimal interval $[a; a + da]$.

However, both methods lead to the same results and this has been confirmed by numerically recalculating integral [1] for some selected cases.

The probability of exceedance of the acceleration a can also be provided for different return periods, such as 50 years, and is then denoted $P_{50y}(a)$.

Assuming that earthquakes occur independently in time, *i.e.* the probability of an earthquake occurring does not depend on the time elapsed since the last earthquake, the probability $P_{\Delta t}(a)$ follows a Poisson model. The relation which links the return period of a seismic event of intensity greater than a , $T(a)$, and the probability of occurrence of this event over a duration Δt is then written:

$$P_{\Delta t}(a) = 1 - e^{-\frac{\Delta t}{T(a)}} \quad [2]$$

Considering that earthquakes are sufficiently rare events, the following approximation can be made:

$$P_{1y}(a) \approx \lim_{T(a) \rightarrow \infty} \left(1 - e^{-\frac{1}{T(a)}} \right) = \frac{1}{T(a)} \quad [3]$$

Using equation [2] to write the probability of exceedance over 50 years and the approximation [3] leads to the following expression to convert 50-year probabilities to annual probabilities:

$$P_{1y} \approx \frac{1}{T} = -\frac{\ln(1 - P_{50y})}{50} \quad [4]$$

2.2. Seismic risk - Numerical computations

In Drif et al. 2020, an approximation (actually, an upper bound) for calculating integral [1] is used in order to simplify risk calculation. This approximation is only exact under two conditions:

- The hazard curve is replaced by its tangent line in log-log scale at the point corresponding to a defined return period, T_{ref} , as illustrated on **Figure 1a**,
- Fragility curves are log normally distributed, as illustrated on **Figure 1b**.

Under these assumptions, calculation of the convolution integral for seismic risk is simplified as follows:

$$R_D = \int_0^{\infty} -P'_{1y}(a) F_D(a) da \approx \frac{1}{T_{\text{ref}}} \left(\frac{a_{\text{ref}}}{a_D^c} \right)^n \exp\left(\frac{n^2 \beta_D^{c2}}{2} \right) \quad [5]$$

Where:

- T_{ref} : return period selected for establishing the probabilistic seismic hazard analysis,
- a_{ref} : PGA at the considered T_{ref} ,
- a_D^c : median value of PGAs generating a damage grade D in a building of vulnerability class \mathcal{C} ,
- β_D^c : standard deviation of the logarithm of the PGAs generating a damage grade D in a building of vulnerability class \mathcal{C} ,
- n : slope in log-log scale at a_{ref} of the line tangent to the seismic hazard curve at the considered point of the hazard curve.

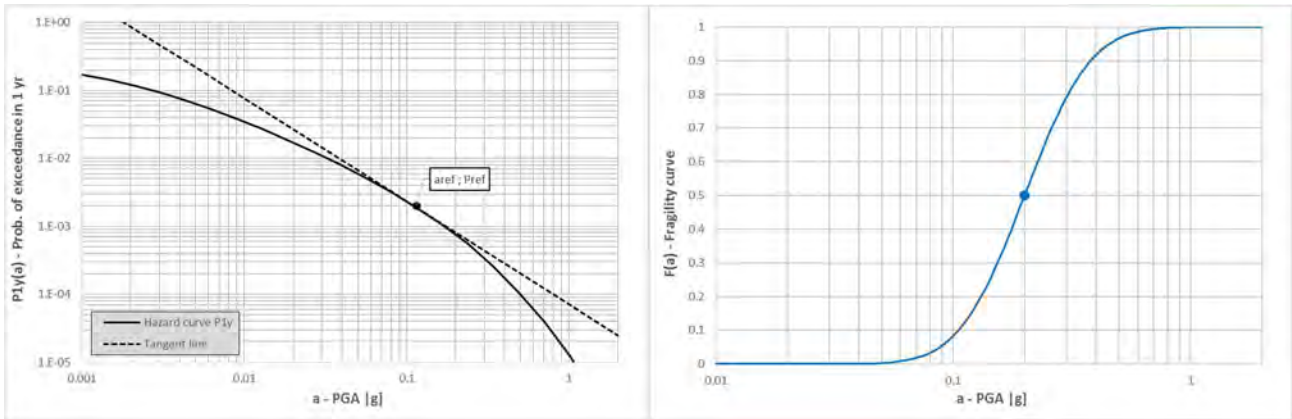


Figure 1a,b: Scheme of seismic hazard curve, parameters T_{ref} and a_{ref} , and tangent line at a_{ref} (left) and typical lognormal fragility curve plotted for median PGA with $a_D^C = 0.2$ g and $\beta_D^C = 0.5$ (right)

In the present study, the hazard curve is no longer approximated by its tangent. Instead, the convolution integral [1] for calculation of seismic risk R_D is numerically computed by discretizing the acceleration interval:

$$P_{1y}(a) = P_{1y}(a_i) \quad ; \quad F_D(a) = F_D(a_i) \quad ; \quad i \in [1; N] \quad [6]$$

The derivative function $P'_{1y}(a)$ in expression [1] is given by the central difference formula:

$$P'_{1y}(a_i) = \frac{P_{1y}(a_{i+1}) - P_{1y}(a_{i-1})}{a_{i+1} - a_{i-1}} \quad [7]$$

In the numerical calculations, this derivative is calculated in the log-log space.

The risk is then calculated using the trapezoidal rule, which yields the following sum:

$$R_D = - \sum_{i=1}^{N-1} \frac{1}{2} (a_{i+1} - a_i) [P'_{1y}(a_{i+1})F_D(a_{i+1}) + P'_{1y}(a_i)F_D(a_i)] \quad [8]$$

This approach allows to extend the seismic risk calculation with real hazard curves (and possibly other fragility curves than log-normal ones). This approach is illustrated on **Figure 2**.

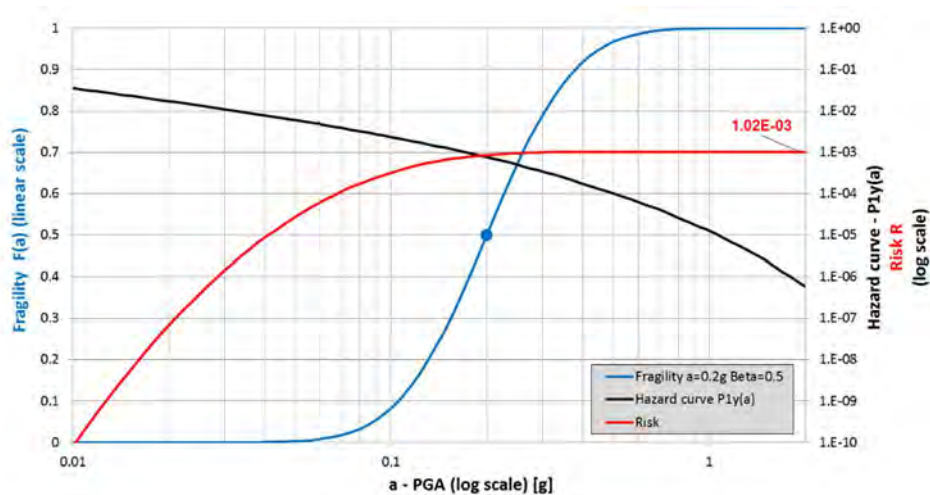


Figure 2: Risk calculation from Hazard Curve $P_{1y}(a)$ and Fragility curve $F(a)$, $a_D = 0.2$ g, $\beta_D = 0.5$

This figure presents a log-normal fragility $F(a)$ in blue that can be read on left axis (linear scale), and the hazard curve in annual probability in black, $P_{1y}(a)$ and the computed risk R obtained with these fragility and hazard curve, in the right axis (log scale).

In the example of **Figure 2**, using Eq. [5] would give a value of risk of $1.23e^{-3}$ (20 % higher than the numerical calculation), which gives an order of magnitude of the over-estimation of the risk when using the simplified formula [5].

2.3. Hazard curves – European Seismic Hazard Model - ESHM20

Hazard curves for the calculation of seismic risk in Continental France have been obtained from the new hazard map of the European Seismic Hazard Model ESHM20.

Hazard curves are given in terms of annual probability of exceedance of the acceleration for about 20 values of acceleration. For the calculation of seismic risk, the ESHM20 hazard curves are interpolated on 500 points evenly distributed in log-log scale in the interval $[a_{\min}, a_{\max}]$, where a_{\min} , a_{\max} are respectively the minimum and maximum values of the intensity measure used in the definition of hazard curves. The interpolation scheme used for the hazard curve is a linear interpolation in the log scale.

Hazard curves can be provided for different Intensity Measures such as the spectral acceleration at different periods T (ranging from 0.05 s to 5.0 s), and for the Peak Ground Acceleration (PGA) which is identified with spectral acceleration for $T = 0$ s. In this study, we have used hazard curves defined on the basis of PGA as Intensity Measure. One reason for this choice is that fragility curves used in the calculations are also defined based on PGA.

Moreover, hazard curves are provided for different statistical fractiles (percentiles) coming from the PSHA study, namely: mean value and 5%, 16%, 50% (median), 84% and 95% percentiles. However, no actual branches of the PSHA study are provided.

Finally, this study is carried out by computing the seismic risk on 115 points in Continental France, cf. §2.5, and the hazard curves are provided for each of these points. The selected 115 points are classified into 8 geographic domains, which are exactly the same as the ones defined in Drif et al. (2020).

Appendix 2 presents hazard curves from ESHM20, for one point of each geographic domain. A first set of figures is presented for displaying the retained hazard curve percentiles (5%, 16%, 50%, 84%, 95%) plus the mean hazard curve from the ESHM20 hazard map.

2.4. Fragility curves

We use fragility curves following the commonly adopted log-normal distribution: the probability $F_D(a)$ that a given acceleration a induces a level of damage greater than a given level D , is defined by the following equation:

$$F_D(a) = \frac{1}{\beta_D \sqrt{2\pi}} \int_{-\infty}^{\ln a} \exp \left[-\frac{1}{2} \left(\frac{a - a_D}{\beta_D} \right)^2 \right] da \quad [9]$$

With:

- a_D : Median value,
- β_D : Log-normal standard deviation.

This definition of fragility is particularly convenient because it reduces to the definition of only two parameters $\{a_D, \beta_D\}$.

Fragility curves are then defined for:

- Two vulnerability classes: B, C,
- Three damage degrees: D2, D3, D4,

Fragility curves used in the present study are the same as the ones used in Drif et al., 2020. These are:

- the set of curves proposed by Lagomarsino & Cattari (2014) using the conversion equation Intensity/PGA of Murphy & O'Brien (1977),
- the set of curves proposed by Lagomarsino & Cattari (2014) using the conversion equation Intensity/PGA of Faccioli & Cauzzi (2006).

Table 1 hereafter indicates the values of a_D and β_D that define these fragility curves.

Vulnerability Class B	D2		D3		D4	
	a_D	β_D	a_D	β_D	a_D	β_D
Lagomarsino & Cattari (2014), Murphy & O'Brien (1977)	0.118	0.62	0.204	0.61	0.355	0.63
Lagomarsino & Cattari (2014), Faccioli & Cauzzi (2006)	0.145	0.54	0.240	0.54	0.390	0.56

Vulnerability Class C	D2		D3		D4	
	a_D	β_D	a_D	β_D	a_D	β_D
Lagomarsino & Cattari (2014), Murphy & O'Brien (1977)	0.208	0.62	0.362	0.61	0.631	0.63
Lagomarsino & Cattari (2014), Faccioli & Cauzzi (2006)	0.243	0.54	0.397	0.54	0.650	0.56

Table 1 - Definition of parameters a_D [g] and β_D for fragility curves (expressed as functions of the PGA), associated to vulnerability classes B and C and damage degrees D2, D3, D4, according to Lagomarsino & Cattari (2014), Murphy & O'Brien (1977) and Faccioli & Cauzzi (2006).

These fragility curves are displayed on **Figure 3** hereafter:

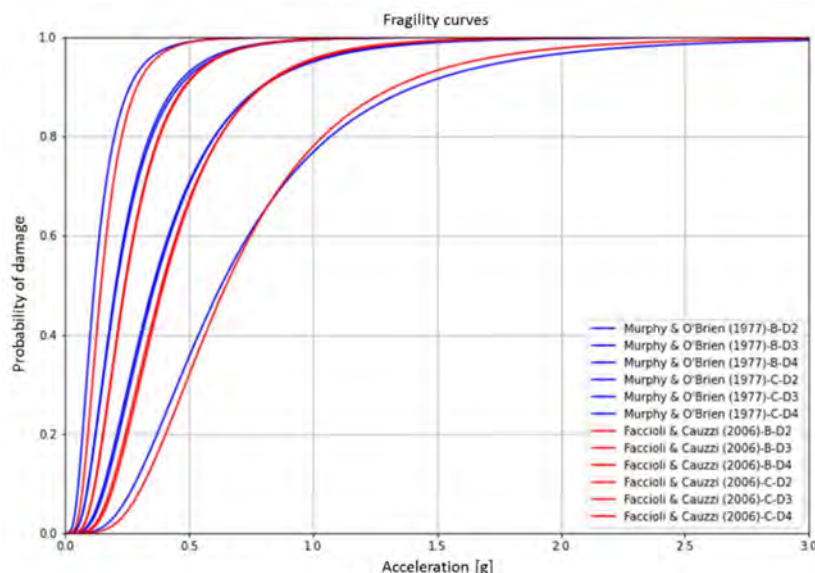



Figure 3: Fragility curves Lagomarsino & Cattari (2014) and conversion equation of Murphy & O'Brien (1977) or Faccioli & Cauzzi (2006). Vulnerability classes B and C and damage degrees D2, D3, D4

It can be noted that the initial set of 6 fragility curves (3 damages states \times 2 vulnerability classes) can actually be reduced to 4 curves: this is because there is a correspondence between case B/D3 and

	Research and Development Program on Seismic Ground Motion	Ref : SIGMA2-2021-04-01
		Page 9/63

C/D2 and also between B/D4 and C/D3. Consequently, the cases for fragility functions are reduced from six to four as follows:

- Vulnerability class B - damage state D2
- Vulnerability class B - damage state D3 (equivalent to vulnerability class C - damage state D2)
- Vulnerability class B - damage state D4 (equivalent to vulnerability class C - damage state D3)
- Vulnerability class C - damage state D4

For the presented calculations, it can be considered that reference risk values are obtained using the fragilities proposed by Lagomarsino & Cattari (2014) and the conversion equation by Faccioli & Cauzzi (2006) which are more recent. As a means for studying the variability of fragility definition in the calculated risk, we present in the **Appendices 5, 6 and 7** additional risk calculations performed using the conversion equation by Murphy & O'Brien (1977). As it can readily be seen from Figure 3, Murphy & O'Brien conversion equation leads to fragilities that are generally envelope to the ones obtained using Faccioli & Cauzzi (2006) conversion equation for the most relevant values of PGA and for all four considered vulnerability class / damage level cases. The calculated risks using Murphy & O'Brien conversion equation are consequently expected to be more significant than the ones obtained using the one proposed by Faccioli & Cauzzi (2006).

Although, there have been other, more recent proposals for the definition of fragility curves (Rota et al. (2010), Simoes et al. (2019), Milosevic et al. (2019) *etc.*), these curves are not directly applicable to the present context for the following reasons:

- These fragility curves have been obtained for very specific types of buildings and are characterized by relatively low β values, which are not sufficient for covering the variability of buildings in a given vulnerability class
- The authors do not mention the vulnerability class (in terms of EMS 98, Grünthal (1998)) in which the considered buildings fit. This could be inferred from the building description, but due to the low β values, these curves cannot be regarded as representative of a vulnerability class, as necessary for the purpose of the presented research.

Appendix 8 provides a comparison of the computed risk using additional fragility curves from a more recent study by Rosti et al. (2020). In this study, authors defined five damage levels consistent with the European Macroseismic Scale (EMS-98, Grünthal (1998)), but used building typologies related to three vulnerability classes (A: high vulnerability, B: medium vulnerability, C1: low vulnerability) that are note equivalent to vulnerability classes of EMS 98.

2.5. Geographic domains

The present study is carried out for Continental France, divided into 8 geographic domains. The definition of these domains is inherited from the initial study by Drif et al. (2020). These 8 reasonably homogeneous domains (from the point of view of seismic hazard) are established relying on the seismotectonic studies that were conducted by Drouet et al. (2020) and are presented on **Figure 4**.

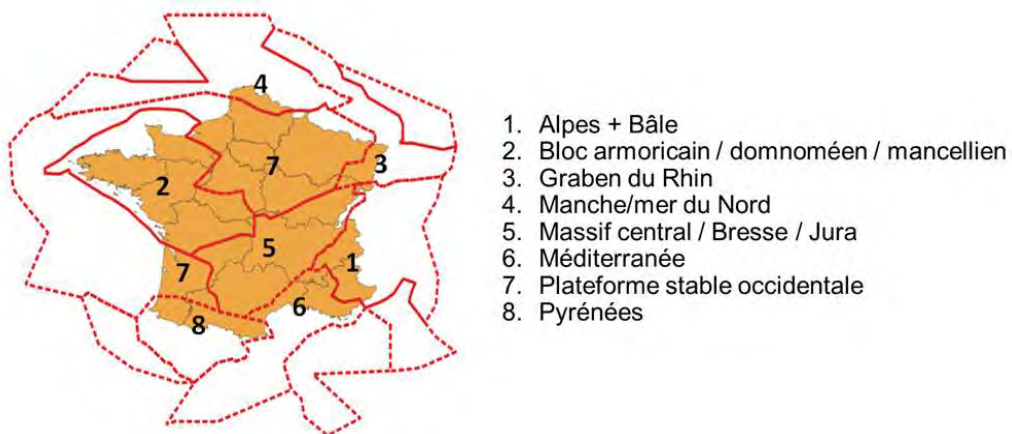


Figure 4: Seismo-tectonic geographic domains across Continental France

The risk calculation is performed for 115 points evenly distributed on this territory as shown on **Figure 5**.

The coordinates of the selected points are given in **Appendix 1**.



Figure 5 : Grid of points selected for risk calculation within each domain

3. Risk calculations

3.1. Seismic risk derived from historical seismicity

3.1.1. Results inherited from the work by Drif et al. 2020

Drif et al. (2020), describe in detail the method for calculating the so-called “historical” seismic risk by combining seismic hazard expressed in Intensity and the EMS-98 scale. Historical risk is calculated separately for each of the 8 geographic domains defined above and also for the entire area of Continental France. The results are given in **Table 2** below for damage degrees D2, D3, D4 and vulnerability classes B and C (note the correspondence between B-D3, C-D2 and B-D4, C-D3 as explained above):

VULNERABILITY CLASS B	Damage D2	Damage D3	Damage D4
Domain	Historical risk	Historical risk	Historical risk
ALPES + BALE	5.240E-04	8.260E-05	1.160E-05
BLOC ARMORICAIN	3.220E-05	4.000E-06	4.580E-07
GRABEN DU RHIN	6.900E-05	4.060E-07	2.390E-09

MANCHE / MER DU NORD	4.210E-05	9.660E-07	2.210E-08
MASSIF CENTRAL	5.730E-06	1.150E-07	2.310E-09
MEDITERRANEE	1.510E-04	4.090E-05	9.990E-06
PLATEFORME OCCIDENTAL	3.880E-07	7.810E-09	1.560E-10
PYRENEES	5.220E-04	3.940E-05	7.160E-07
FRANCE CONTINENTALE	8.020E-05	1.080E-05	1.540E-06
VULNERABILITY CLASS C	Damage D2	Damage D3	Damage D4
Domain	Historical risk	Historical risk	Historical risk
ALPES + BALE	8.260E-05	1.160E-05	1.100E-06
BLOC ARMORICAIN	4.000E-06	4.580E-07	3.720E-08
GRABEN DU RHIN	4.060E-07	2.390E-09	1.370E-11
MANCHE / MER DU NORD	9.660E-07	2.210E-08	4.610E-10
MASSIF CENTRAL	1.150E-07	2.310E-09	4.270E-11
MEDITERRANEE	4.090E-05	9.990E-06	1.420E-06
PLATEFORME OCCIDENTAL	7.810E-09	1.560E-10	2.890E-12
PYRENEES	3.940E-05	7.160E-07	1.210E-08
FRANCE CONTINENTALE	1.080E-05	1.560E-06	1.770E-07

Table 2: Historical seismic risk evaluation for D2, D3, D4 damage degrees and vulnerability classes B and C.

3.1.2. Summary of the method implemented in Drif et al. (2020)

The reader may refer to the SIGMA2 report by Drif et al. (2020) for a detailed description of the method that has been implemented for the calculation of seismic risk derived from historical seismicity. For reasons of completeness of the present report we provide hereafter a brief summary of the methodology implemented in Drif et al. 2020.

The method is based on a definition of historical seismicity for Continental France via an atlas of isoseismal maps. These maps have been elaborated in the framework of the SIGMA research project (Pecker et al. (2017)). The SIGMA atlas of isoseismal maps is an exhaustive set of manually drawn isoseismals for the 194 events with epicentral intensities of degree VI (MSK) or greater, that occurred over the period from 1900 to 2007, and were felt in continental France or its immediate vicinity.

Continental France is a moderate seismicity area. The activity is usually diffuse and nonhomogeneous across the territory. In order to identify reasonably homogeneous domains, seismo-tectonic studies conducted by Drouet et al. (2020) have been used to individualize crustal units with homogenous seismogenic characteristics. These deemed homogeneous geographic domains (8 in total, within Continental France) are actually the ones presented in section 2.5 and they have been the geographic domains used in the present study and in Drif et al (2020) report for seismic risk calculation based both on historical seismicity and on the several hazard maps (including the ESHM20).

The calculation of seismic hazard based on historical seismicity considers the ratio of the annual average area affected by an intensity equal to or larger than I in a region of interest over the total area of this region. Denoting by A_I the average area (within a given geographic domain) that is yearly affected by an intensity equal to or larger than I , the annual frequency of observing at least one intensity equal to or larger than I at any location in the territory reads:

$$p(I) = \frac{A_I}{A} \quad [10]$$

Conceptually, if comprehensive macro-seismic data were available on a very long period of time (T years), calculating A_I would be easily achieved as follows: for every event i occurring over T and denoting by $A_{I,i}$ the area affected by an intensity larger than or equal to I , quantity A_I would be obtained by the following expression:

$$A_I = \frac{\mathcal{A}_I}{T} \quad \text{with} \quad \mathcal{A}_I = \sum \mathcal{A}_{I,i} \quad [11]$$

Practical implementation of the above approach requires a comprehensive macro-seismic dataset and for this purpose the SIGMA atlas of isoseismal maps has been used in the work by Drif et al (2020). This enables to derive, for $I \geq VI$, an estimated value $p'(I)$ of $p(I)$ as follows:

$$p(I) \approx p'(I) = \frac{A'_I}{A} \quad [12]$$

$$A'_I = \frac{\mathcal{A}'_I}{108} \quad \text{with} \quad \mathcal{A}'_I = \sum \mathcal{A}_{I,i} \quad \text{on 1900-2007} \quad [13]$$

Since Continental France cannot be regarded as homogeneous in terms of seismic activity, the territory is separated into the 8 geographic domains defined above, in such a way so that the activity can be regarded as reasonably homogeneous inside each domain.

After having derived $p'(I)$ for each geographic domain and intensity, the EMS-98 scale (Grünthal 1998) is selected for calculating seismic risk from historical seismic hazard. The calculation is performed for masonry buildings, for which the EMS-98 scale defines six vulnerability classes (A to F) and five damage levels (D1 to D5). For each intensity level, EMS-98 provides in a qualitative way, the damage level that is developed in a certain vulnerability class. A quantification assumption for the qualitative terms of EMS-98 is introduced in Drif et al. 2020 to allow calculation of seismic risk. The proposed quantification is the following: *all* = 100%, *most* = 80%, *many* = 35%, *few* = 8%. As an example, **Table 3** below provides the transition from hazard to damage for intensity level VIII according to ESM-98 is provided below:

Intensity VIII	Vulnerability classes				
Degree of damage	A	B	C	D	E
1	all	all	most	many	-
2	all	most	many	few	-
3	most	many	few	-	-
4	many	few	-	-	-
5	few	-	-	-	-

Table 3: Transition from the seismic hazard in intensity to damage to buildings, for intensity level VIII

In the above table, black terms are explicitly mentioned in EMS-98 and green terms are proposed by Drif et al. 2020. Similar tables are defined for intensities V to IX. Tables with qualitative terms (*all*, *most*, *many*, *few*) are converted to matrices containing quantitative terms following the aforementioned quantification assumption.


The above definitions allow introducing quantity $F_D^C(I)$, which expresses the probability that a damage $\geq D$ occurs in a building of vulnerability class C in case an intensity I is observed or assumed.

Combining quantities $p(I)$ and $F_D^C(I)$, it is possible to calculate seismic risk $R^C(D)$ as follows:

$$R^C(D) = \sum_{I=VI}^{IX} p(I) F_D^C(I) \quad [14]$$

Because no information on Intensity V is included in the SIGMA atlas of isoseismal maps, the summation in the above equation must start at $I = VI$. Additionally, it follows from the definitions of ESM-98, that the above formula is only valid for $D > 1$.

The results presented by Drif et al. (2020) are considered firm for the present study. In the following paragraph, we focus our attention on the calculation of seismic risk based on the ESHM20 hazard map.

	Research and Development Program on Seismic Ground Motion	Ref : SIGMA2-2021-04-01 <hr/> Page 13/63
---	--	---

3.2. Comparison between ESHM20 risk and historical risk

3.2.1. Methodology

The seismic risk based on ESHM20 hazard map is computed for the following cases:

- 5%, 15%, 50%, 84%, 95% percentiles of hazard curves
- 8 geographic domains + the entire area of Continental France,
- Vulnerability classes B and C,
- Damage degrees D2, D3 and D4,
- Fragility curves from Lagomarsino & Cattari (2014) with two conversion equations: Faccioli & Cauzzi (2006) and Murphy & O'Brien (1977).

The results are presented in tabular and graphical form and are organized:

- a) based on geographic region (one figure per geographic region)
- b) based on the damage level (one figure per damage level)

In case a), for the 8 geographic domains and for Continental France, a graph displays the seismic risk comparison (ESHM20 vs historical) for the 4 considered cases of {Vulnerability Class – Damage degree} couples:

- {Vuln. Class B – D2},
- {Vuln. Class B – D3} considered equivalent to {Vuln. Class C – D2},
- {Vuln. Class B – D4} considered equivalent to {Vuln. Class C – D3},
- {Vuln. Class C – D4},

In these curves the risk per geographic domain corresponds to the mean value of the risks calculated in the points belonging to each domain. These 9 graphs are given in §3.2.2 using the 5 aforementioned percentiles of hazard curves, and in **Appendix 3** using the median hazard curves and highlighting with an error bar the variability in risk among all points in each domain.

For case b), 4 graphs are presented corresponding to the 4 considered cases of {Vulnerability Class – Damage degree}. These 4 graphs are given in §3.2.3 using the 5 aforementioned percentiles of hazard curves. The same 4 graphs are presented in **Appendix 4** for median hazard curves alone, but by displaying the variability between the points belonging to each domain. The error bars correspond to the minimum and maximum risks from all the points in each domain.

In the present report (main text and appendices), we invariably use the following coloration convention:

- ESHM20, Lagomarsino & Cattari (2014) fragility, Faccioli & Cauzzi (2006) conversion eq.: red,
- ESHM20, Lagomarsino & Cattari (2014) fragility, Murphy & O'Brien (1977) conversion eq.: blue,
- Historical: grey.

The 2 paragraphs hereafter only present results obtained with Lagomarsino & Cattari (2014) fragility curves and Faccioli & Cauzzi (2006) conversion equation (Intensity/PGA) which can be considered reference values for the present study. However, **Appendix 7** presents these same results obtained with Murphy & O'Brien (1977) conversion equations and compares risks obtained from the conversion equations of Faccioli & Cauzzi (2006). It confirms that using either of these equations does not lead to a significant change on computed risk. Faccioli & Cauzzi (2006) conversion equations yield in all cases slightly lower risks than the conversion equations proposed by Murphy & O'Brien (1977).

The computed risks based on ESHM20 maps correspond to the mean values from all the points belonging to a specific geographic domain. This is relevant with the fact that these points are evenly distributed on the territory. Moreover, error bars (*cf.* **Appendix 4**) indicate the range between the minimal

and the maximal risk among the computed values for all the points in each geographic domain. This gives a measure of the variability that is inherent in the definition of risk within a geographic zone.

The minimal risk on the vertical axis is set equal to 10^{-8} even if the computed historical risk (*cf.* **Table 2**) can be lower. Indeed, for regions of very low seismicity and for high damage levels (*i.e.* vulnerability class C and damage degree D4) historical risk can be as low as $2.89 \cdot 10^{-12}$ (see the case of “Plateforme Occidentale” in **Table 2**). Such a low value cannot be considered relevant but it rather indicates a lack of historical data. This is the reason why in graphs for risk comparison provided in the following sections, no risk lower than 10^{-8} is displayed.

The presented graphs are accompanied by a table, displayed at the lower part of the figure, providing the numerical values corresponding to each plot.

3.2.2. Results by geographic domains, for each percentile (5%, 16%, 50%, 84%, 95%) of hazard curves

This paragraph contains 9 figures, one for each of the 8 geographic zone considered in the present study plus one for the entire France. In each figure, we provide a comparison of historical risk with the risk calculated with hazard curves percentiles of ESHM hazard map. Computed risks from median hazard curves are designated with a circular marker. Risks from the other considered percentiles are designated with a diamond marker (16%, 84%) or with a thin diamond marker (5%, 95%).

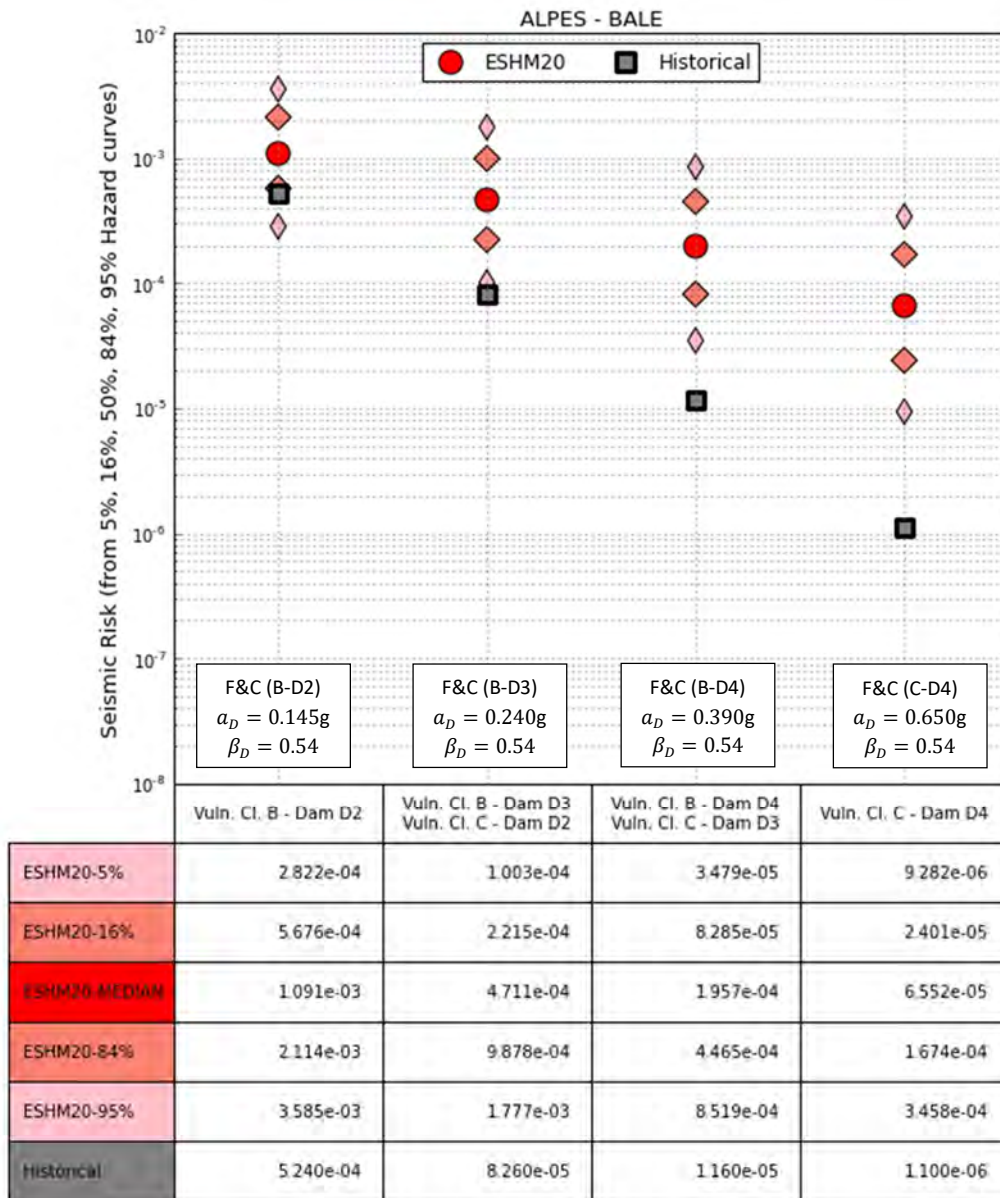


Figure 6: Seismic risk (5%, 16%, 50%, 84%, 95% percentiles of hazard curves) – Alpes Bâles

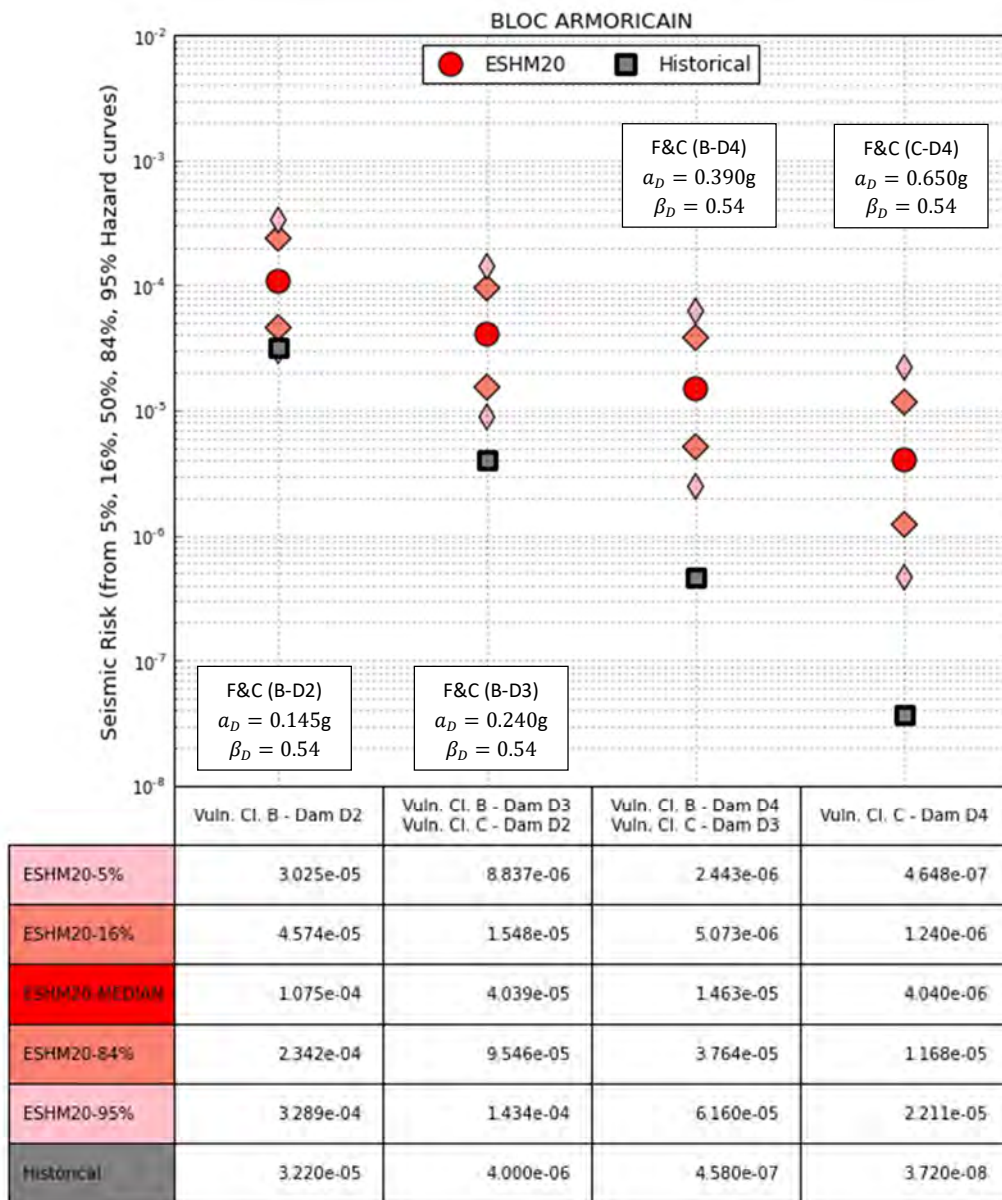


Figure 7: Seismic risk (5%, 16%, 50%, 84%, 95% percentiles of hazard curves) – Bloc Armoricaïn

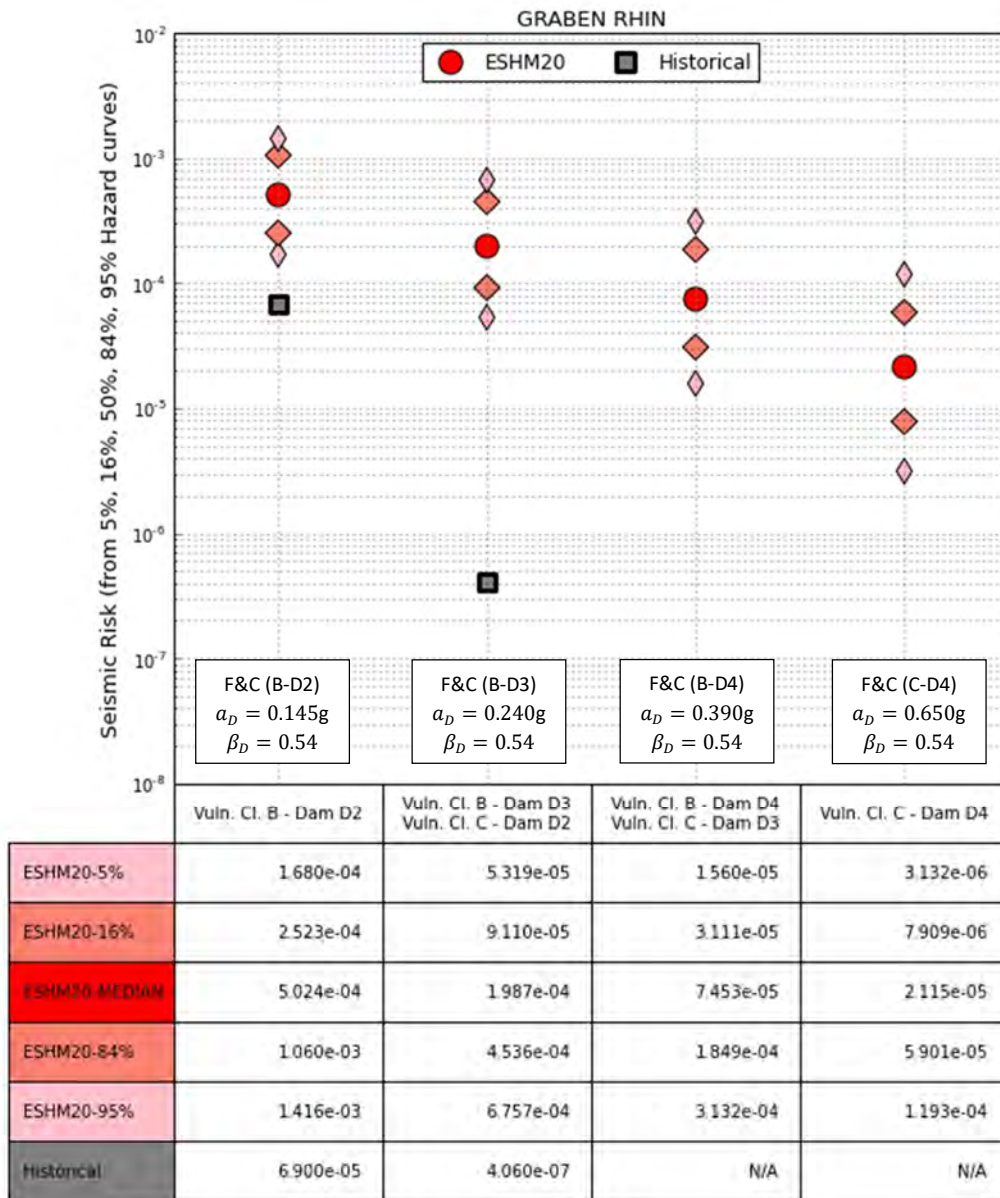


Figure 8: Seismic risk (5%, 16%, 50%, 84%, 95% percentiles of hazard curves) – Graben du Rhin

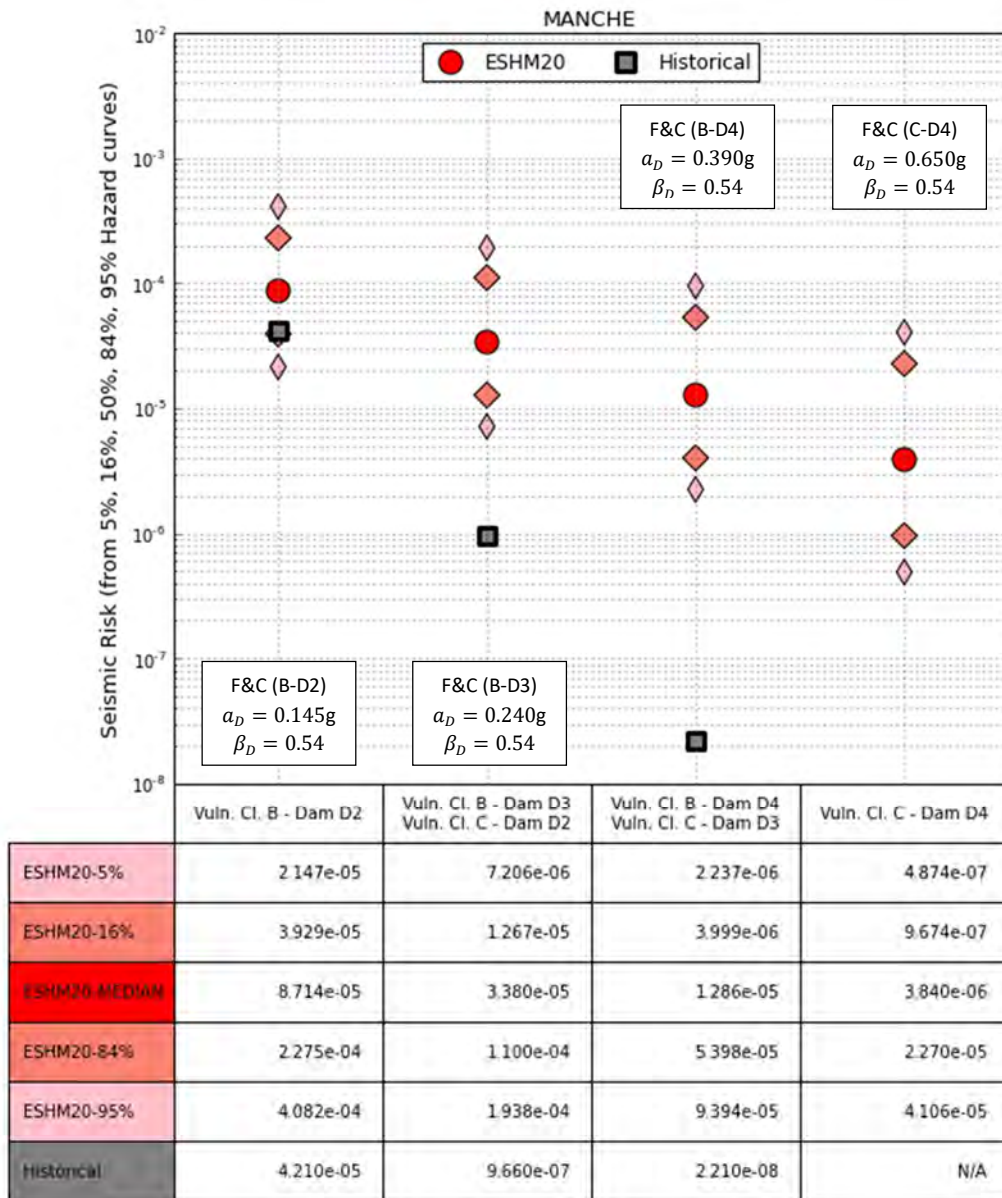


Figure 9: Seismic risk (5%, 16%, 50%, 84%, 95% percentiles of hazard curves) – Manche

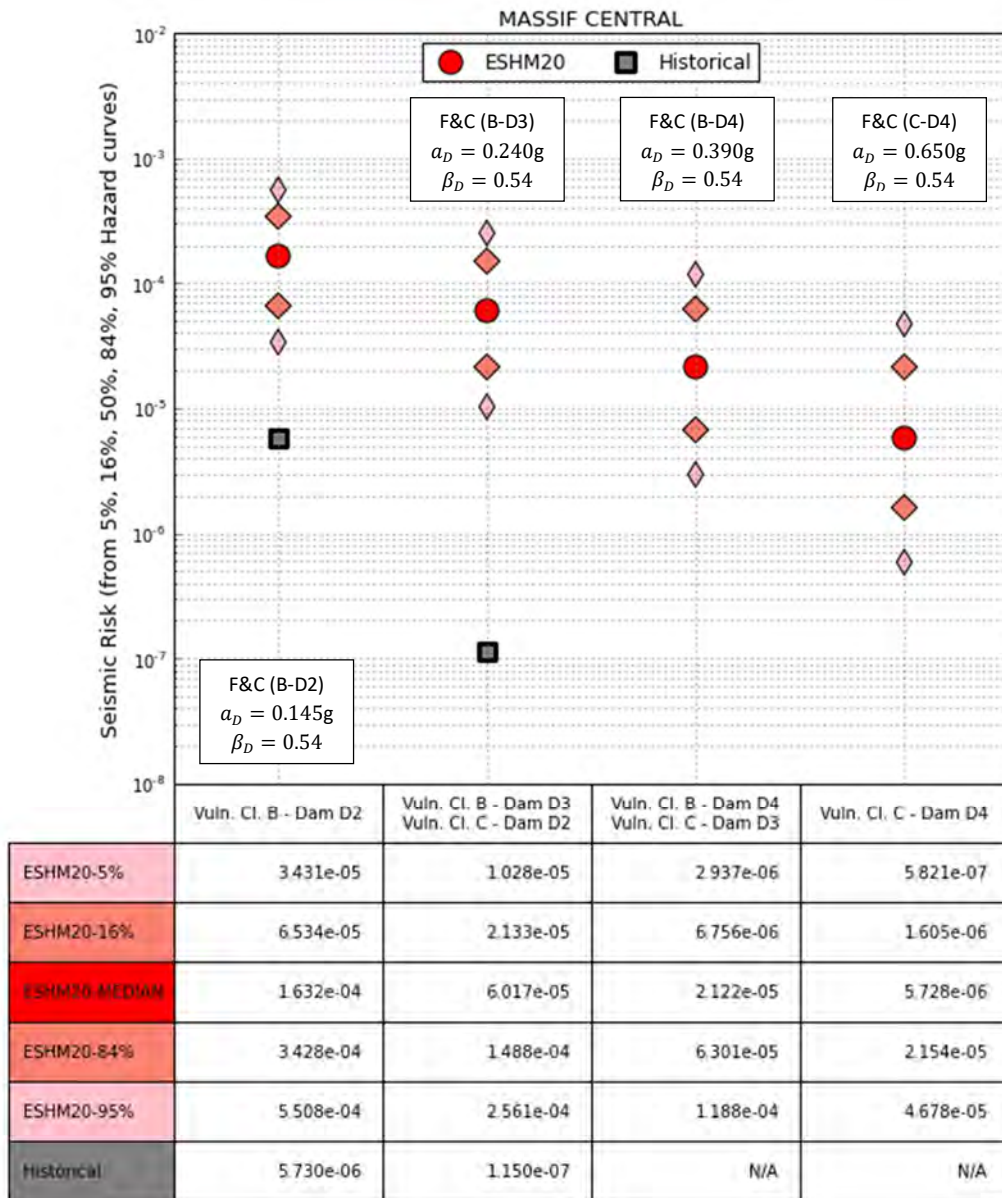


Figure 10: Seismic risk (5%, 16%, 50%, 84%, 95% percentiles of hazard curves) – Massif Central

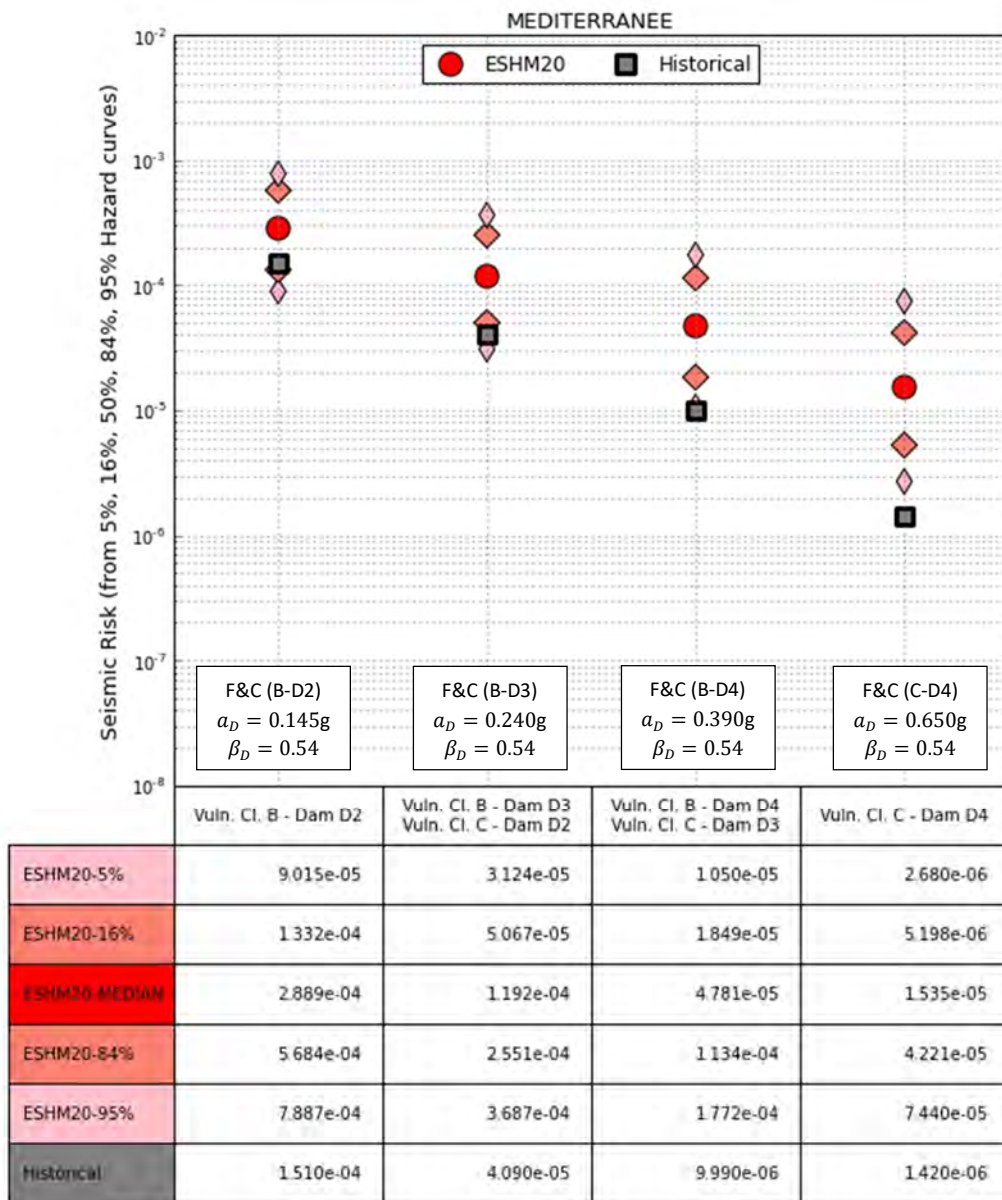


Figure 11: Seismic risk (5%, 16%, 50%, 84%, 95% percentiles of hazard curves) – Méditerranée

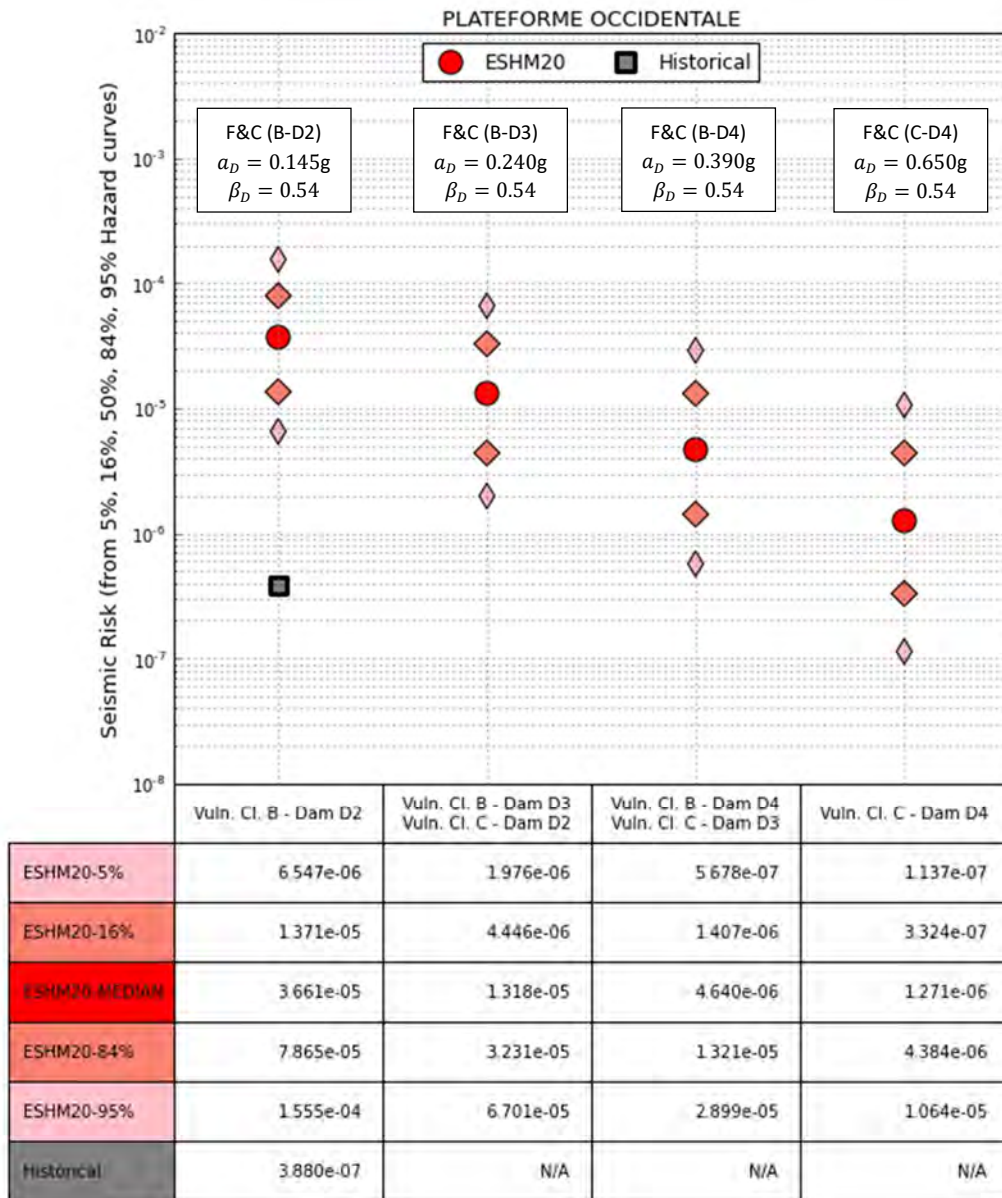


Figure 12: Seismic risk (5%, 16%, 50%, 84%, 95% percentiles of hazard curves) – Plateforme Occidentale

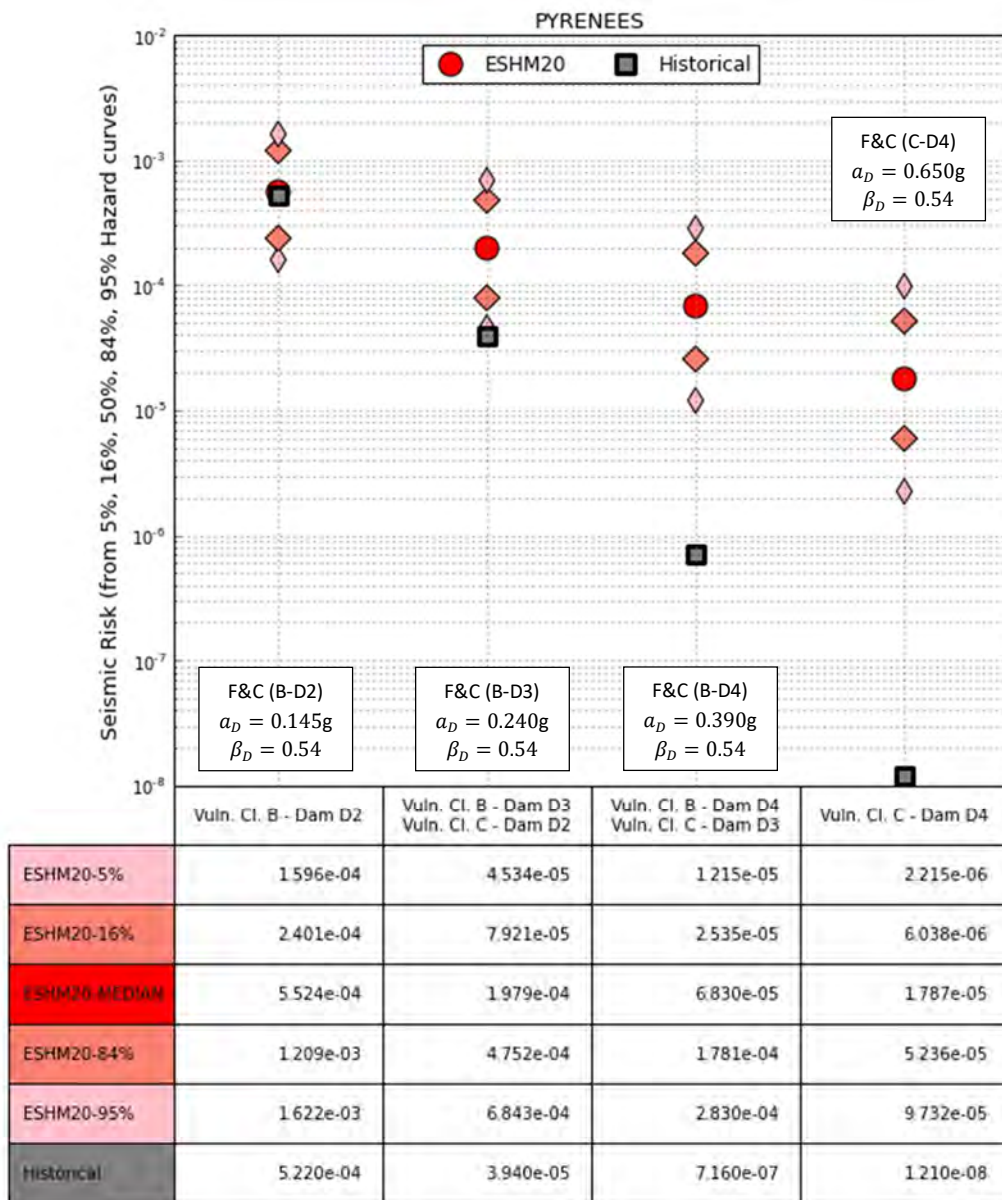


Figure 13: Seismic risk (5%, 16%, 50%, 84%, 95% percentiles of hazard curves) – Pyrénées

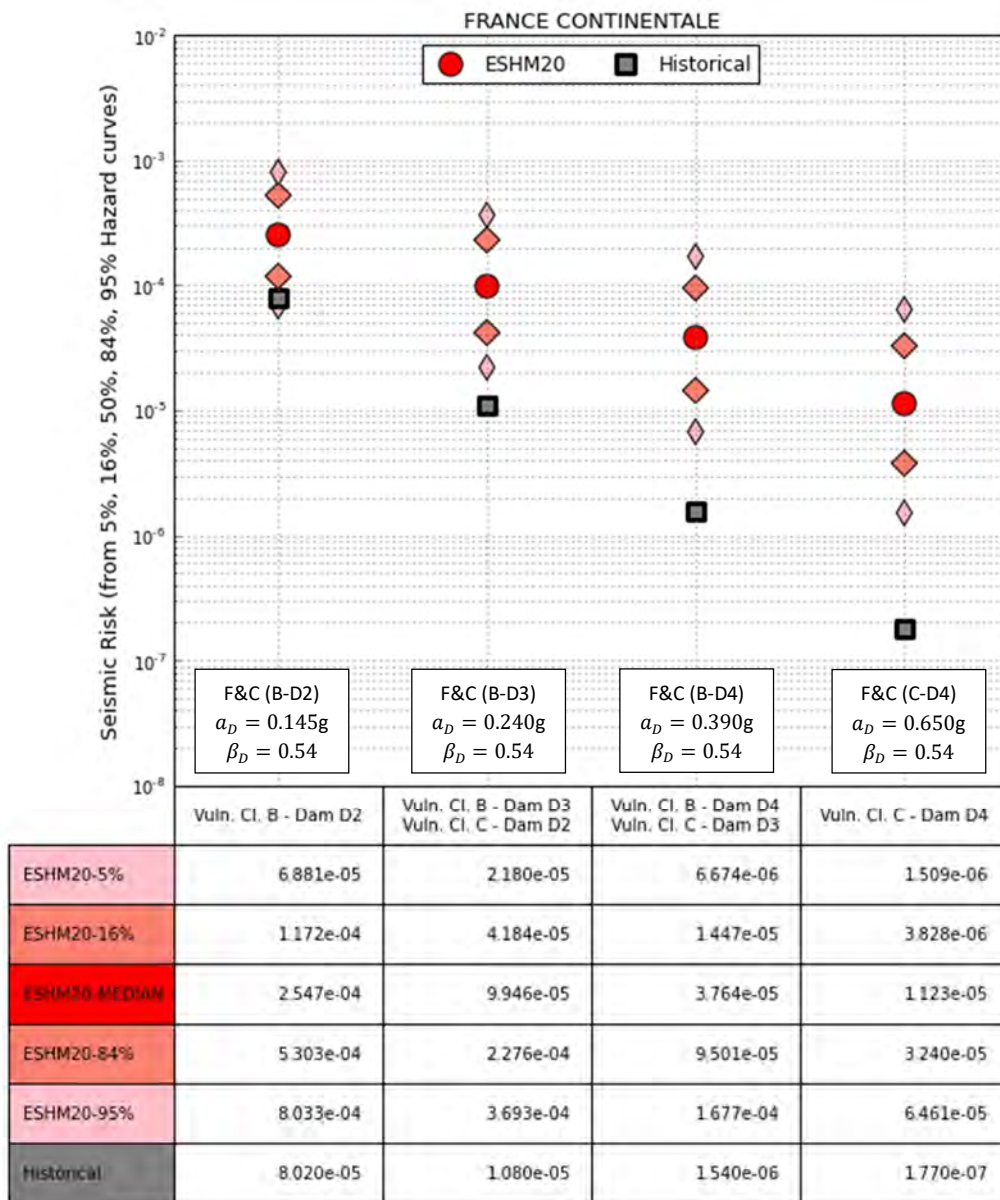


Figure 14: Seismic risk (5%, 16%, 50%, 84%, 95% percentiles of hazard curves) – France Continentale

3.2.3. Results by damage degree and vulnerability class, for each percentile (5%, 16%, 50%, 84%, 95%) of hazard curves

This paragraph contains 4 figures, one for each of the four couples of vulnerability class and damage degree considered in the present study. In each figure, we provide a comparison of historical risk with the risk calculated with hazard curves percentiles of ESHM hazard map. Computed risks from median hazard curves are designated with a circular marker. Risks from the other considered percentiles are designated with a diamond marker (16%, 84%) or with a thin diamond marker (5%, 95%). Each figure contains 8+1 plots corresponding the considered geographic zones and to the entire area of Continental France.

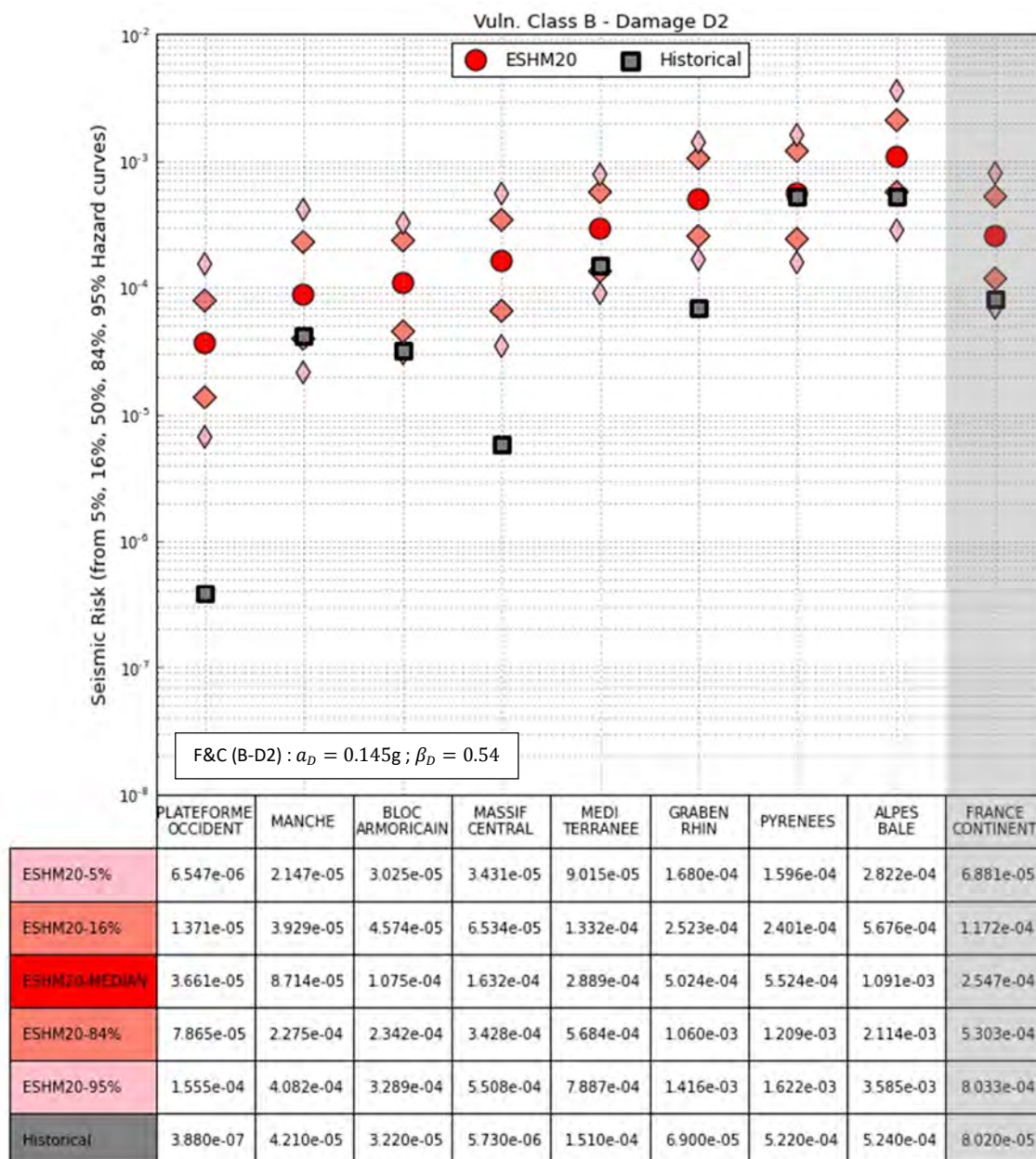


Figure 15: Seismic risk (5%, 16%, 50%, 84%, 95% percentiles of hazard curves) – Vuln. Class B – Damage D2

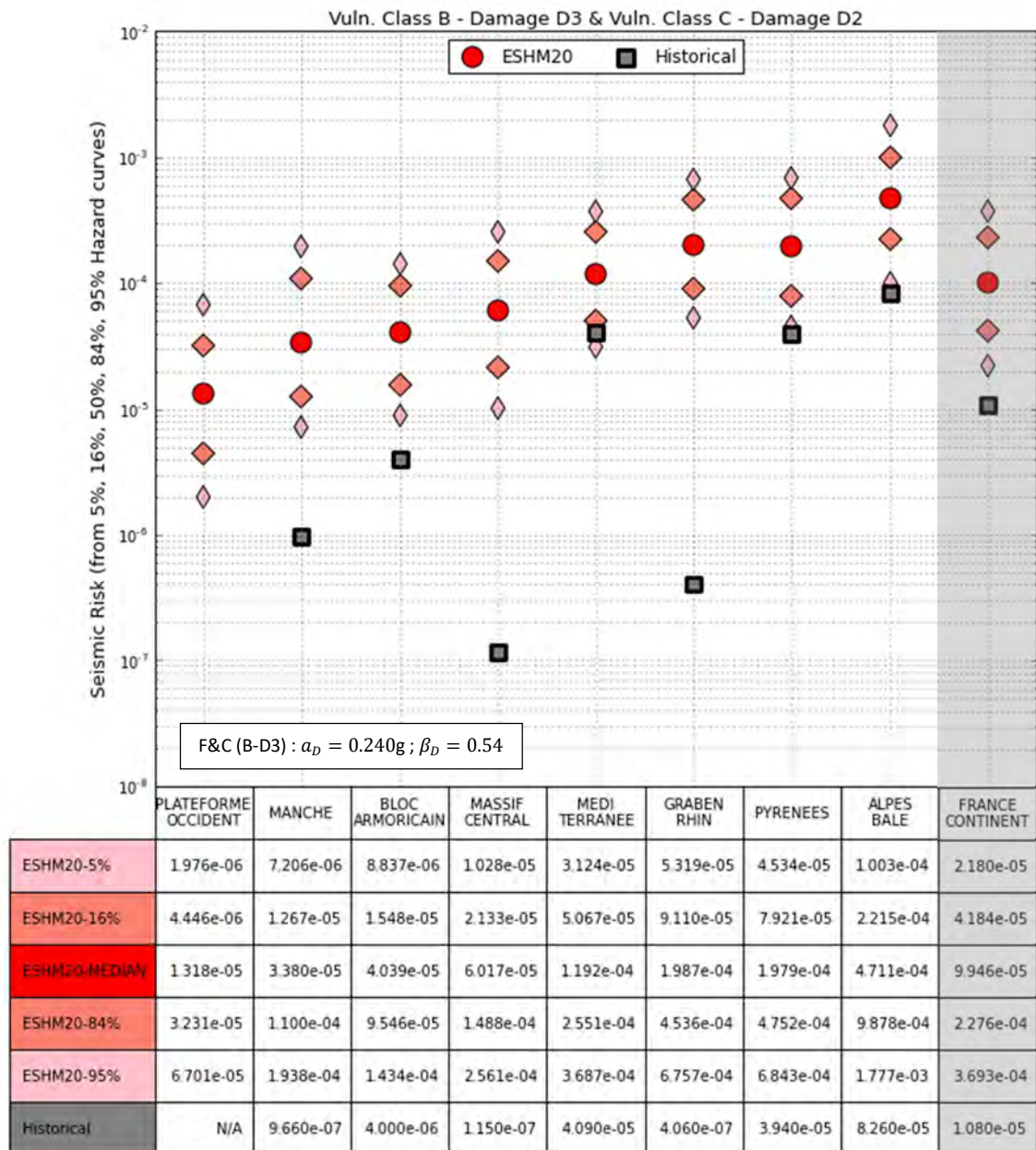


Figure 16: Seismic risk (5%, 16%, 50%, 84%, 95% percentiles of hazard curves) – Vuln. Class B – Damage D3 (equivalent to Vuln. Class C – Damage D2)

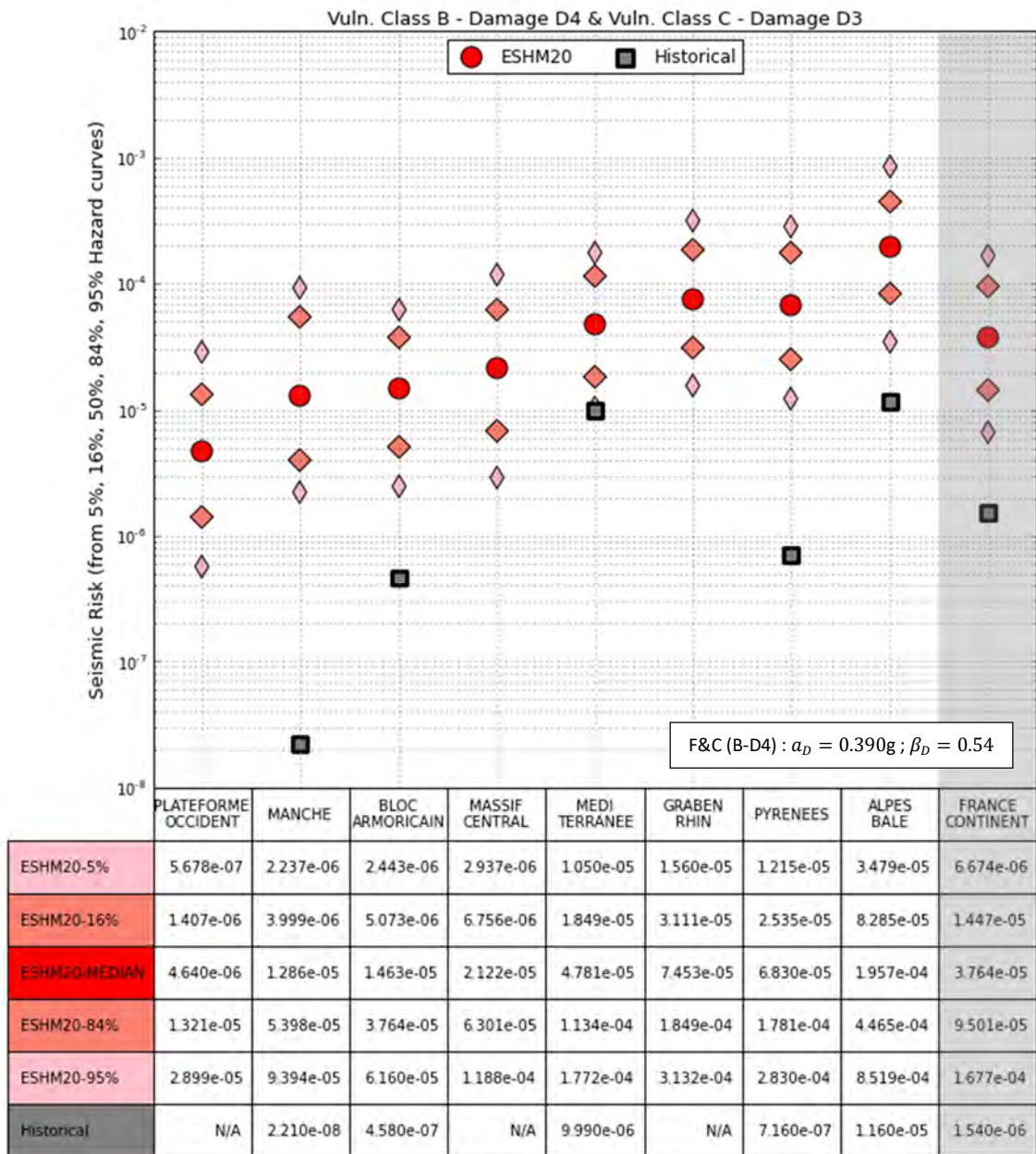


Figure 17: Seismic risk (5%, 16%, 50%, 84%, 95% percentiles of hazard curves) – Vuln. Class B – Damage D4 (equivalent to Vuln. Class C – Damage D3)

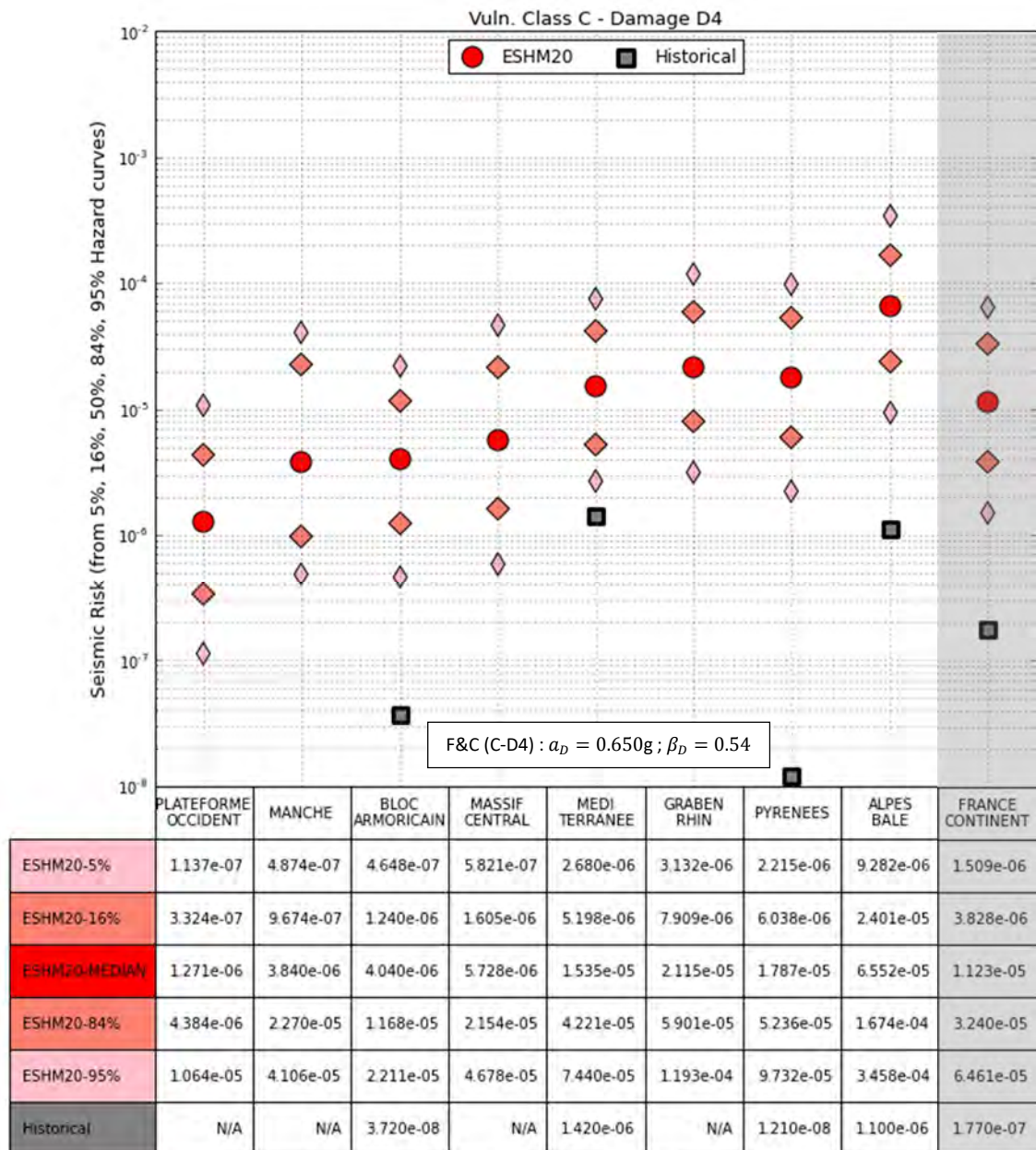


Figure 18: Seismic risk (5%, 16%, 50%, 84%, 95% percentiles of hazard curves) – Vuln. Class C – Damage D4

3.2.4. Discussion on the obtained results

Examination of the provided graphs and tables that provide the comparison of historical risk with the computed risk based on the ESHM20 hazard maps leads to the following remarks:

- The risk calculated from ESHM20 maps using median hazard curves is generally larger than the historical risk (and this, despite of the fact that ESHM20 hazard curves do not encapsulate local site effects whereas historical risk does). However, depending on the geographic region and the considered fragility curve / conversion equation set, there are cases in which the ESHM20-based risk (mean value per region) can be comparable to the historical risk. This is, for example, the case of the Pyrénées region, damage level B-D2 and Faccioli & Cauzzi conversion equation (*cf. Figure 13 and Figure 15*).
- If it can generally be considered that ESHM-based risk is larger than historical risk, this gap is decreasing for regions of higher seismicity (such as regions “Méditerranée”, “Alpes+Bâles”) and is increasing for regions of very low seismicity (such as “Massif Central”, “Plateforme occidentale”) for a given damage level. For most of those low seismicity regions, the historical risk is lower than the computed risk obtained with 5% percentile hazard curves and even for Vulnerability Class B and Damage degree D2.
- Similarly, this gap increases when vulnerability class passes from B to C and/or the damage degree increases (D2 → D3 → D4): this can be understood either by the fact that data for historical seismicity become scarcer as damage level increases, yielding very low historical risks or because ESHM20 hazard curves might over-estimate long return period seismic motion, due to some underlying assumptions of the ESHM20 study.
- Considering only the Vulnerability Class B, the Damage degree D2, and the 3 regions with the highest seismicity level, in other words, the hypotheses that lead to the best match between historical and computed risks, we can make the following observations:

$$\text{Alpes Bales: } R_{ESHM20 V12-5\%} = 2.8e^{-4} < R_{hist} = 5.2e^{-4} < R_{ESHM20 V12-16\%} = 5.7e^{-4}$$

$$\text{Méditerranée: } R_{ESHM20 V12-16\%} = 1.3e^{-4} < R_{hist} = 1.5e^{-4} < R_{ESHM20 V12-50\%} = 2.9e^{-4}$$

$$\text{Pyrénées: } R_{ESHM20 V12-16\%} = 2.4e^{-4} < R_{hist} = 5.2e^{-4} < R_{ESHM20 V12-50\%} = 5.5e^{-4}$$

Moreover, the same analysis for the entire continental France leads to the following results:

$$\text{Cont. France: } R_{ESHM20 V12-5\%} = 6.9e^{-5} < R_{hist} = 8.0e^{-5} < R_{ESHM20 V12-16\%} = 1.2e^{-4}$$

These results highlight that there can be a certain percentile of the hazard curves that matches historical risk but only for the regions of relatively strong seismicity within France and for the less severe couples of vulnerability class and damage degree.

- Although this comparison is not presented herein, the ESHM20-based risk is typically lower than the risks obtained with MEDD, SHARE and GEOTER maps (these results have been presented in Drif et al. (2020)) and can thus be considered to be more compatible with respect to historical seismicity.

- The use of conversion equation proposed by Faccioli & Cauzzi (2006) (in fragility curves from Lagomarsino & Cattari (2014)) yields computed risks that are lower than the ones predicted using the conversion equation by Murphy & O'Brien (1977). Gap between these two risks remains nevertheless low compared to the gap between computed and historical risks. Faccioli & Cauzzi are by the way more recent and should thus be considered more reliable.
- The error bars plotted in the graphs highlight the variability in the value of calculated risk within a zone. As expected, the size of the error bars increases for regions of larger surface area since these regions contain a larger number of control points.

In addition to the previous observations, the following considerations have also to be taken into account:

- In order to better compare the observed risk (that incorporates site effects), calculated risk should take into consideration site amplification which is not extremely complicated to account for, even if some additional considerations regarding site conditions variability among a given area should still be carefully addressed. As a perspective of our study, we could use data such as the part of French territory belonging to zones A, B, C, D, E according to the Eurocode, and introduce an adapted coefficient for site amplification.
- As the historical risk was estimated based on the 20th century observed seismicity, there is a possibility that an occurrence variability is present in the calculations due to this time window of observation. This does not seem to be the case at the entire French metropolitan territory but it could be the case for smaller areas. This aspect could be taken into consideration in the future by implementing an occurrence model in the process (*i.e.*, Poisson's model) in order to assess the likelihood of having observed what was actually observed compared with the calculated risk. A complementary way would be to work with a smaller number of zones, by merging zones that exhibit similar levels of seismicity.

This is particularly true for a low-to-moderate seismicity country like France, and this study could be extended to a higher seismicity country (e.g. Italy) where the results would be less influenced by the small number of observed earthquakes in historical risk calculation. Actually, such an analysis has been performed for the southeastern region of France and northwestern region of Italy, with the hazard map developed within the SHARE project, in the work by Sopranzi (2018).

- Ideally, the comparisons between hazard map-based risk and historical risk should be performed based on the results from the entire logic tree of the PSHA study (not only percentiles) in order to provide PSHA actors with useful feedback in order to let them adjust weight of the whole logic tree (even reconsider some branches), regarding the comparison to observation. This was not done in this study due to time delay and organizational issues, but this could be done in a future work.
- Regarding risk calculation, it should also be pointed out that one additional bias could also originate from the fragility curves data that are used to calculate risk. If the median value of a given fragility curve is biased, the calculated risk will be biased consequently. This possible bias could be highlighted and discussed by comparing risk testing to instrumental seismicity testing in order to quantify its contribution and possibly identify axes of improvement of building fragility models.
- In addition, the fragility model parameter β_D includes some epistemic uncertainties that lead to an increase to the value of β_D and thus to an increase of the calculated risk (as shown in eq. 5

of Drif et al. (2020)). A way to cope with this situation would be to separate aleatory and the epistemic contributions to β_D and calculate a risk distribution (instead of a single value)

Crosscheck of risk testing results presented in this report with instrumental and historical seismicity testing results obtained through a SIGMA-2 parallel study (Drouet & Secanell):

- The results presented in this study may be compared to the results obtained through a SIGMA-2 parallel study (Drouet & Secanell). Even if the scope of these studies and the way of evaluating ESHM20 results based on observation are not strictly comparable, the consistency of their outcomes and conclusions can be compared. **Figure 19** hereafter illustrates how these two studies are connected and complement to each other in terms of level of hazard (or range of the hazard curve) they allow to explore. Drouet & Secanell study explores the range 0.01 g to 0.15 g of ESHM20 results when this study explores the range 0.15 g to 0.65 g. Focusing at the border between the two studies ranges, **Figure 19** (middle to right connection) shows that the trends and conclusions are quite in a good agreement (both of them show that ESHM20 centiles 5% and 16% are in good agreement with observations regarding 0.15 g PGA hazard range).

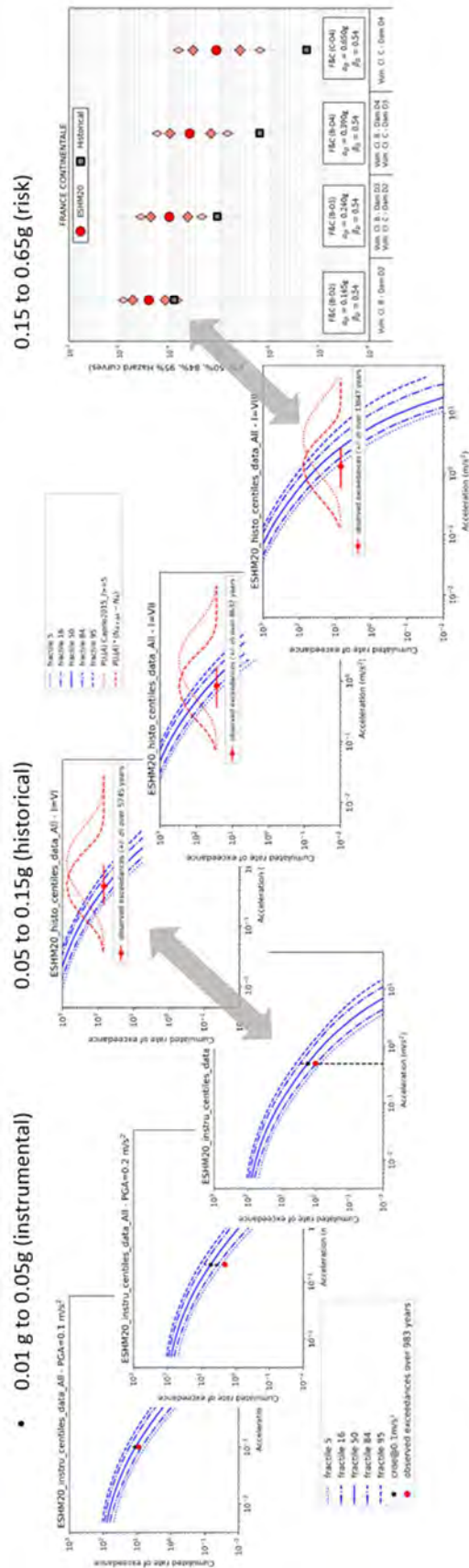


Figure 19: Comparison and complementarity illustration of this study (right) and Drouet & Secanell study (left and middle)

4. Conclusions and perspectives

As a general conclusion of this study, we can consider that ESHM20 provides with hazard characterization that is much more consistent with observations as compared with previous studies, even if still higher than seismic risk observed on the French metropolitan territory.

The difference between calculated risk and observed risk seems to be lower (in better agreement) in areas with high seismicity. This means that ESHM20 may overestimate hazard more in low-to-moderate seismicity areas than in high seismicity areas).

For Vulnerability Class B, Damage degree D2, the three areas with higher seismicity, which are Alpes-Bales, Méditerranée and Pyrénées present an historical risk which is respectively $5.2e^{-4}$, $1.5e^{-4}$ and $5.2e^{-4}$. These values correspond approximately to the 50% percentile of ESHM20 V8-based risk (respectively $5.1e^{-4}$, $1.6e^{-4}$ and $3.4e^{-4}$), and around the 16% to 50% percentiles of ESHM20 V12-based risk (resp. $5.7e^{-4}$ (50%), $1.3e^{-4}$ (16%) and $5.5e^{-4}$ (50%)).

For the entire area of continental France, historical risk ($8.0e^{-5}$) is better fitted to the 16% percentile of ESHM20 V8 hazard curves (computed risk is $8.2e^{-5}$) and to the 5% percentile of ESHM20 hazard curves (computed risk is $6.9e^{-5}$).

The main perspectives of the present work are the following:

- To improve risk calculation by taking into consideration site amplification,
- To extend historical risk estimated either by the assessment of a larger time window or by taking into consideration an occurrence model in the process (*ie.* Poisson's model),
- To perform this process based on the results from the entire logic tree of the PSHA study (not only percentiles), in order to provide PSHA actors with feedback and to let them adjust the weights within the PSHA logic tree (even reconsider some branches) via Bayesian update,
- To continue comparing the risk testing results presented in this report with instrumental and historical seismicity testing in order to build a global framework of evaluation of PSHA results based on observations, exploring a wide range of hazard curves and contributing to assess the likelihood of PSHA logic tree branches and to update their weights.

The computations presented in this report have been performed using a dedicated computer tool that has been developed for this purpose. It is expected to be able to share this tool with a larger scientific community in order to disseminate good practices, consolidate and develop the inherent scientific background and finally improve confidence in seismic hazard assessment and seismic risk evaluations.

5. References

- Drif K, Labbé P, Senfaute G, (2020)**, Sigma2 Work Package #5 « PSHA » - Evaluation of Probabilistic Seismic Hazard Analyses based on macroseismic observations. SIGMA2-2018-D5-016. Rev 1. 2020/11/09
- Drouet S, Ameri G, Le Dortz K, Secanell R, Senfaute G, (2020)**, A Probabilistic seismic hazard map for the metropolitan France, Bulletin of Earthquake Engineering.
- Faccioli E, Cauzzi C (2006)**: Macroseismic intensities for seismic scenarios, estimated from instrumentally based correlations. First European Conference on Earthquake Engineering and Seismology, Geneva.
- Grünthal G (1998)**: European Macroseismic Scale 1998 (EM98). Edition A. LEVRET
- Lagomarsino S, Cattari S (2014)**: *Fragility Functions of Masonry Buildings* in K. Pitilakis et al. (eds.), *SYNER-G: Typology Definition and Fragility Functions for Physical Elements at Seismic Risk, Geotechnical, Geological and Earthquake Engineering 27*, DOI 10.1007/978-94-007-7872-6_5, © Springer Science + Business Media Dordrecht 2014
- Milosevic J, Cattari S, Bento R (2020)**: Definition of fragility curves through nonlinear static analyses: procedure and application to a mixed masonry-RC building block. Bulletin of Earthquake Engineering 2020, 18: 513-545
- Murphy JR, O'Brien LJ (1977)**: The correlation of peak ground acceleration amplitudes with seismic intensity and other physical parameters. Bulletin of the Seismological Society of America. Vol. 67, No. 3.
- Pecker A, Faccioli E, Gurpinar A, Martin C, Renault P (2017)**: An overview of the SIGMA research project, Springer.
- Rosti A, Rota M, Penna A (2020)**: Empirical fragility curves for Italian URM buildings.
- Rota M, Penna A, Magenes G (2010)**: A methodology for deriving analytical fragility curves for masonry buildings based on stochastic nonlinear analyses. J Eng Struct 32:1312–1323.
- Simoes AG, Bento R, Lagomarsino S, Cattari S, Lourenço PB (2019a)**: Fragility functions for tall URM buildings around early 20th century in Lisbon. Part 1: method description and application to a case study. International Journal of Architectural Heritage (submitted)
- Simoes AG, Bento R, Lagomarsino S, Cattari S, Lourenço PB (2019b)**: Fragility functions for tall URM buildings around early 20th century in Lisbon. Part 2: application to different classes of buildings. International Journal of Architectural Heritage (submitted)
- Sopranzi U (2018)**: Seismic risk evaluation with PSHA methods in southeastern France and northwestern Italy – Master of Environmental Engineering for Sustainability, Politecnico di Milano.

APPENDIX 1

Grid of points selected for risk calculation within each domain



1. Alpes + Bâle
2. Bloc armoricain / domnoyéen / mancellien
3. Graben du Rhin
4. Manche/mer du Nord
5. Massif central / Bresse / Jura
6. Méditerranée
7. Plateforme stable occidentale
8. Pyrénées



Point nb.	Domain number
1	1
2	
3	
4	
5	
6	
7	
8	

Long. (ESHM20)	Lat. (ESHM20)
6.78	46.00
5.88	45.30
6.78	45.40
6.28	45.00
6.48	44.50
6.28	43.90
7.28	43.90
6.18	45.70

Point nb.	Domain number	Long. (ESHM20)	Lat. (ESHM20)
9	2	-1.62	49.40
10		-1.22	48.80
11		-0.12	48.80
12		-4.42	48.50
13		-3.22	48.50
14		-3.72	48.00
15		-2.42	48.10
16		-0.72	48.10
17		-2.22	47.40
18		-1.02	47.40
19		0.28	47.40
20		-1.82	46.80
21		-0.62	46.80
22		0.98	46.80
23		2.28	46.80
24		-0.82	46.00
25		0.38	46.00
26	1.58	46.00	
27	-0.22	45.50	
28	3	7.48	48.70
29		6.58	48.00
30		7.48	48.00
31		6.28	47.70
32	4	1.68	50.90
33		2.38	51.00
34		2.28	50.60
35		2.98	50.40
36		3.68	50.30

Point nb.	Domain number	Long. (ESHM20)	Lat. (ESHM20)
37	5	6.48	47.40
38		4.68	46.80
39		5.78	46.70
40		2.98	46.00
41		4.18	46.00
42		5.28	46.00
43		6.08	46.00
44		0.98	45.40
45		2.08	45.40
46		3.58	45.40
47		4.68	45.40
48		1.38	44.90
49		2.58	45.00
50		4.08	45.00
51		4.98	45.00
52		1.38	44.30
53		2.18	44.40
54		3.38	44.40
55		1.68	43.80
56	2.88	43.90	
57	1.88	43.40	
58	6	4.58	44.40
59		5.58	44.50
60		5.18	44.10
61		4.08	43.80
62		4.98	43.50
63		2.88	43.20
64		5.68	43.30
65		6.68	43.50
66		3.58	43.50

Point nb.	Domain number	Long. (ESHM20)	Lat. (ESHM20)
67	7	1.68	50.30
68		1.08	49.80
69		1.98	49.90
70		3.28	49.80
71		4.68	49.80
72		0.28	49.40
73		1.68	49.40
74		2.98	49.40
75		4.38	49.30
76		5.58	49.30
77		1.38	48.70
78		2.38	48.70
79		3.88	48.70
80		4.98	48.70
81		6.28	48.80
82		0.98	48.00
83		2.08	48.00
84		3.48	48.10
85		4.68	48.00
86		5.58	48.10
87		1.48	47.40
88		2.98	47.40
89		4.18	47.40
90		5.38	47.40
91		3.48	46.90
92		-1.12	44.90
93		-0.02	44.90
94		-1.22	44.30
95		-0.32	44.40
96		0.58	44.40
97		0.28	43.80
98		-1.02	45.30
99		-0.82	44.00

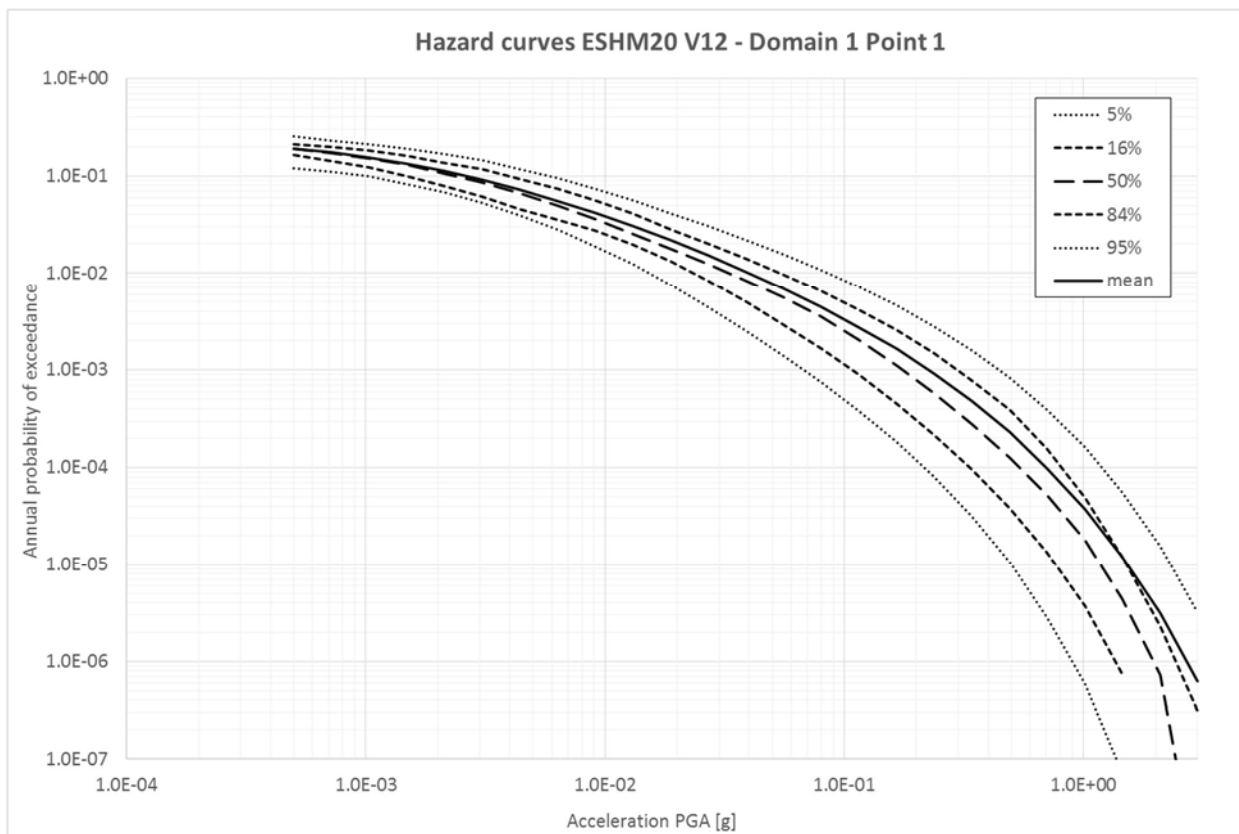
Point nb.	Domain number	Long. (ESHM20)	Lat. (ESHM20)
100	8	-1.32	43.70
101		-0.82	43.70
102		-0.32	43.50
103		-1.52	43.40
104		-1.12	43.30
105		-0.62	42.90
106		-0.02	42.80
107		0.28	43.40
108		0.48	42.80
109		0.58	43.10
110		1.48	43.10
111		1.48	42.70
112		1.98	43.00
113		2.58	42.80
114		2.48	42.50
115	2.88	42.60	

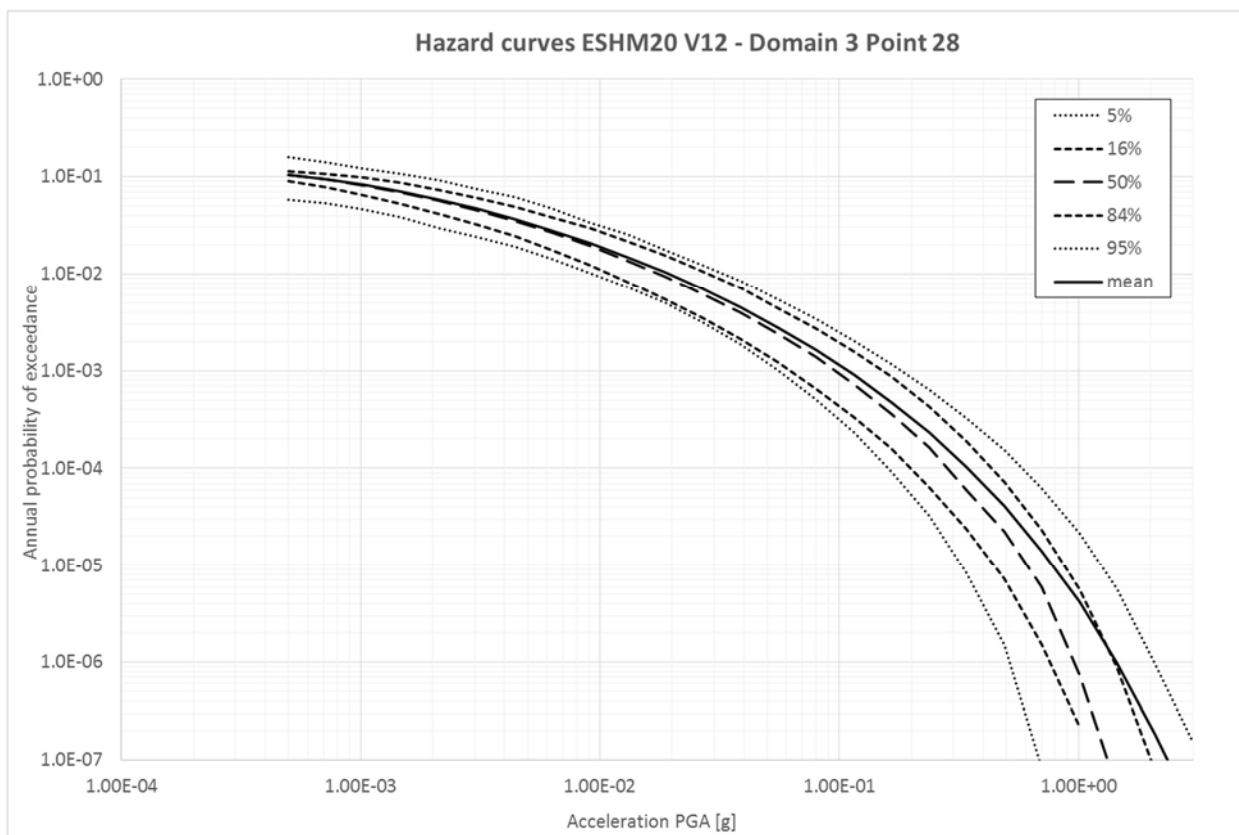
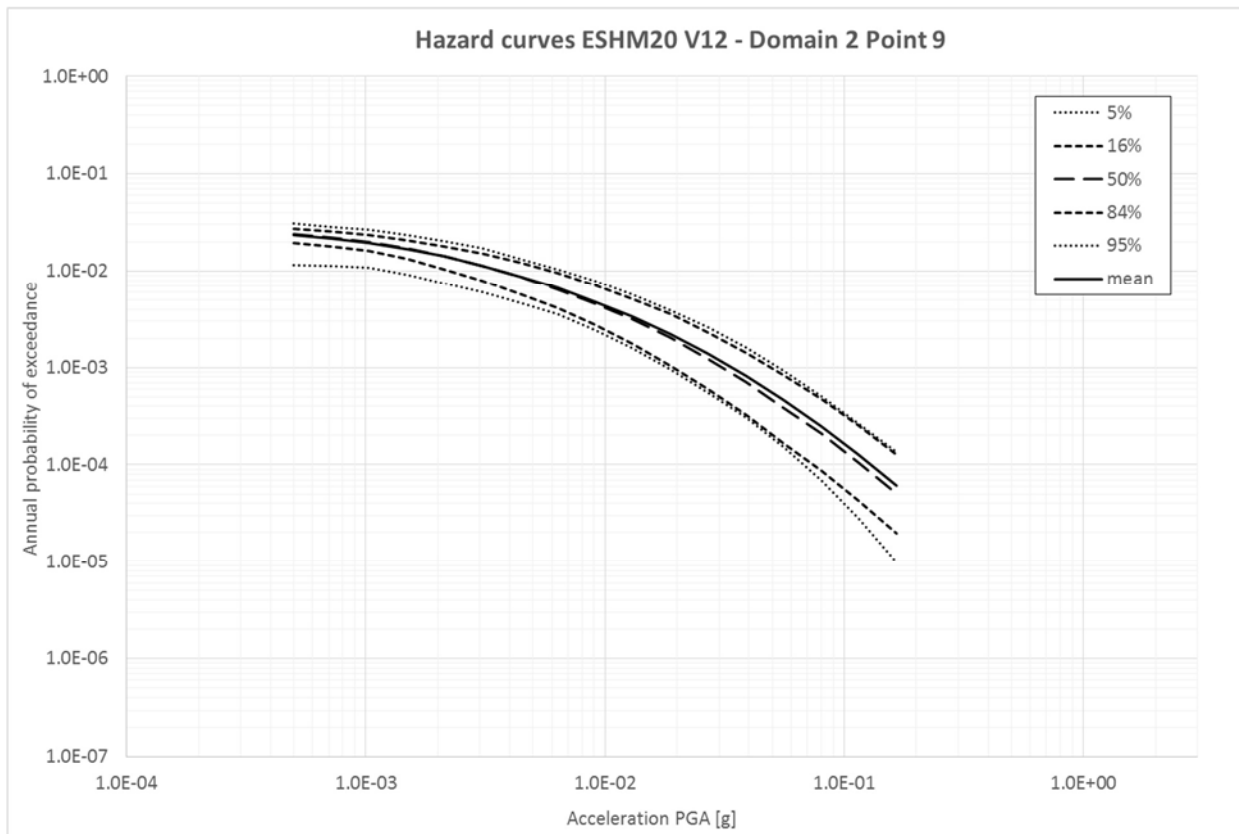
APPENDIX 2

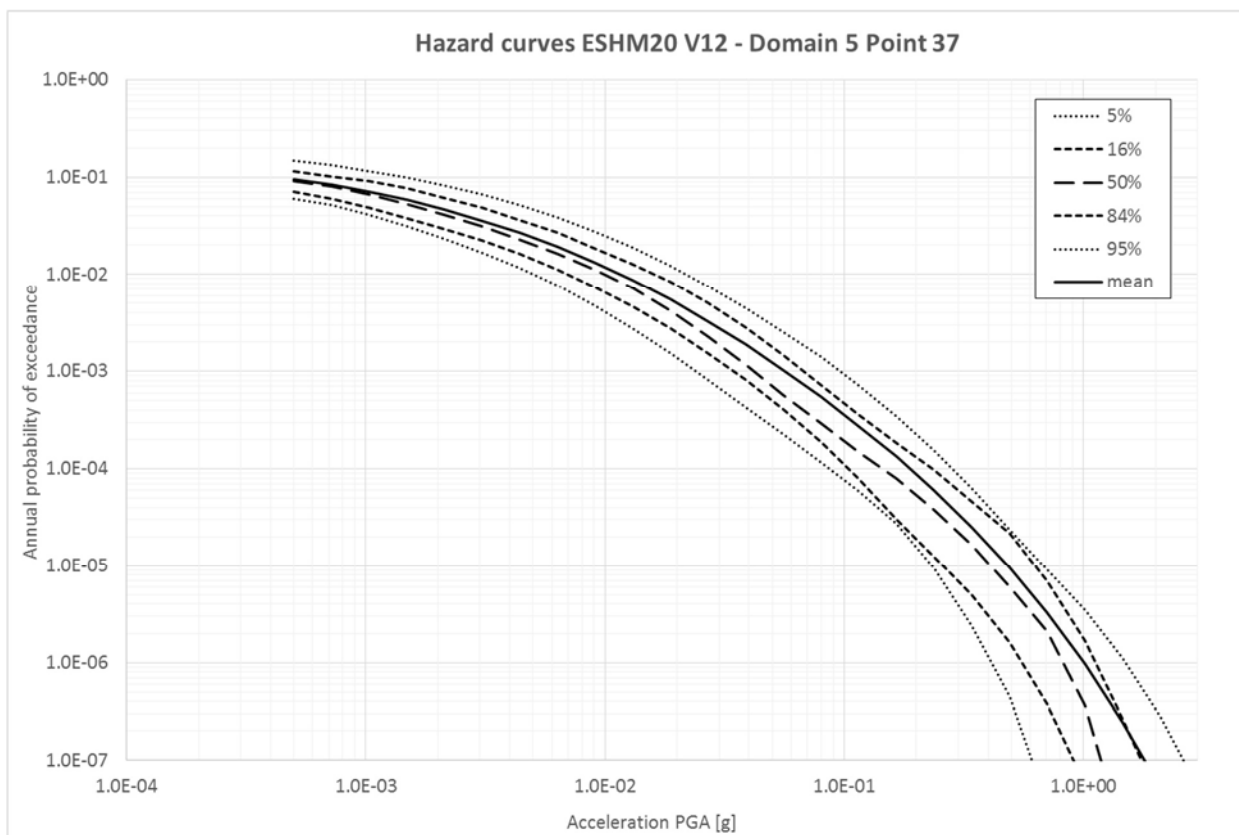
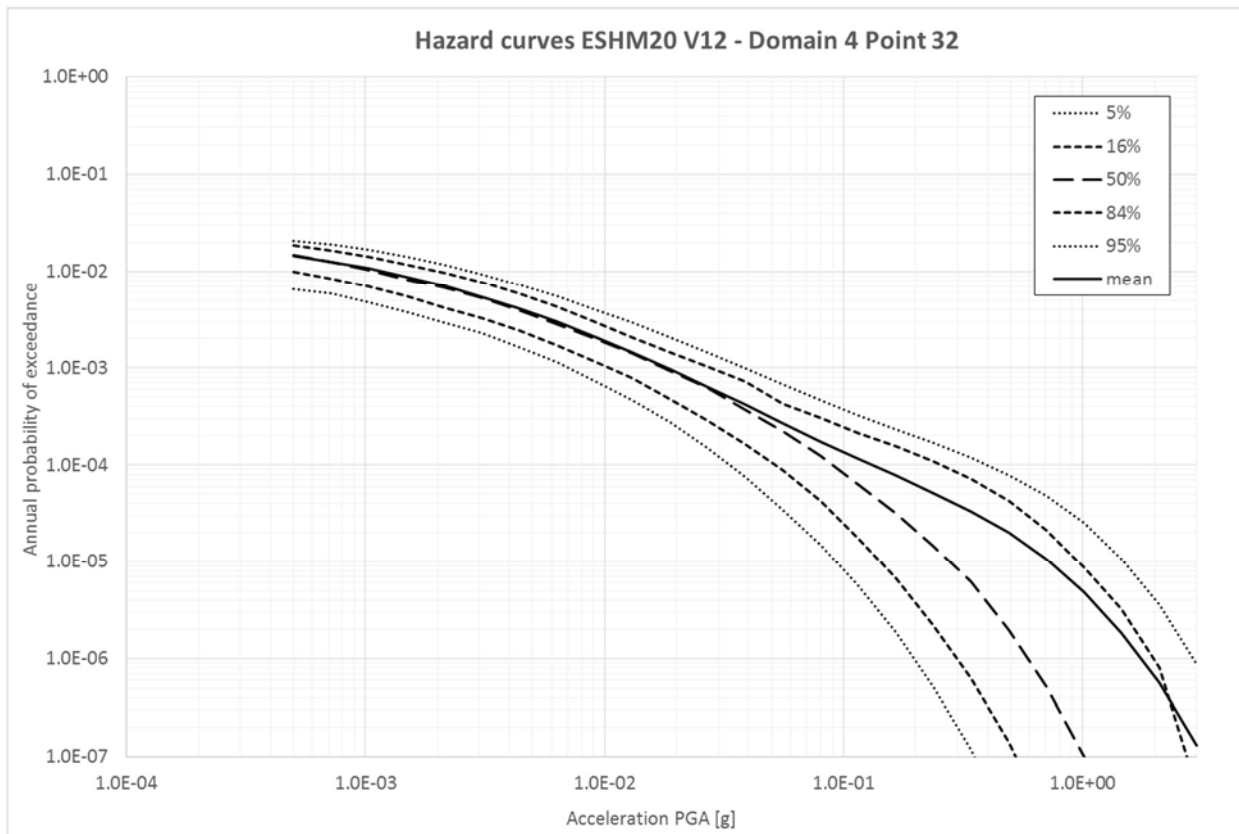
Hazard curves from ESHM20

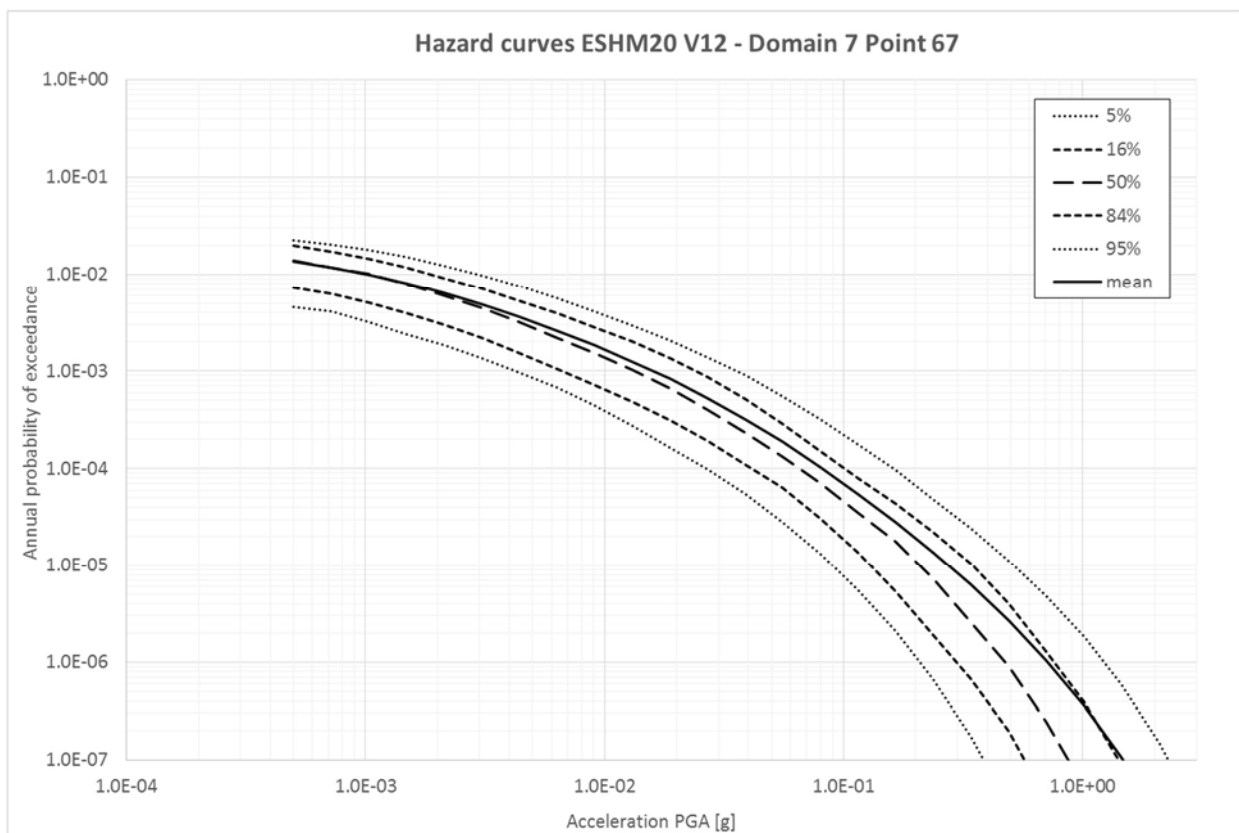
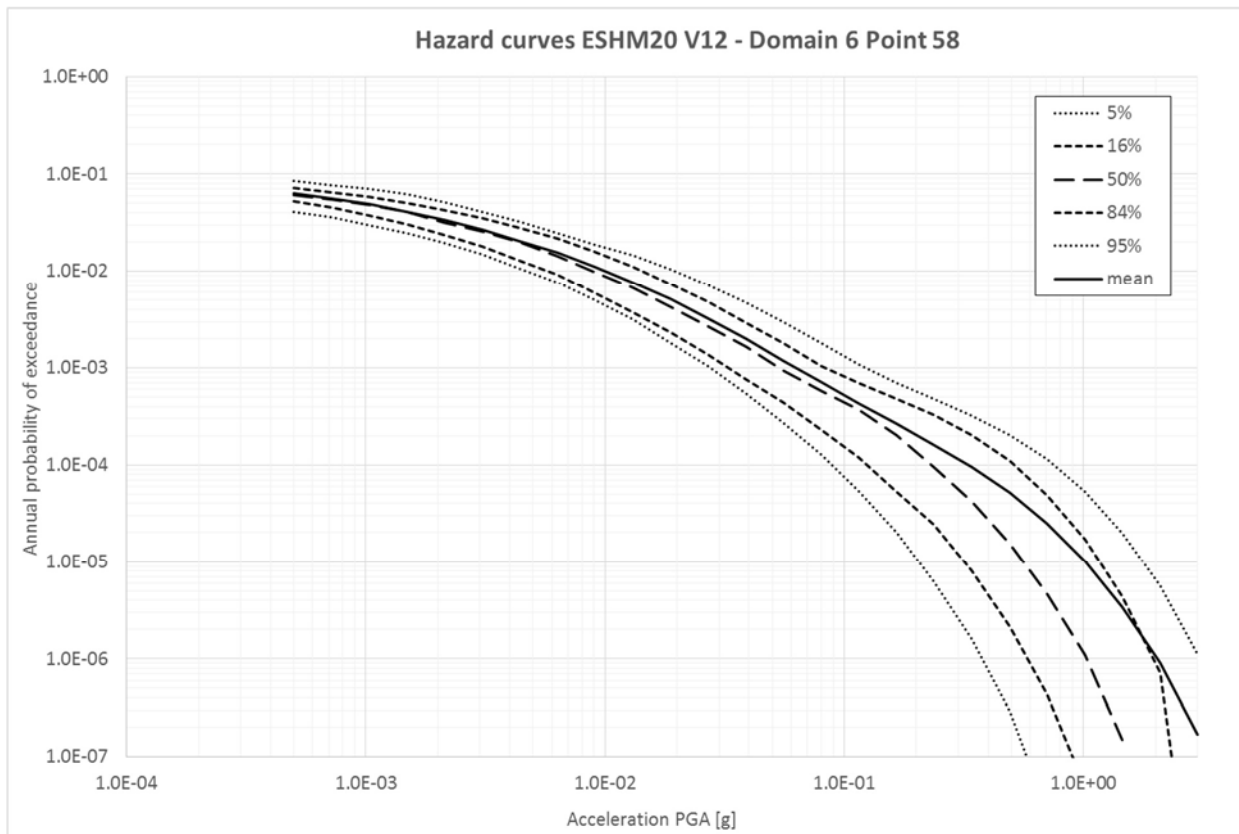
Hazard curves from ESHM20 (V12) are displayed hereafter for 5%, 16%, 50%, 84%, 95% percentiles and the mean, and for the first point of each geographic domain.

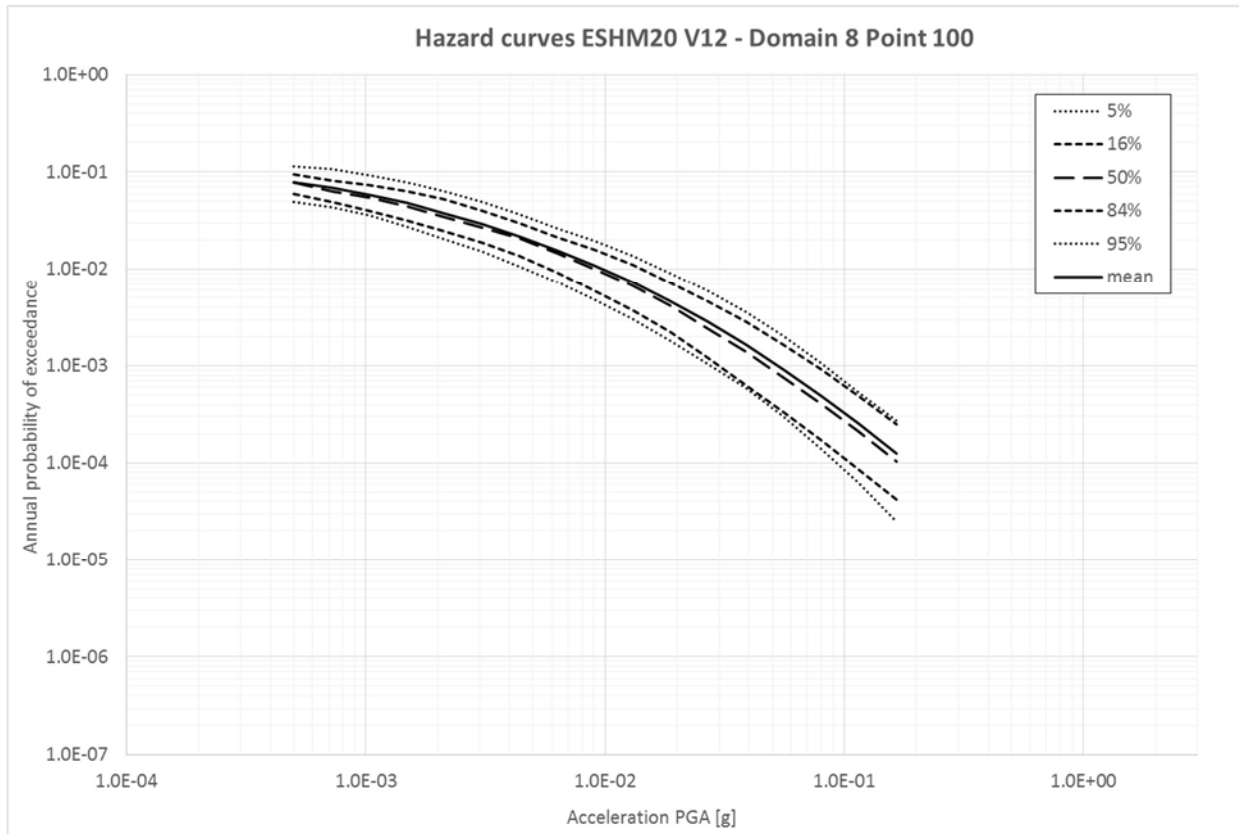
Point nb.	Domain number	Long. (ESHM20)	Lat. (ESHM20)
1	1	6.78	46.00
9	2	-1.62	49.4
28	3	7.48	48.7
32	4	1.68	50.9
37	5	6.48	47.4
58	6	4.58	44.4
67	7	1.68	50.3
100	8	-1.32	43.7











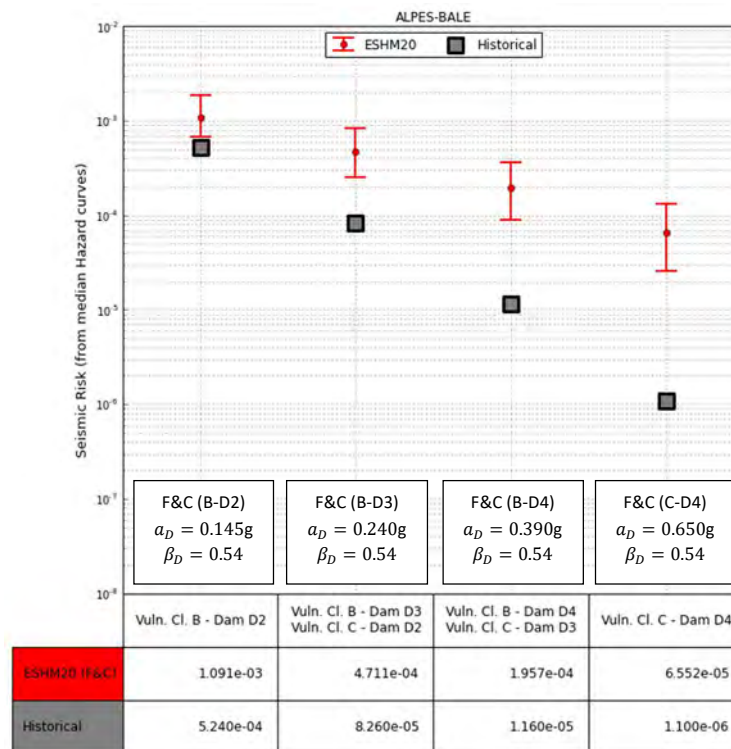
APPENDIX 3

Comparison between ESHM20 risk and historical risk

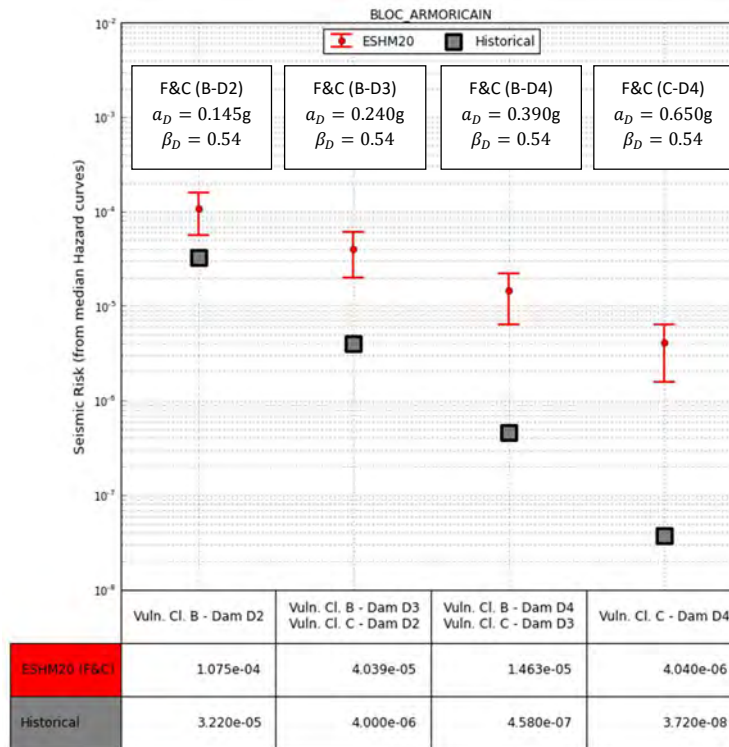
Results by geographic domains, 50% percentile of hazard curves, variability among the different points in each domain

Figures in this appendix provide computed risks exclusively from median hazard curves. The error bars plotted in the graphs highlight the variability in the value of calculated risk coming from all considered points within a geographic zone. Figures are organized with respect to geographic zones.

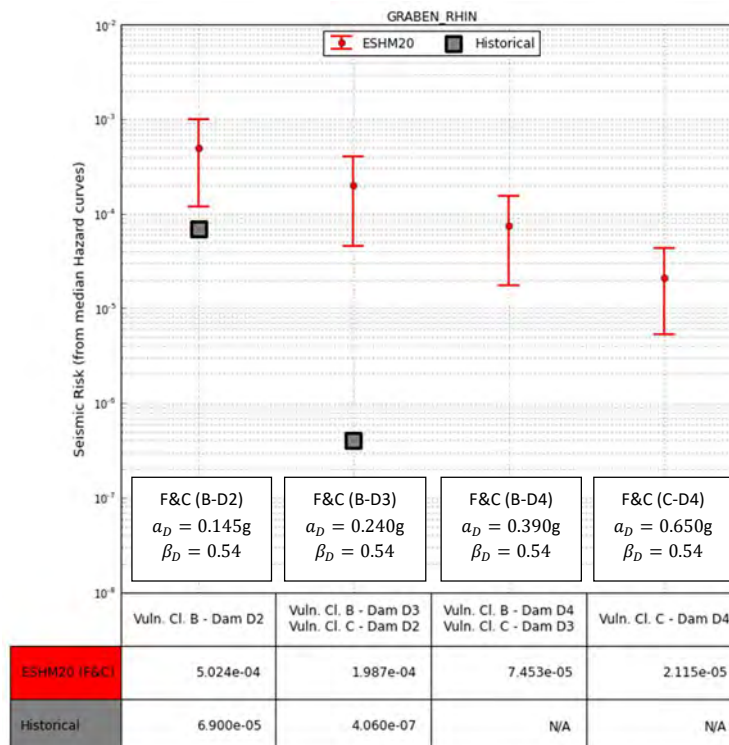
Appendix 4 presents the same results but figures are organized with respect to vulnerability class and damage level.



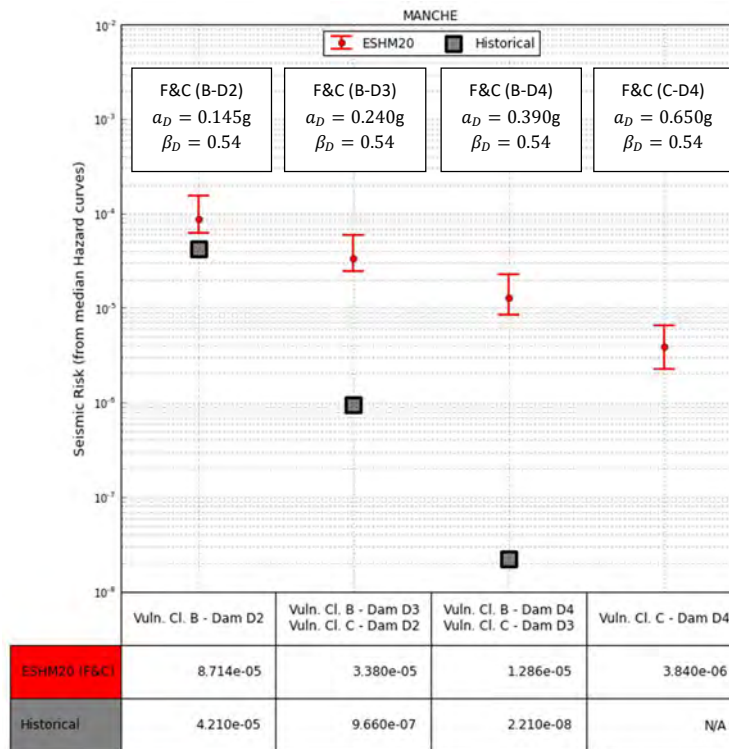
Seismic risk (median hazard curves) – Alpes – Bâles



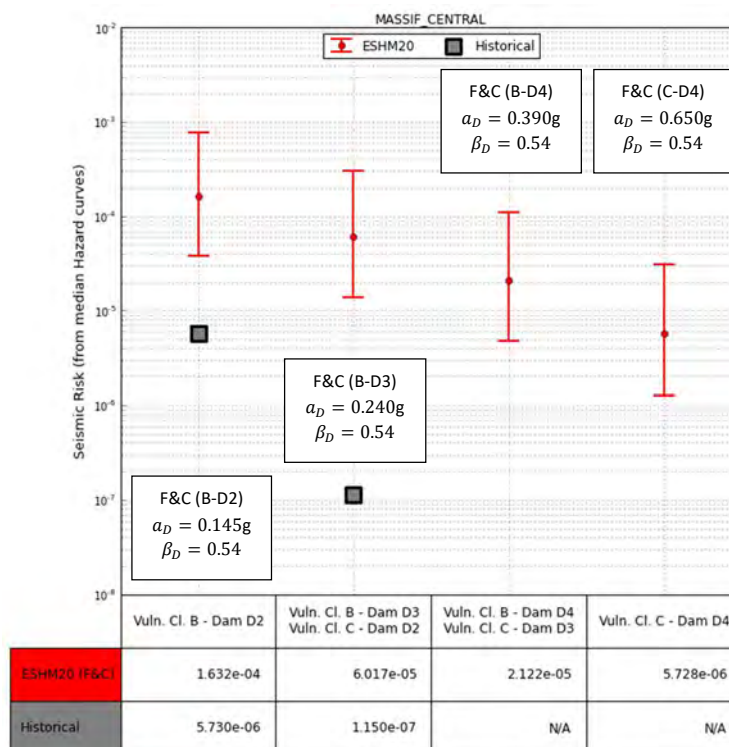
Seismic risk (median hazard curves) – Bloc Armoricaín



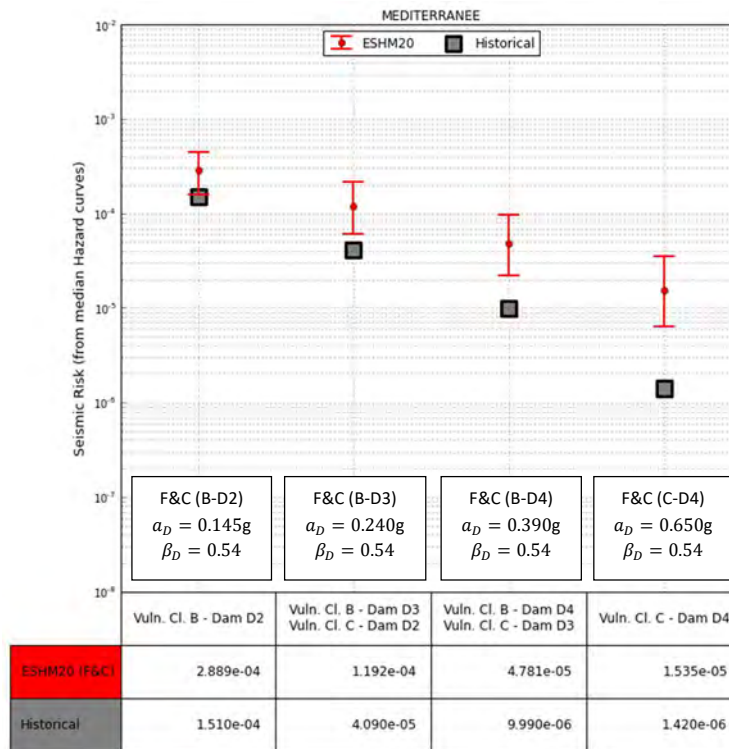
Seismic risk (median hazard curves) – Graben du Rhin



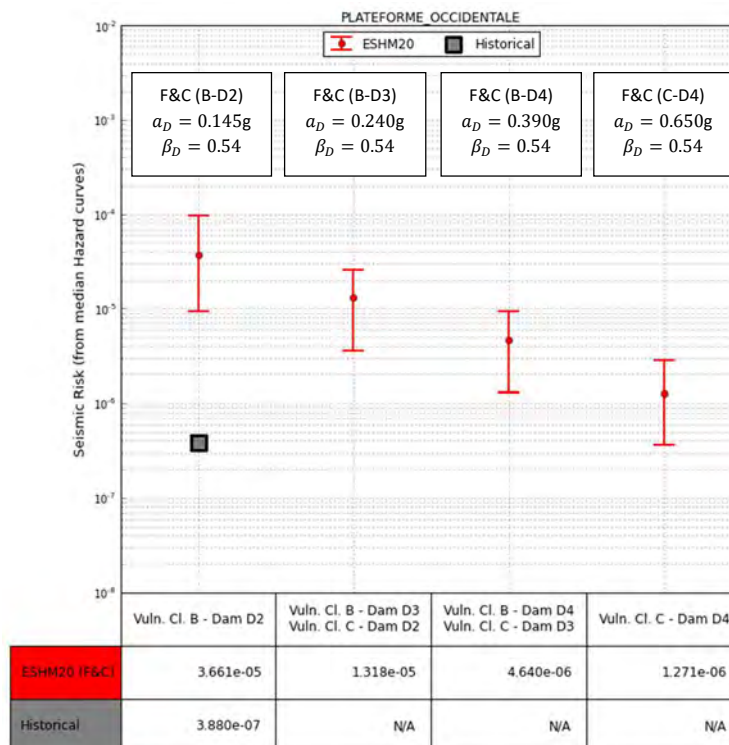
Seismic risk (median hazard curves) – Manche



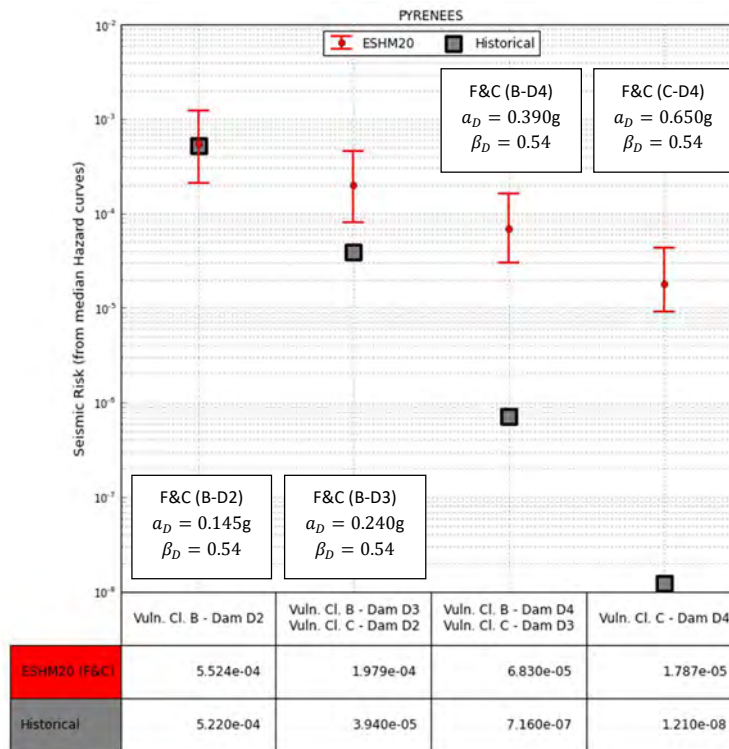
Seismic risk (median hazard curves) – Massif Central



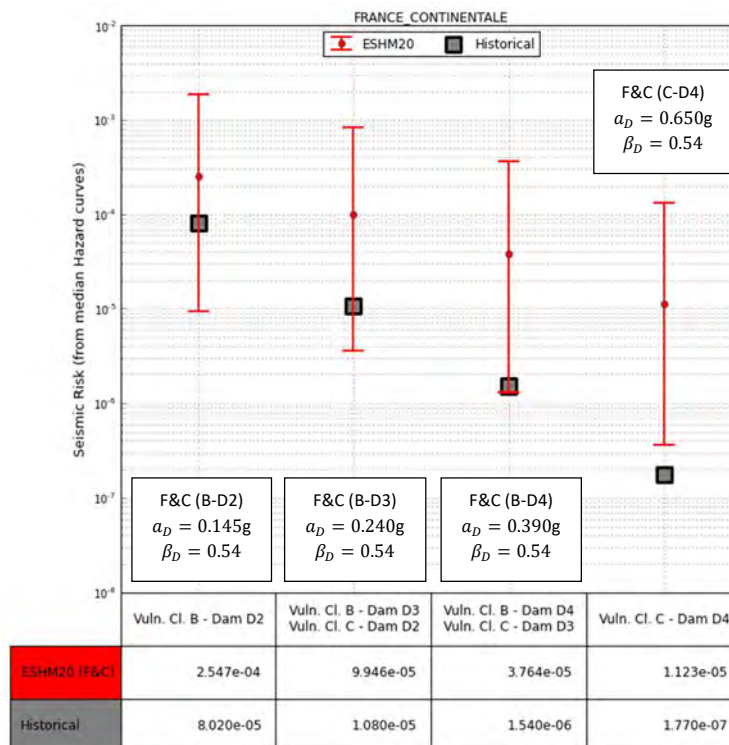
Seismic risk (median hazard curves) – Méditerranée



Seismic risk (median hazard curves) – Plateforme Occidentale



Seismic risk (median hazard curves) – Pyrénées



Seismic risk (median hazard curves) – France Continentale

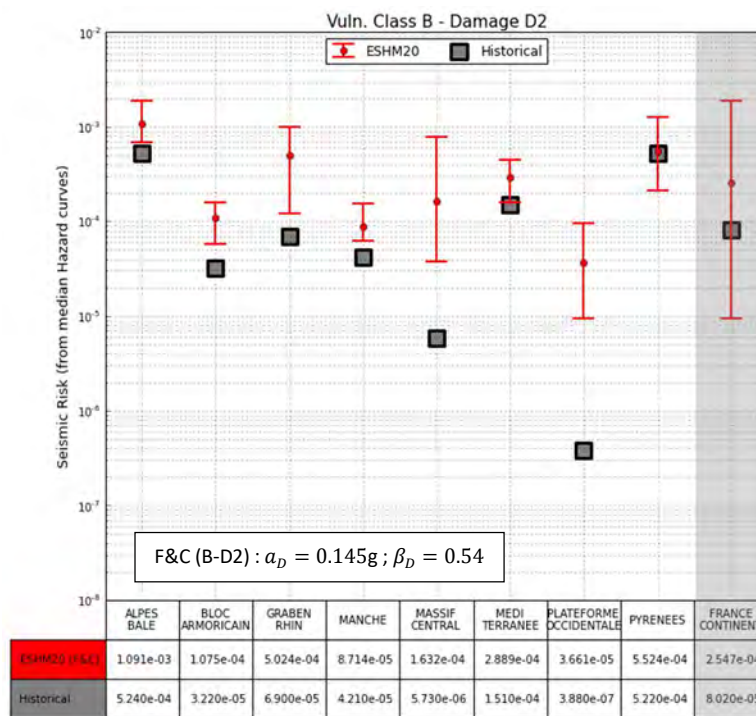
APPENDIX 4

Comparison between ESHM20 risk and historical risk

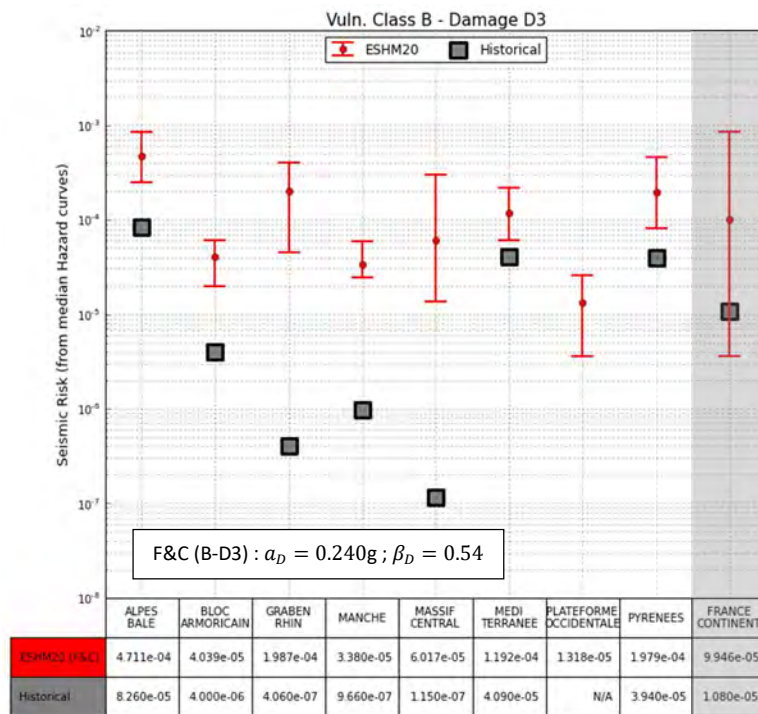
Results by damage degree and vulnerability class, 50% percentile of hazard curves, variability among the different points in each domain

Figures in this appendix provide computed risks exclusively from median hazard curves. The error bars plotted in the graphs highlight the variability in the value of calculated risk coming from all considered points within a geographic zone. Figures are organized with respect to vulnerability class and damage level.

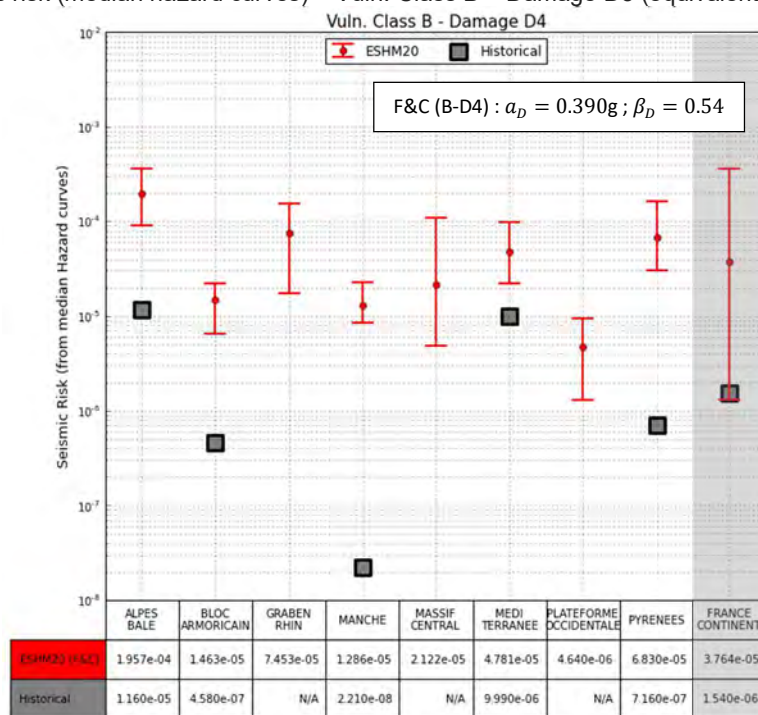
Appendix 3 presents the same results but figures are organized with respect to geographic domains.



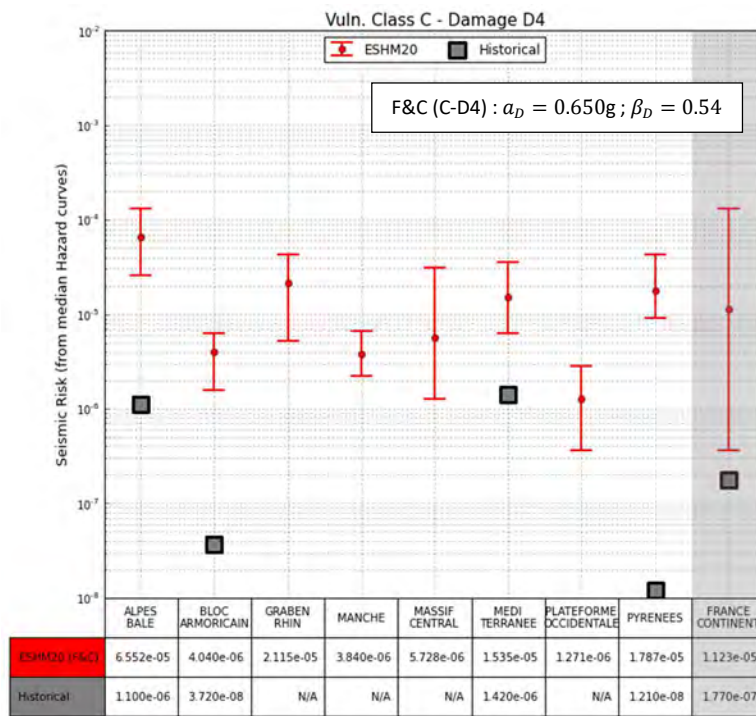
Seismic risk (median hazard curves) – Vuln. Class B – Damage D2



Seismic risk (median hazard curves) – Vuln. Class B – Damage D3 (equivalent to C-D2)



Seismic risk (median hazard curves) – Vuln. Class B – Damage D4 (Equivalent to C-D3)



Seismic risk (median hazard curves) – Vuln. Class C – Damage D4

APPENDIX 5

Seismic risk for each geographic domain

Seismic risk for each domain (Mean value from the points in the domain)

Vulnerability Class B and C – Damage grade D2

ESHM20 V8 and V12 – 5% - 16% - 50% - 84% - 95% percentiles

Fragility curves: Lagomarsino & Cattari (2014)

Conversion equations: Murphy & O'Brien (1977), Faccioli & Cauzzi (2006)

VULNERABILITY CLASS B		D2					
Murphy & O'Brien (1977)	V12-0.05	V12-0.16	V12-0.50	V12-0.84	V12-0.95	Historical	
ALPES + BALE	4.81E-04	9.04E-04	1.64E-03	3.05E-03	4.97E-03	5.24E-04	
BLOC ARMORICAIN	5.67E-05	8.01E-05	1.77E-04	3.66E-04	4.95E-04	3.22E-05	
GRABEN DU RHIN	2.94E-04	4.14E-04	7.92E-04	1.59E-03	2.04E-03	6.90E-05	
MANCHE / MER DU NORD	3.71E-05	6.87E-05	1.42E-04	3.34E-04	5.94E-04	4.21E-05	
MASSIF CENTRAL	6.46E-05	1.16E-04	2.66E-04	5.23E-04	8.13E-04	5.73E-06	
MEDITERRANEE	1.55E-04	2.16E-04	4.49E-04	8.48E-04	1.18E-03	1.51E-04	
PLATEFORME OCCIDENTAL	1.23E-05	2.48E-05	6.22E-05	1.27E-04	2.40E-04	3.88E-07	
PYRENEES	3.03E-04	4.26E-04	9.20E-04	1.89E-03	2.47E-03	5.22E-04	
FRANCE CONTINENTALE	1.24E-04	1.98E-04	4.07E-04	8.03E-04	1.18E-03	8.02E-05	
VULNERABILITY CLASS B		D2					
Faccioli & Cauzzi (2006)	V12-0.05	V12-0.16	V12-0.50	V12-0.84	V12-0.95	Historical	
ALPES + BALE	2.82E-04	5.68E-04	1.09E-03	2.11E-03	3.58E-03	5.24E-04	
BLOC ARMORICAIN	3.02E-05	4.57E-05	1.08E-04	2.34E-04	3.29E-04	3.22E-05	
GRABEN DU RHIN	1.68E-04	2.52E-04	5.02E-04	1.06E-03	1.42E-03	6.90E-05	
MANCHE / MER DU NORD	2.15E-05	3.93E-05	8.71E-05	2.28E-04	4.08E-04	4.21E-05	
MASSIF CENTRAL	3.43E-05	6.53E-05	1.63E-04	3.43E-04	5.51E-04	5.73E-06	
MEDITERRANEE	9.02E-05	1.33E-04	2.89E-04	5.68E-04	7.89E-04	1.51E-04	
PLATEFORME OCCIDENTAL	6.55E-06	1.37E-05	3.66E-05	7.86E-05	1.55E-04	3.88E-07	
PYRENEES	1.60E-04	2.40E-04	5.52E-04	1.21E-03	1.62E-03	5.22E-04	
FRANCE CONTINENTALE	6.88E-05	1.17E-04	2.55E-04	5.30E-04	8.03E-04	8.02E-05	
VULNERABILITY CLASS C		D2					
Murphy & O'Brien (1977)	V12-0.05	V12-0.16	V12-0.50	V12-0.84	V12-0.95	Historical	
ALPES + BALE	1.63E-04	3.38E-04	6.77E-04	1.36E-03	2.36E-03	8.26E-05	
BLOC ARMORICAIN	1.63E-05	2.59E-05	6.32E-05	1.42E-04	2.05E-04	4.00E-06	
GRABEN DU RHIN	9.28E-05	1.46E-04	3.01E-04	6.55E-04	9.18E-04	4.06E-07	
MANCHE / MER DU NORD	1.21E-05	2.19E-05	5.19E-05	1.49E-04	2.65E-04	9.66E-07	
MASSIF CENTRAL	1.87E-05	3.65E-05	9.51E-05	2.13E-04	3.53E-04	1.15E-07	
MEDITERRANEE	5.14E-05	7.86E-05	1.76E-04	3.59E-04	5.08E-04	4.09E-05	
PLATEFORME OCCIDENTAL	3.57E-06	7.66E-06	2.12E-05	4.79E-05	9.66E-05	7.81E-09	
PYRENEES	8.54E-05	1.35E-04	3.19E-04	7.21E-04	9.97E-04	3.94E-05	
FRANCE CONTINENTALE	3.81E-05	6.76E-05	1.52E-04	3.28E-04	5.12E-04	1.08E-05	
VULNERABILITY CLASS C		D2					
Faccioli & Cauzzi (2006)	V12-0.05	V12-0.16	V12-0.50	V12-0.84	V12-0.95	Historical	
ALPES + BALE	9.80E-05	2.17E-04	4.62E-04	9.71E-04	1.75E-03	8.26E-05	
BLOC ARMORICAIN	8.59E-06	1.51E-05	3.95E-05	9.35E-05	1.41E-04	4.00E-06	
GRABEN DU RHIN	5.18E-05	8.90E-05	1.95E-04	4.45E-04	6.65E-04	4.06E-07	
MANCHE / MER DU NORD	7.03E-06	1.23E-05	3.31E-05	1.08E-04	1.91E-04	9.66E-07	
MASSIF CENTRAL	1.00E-05	2.08E-05	5.88E-05	1.46E-04	2.52E-04	1.15E-07	
MEDITERRANEE	3.05E-05	4.96E-05	1.17E-04	2.51E-04	3.63E-04	4.09E-05	
PLATEFORME OCCIDENTAL	1.92E-06	4.33E-06	1.29E-05	3.17E-05	6.58E-05	7.81E-09	
PYRENEES	4.40E-05	7.72E-05	1.93E-04	4.65E-04	6.71E-04	3.94E-05	
FRANCE CONTINENTALE	2.12E-05	4.09E-05	9.74E-05	2.23E-04	3.63E-04	1.08E-05	

Seismic risk for each domain (Mean value from the points in the domain)
Vulnerability Class B and C - Damage grade D3
ESHM20 – 5% - 16% - 50% - 84% - 95% percentiles
Fragility curves: Lagomarsino & Cattari (2014)
Conversion equations: Murphy & O'Brien (1977), Faccioli & Cauzzi (2006)

VULNERABILITY CLASS B		D3				
Murphy & O'Brien (1977)	V12-0.05	V12-0.16	V12-0.50	V12-0.84	V12-0.95	Historical
ALPES + BALE	1.65E-04	3.44E-04	6.89E-04	1.38E-03	2.40E-03	8.26E-05
BLOC ARMORICAIN	1.66E-05	2.63E-05	6.42E-05	1.44E-04	2.09E-04	4.00E-06
GRABEN DU RHIN	9.43E-05	1.48E-04	3.06E-04	6.66E-04	9.34E-04	4.06E-07
MANCHE / MER DU NORD	1.23E-05	2.22E-05	5.27E-05	1.51E-04	2.69E-04	9.66E-07
MASSIF CENTRAL	1.90E-05	3.71E-05	9.67E-05	2.17E-04	3.59E-04	1.15E-07
MEDITERRANEE	5.23E-05	7.99E-05	1.79E-04	3.65E-04	5.16E-04	4.09E-05
PLATEFORME OCCIDENTAL	3.63E-06	7.78E-06	2.15E-05	4.87E-05	9.82E-05	7.81E-09
PYRENEES	8.67E-05	1.37E-04	3.24E-04	7.34E-04	1.01E-03	3.94E-05
FRANCE CONTINENTALE	3.87E-05	6.87E-05	1.54E-04	3.34E-04	5.21E-04	1.08E-05
VULNERABILITY CLASS B		D3				
Faccioli & Cauzzi (2006)	V12-0.05	V12-0.16	V12-0.50	V12-0.84	V12-0.95	Historical
ALPES + BALE	1.00E-04	2.21E-04	4.71E-04	9.88E-04	1.78E-03	8.26E-05
BLOC ARMORICAIN	8.84E-06	1.55E-05	4.04E-05	9.55E-05	1.43E-04	4.00E-06
GRABEN DU RHIN	5.32E-05	9.11E-05	1.99E-04	4.54E-04	6.76E-04	4.06E-07
MANCHE / MER DU NORD	7.21E-06	1.27E-05	3.38E-05	1.10E-04	1.94E-04	9.66E-07
MASSIF CENTRAL	1.03E-05	2.13E-05	6.02E-05	1.49E-04	2.56E-04	1.15E-07
MEDITERRANEE	3.12E-05	5.07E-05	1.19E-04	2.55E-04	3.69E-04	4.09E-05
PLATEFORME OCCIDENTAL	1.98E-06	4.45E-06	1.32E-05	3.23E-05	6.70E-05	7.81E-09
PYRENEES	4.53E-05	7.92E-05	1.98E-04	4.75E-04	6.84E-04	3.94E-05
FRANCE CONTINENTALE	2.18E-05	4.18E-05	9.95E-05	2.28E-04	3.69E-04	1.08E-05
VULNERABILITY CLASS C		D3				
Murphy & O'Brien (1977)	V12-0.05	V12-0.16	V12-0.50	V12-0.84	V12-0.95	Historical
ALPES + BALE	4.79E-05	1.10E-04	2.49E-04	5.49E-04	1.02E-03	1.16E-05
BLOC ARMORICAIN	3.77E-06	7.17E-06	1.97E-05	4.89E-05	7.73E-05	4.58E-07
GRABEN DU RHIN	2.33E-05	4.31E-05	9.89E-05	2.37E-04	3.81E-04	2.39E-09
MANCHE / MER DU NORD	3.24E-06	5.77E-06	1.70E-05	6.45E-05	1.13E-04	2.21E-08
MASSIF CENTRAL	4.45E-06	9.72E-06	2.90E-05	7.95E-05	1.45E-04	2.31E-09
MEDITERRANEE	1.47E-05	2.49E-05	6.17E-05	1.40E-04	2.13E-04	9.99E-06
PLATEFORME OCCIDENTAL	8.58E-07	2.03E-06	6.34E-06	1.69E-05	3.63E-05	1.56E-10
PYRENEES	1.91E-05	3.63E-05	9.42E-05	2.37E-04	3.61E-04	7.16E-07
FRANCE CONTINENTALE	9.77E-06	1.99E-05	4.98E-05	1.21E-04	2.06E-04	1.56E-06
VULNERABILITY CLASS C		D3				
Faccioli & Cauzzi (2006)	V12-0.05	V12-0.16	V12-0.50	V12-0.84	V12-0.95	Historical
ALPES + BALE	3.14E-05	7.57E-05	1.82E-04	4.19E-04	8.06E-04	1.16E-05
BLOC ARMORICAIN	2.11E-06	4.54E-06	1.33E-05	3.47E-05	5.75E-05	4.58E-07
GRABEN DU RHIN	1.36E-05	2.80E-05	6.81E-05	1.71E-04	2.95E-04	2.39E-09
MANCHE / MER DU NORD	1.98E-06	3.55E-06	1.18E-05	5.12E-05	8.90E-05	2.21E-08
MASSIF CENTRAL	2.56E-06	6.01E-06	1.92E-05	5.87E-05	1.12E-04	2.31E-09
MEDITERRANEE	9.43E-06	1.68E-05	4.42E-05	1.06E-04	1.68E-04	9.99E-06
PLATEFORME OCCIDENTAL	4.95E-07	1.25E-06	4.20E-06	1.22E-05	2.71E-05	1.56E-10
PYRENEES	1.04E-05	2.26E-05	6.16E-05	1.63E-04	2.63E-04	7.16E-07
FRANCE CONTINENTALE	5.89E-06	1.31E-05	3.45E-05	8.83E-05	1.58E-04	1.56E-06

Seismic risk for each domain (Mean value from the points in the domain)
Vulnerability Class B and C - Damage grade D4
ESHM20 – 5% - 16% - 50% - 84% - 95% percentiles
Fragility curves: Lagomarsino & Cattari (2014)
Conversion equations: Murphy & O'Brien (1977), Faccioli & Cauzzi (2006)

VULNERABILITY CLASS B	D4					
Murphy & O'Brien (1977)	V12-0.05	V12-0.16	V12-0.50	V12-0.84	V12-0.95	Historical
ALPES + BALE	5.31E-05	1.21E-04	2.68E-04	5.86E-04	1.09E-03	1.16E-05
BLOC ARMORICAIN	4.34E-06	8.02E-06	2.17E-05	5.32E-05	8.32E-05	4.58E-07
GRABEN DU RHIN	2.65E-05	4.78E-05	1.08E-04	2.56E-04	4.06E-04	2.39E-09
MANCHE / MER DU NORD	3.65E-06	6.50E-06	1.86E-05	6.82E-05	1.20E-04	2.21E-08
MASSIF CENTRAL	5.09E-06	1.09E-05	3.20E-05	8.56E-05	1.54E-04	2.31E-09
MEDITERRANEE	1.63E-05	2.73E-05	6.69E-05	1.50E-04	2.26E-04	9.99E-06
PLATEFORME OCCIDENTAL	9.81E-07	2.28E-06	7.02E-06	1.83E-05	3.90E-05	1.56E-10
PYRENEES	2.21E-05	4.07E-05	1.04E-04	2.59E-04	3.90E-04	7.16E-07
FRANCE CONTINENTALE	1.11E-05	2.21E-05	5.45E-05	1.30E-04	2.20E-04	1.54E-06
VULNERABILITY CLASS B	D4					
Faccioli & Cauzzi (2006)	V12-0.05	V12-0.16	V12-0.50	V12-0.84	V12-0.95	Historical
ALPES + BALE	3.48E-05	8.29E-05	1.96E-04	4.47E-04	8.52E-04	1.16E-05
BLOC ARMORICAIN	2.44E-06	5.07E-06	1.46E-05	3.76E-05	6.16E-05	4.58E-07
GRABEN DU RHIN	1.56E-05	3.11E-05	7.45E-05	1.85E-04	3.13E-04	2.39E-09
MANCHE / MER DU NORD	2.24E-06	4.00E-06	1.29E-05	5.40E-05	9.39E-05	2.21E-08
MASSIF CENTRAL	2.94E-06	6.76E-06	2.12E-05	6.30E-05	1.19E-04	2.31E-09
MEDITERRANEE	1.05E-05	1.85E-05	4.78E-05	1.13E-04	1.77E-04	9.99E-06
PLATEFORME OCCIDENTAL	5.68E-07	1.41E-06	4.64E-06	1.32E-05	2.90E-05	1.56E-10
PYRENEES	1.21E-05	2.54E-05	6.83E-05	1.78E-04	2.83E-04	7.16E-07
FRANCE CONTINENTALE	6.67E-06	1.45E-05	3.76E-05	9.50E-05	1.68E-04	1.54E-06
VULNERABILITY CLASS C	D4					
Murphy & O'Brien (1977)	V12-0.05	V12-0.16	V12-0.50	V12-0.84	V12-0.95	Historical
ALPES + BALE	1.32E-05	3.28E-05	8.41E-05	2.06E-04	4.13E-04	1.10E-06
BLOC ARMORICAIN	7.88E-07	1.84E-06	5.64E-06	1.55E-05	2.76E-05	3.72E-08
GRABEN DU RHIN	5.15E-06	1.15E-05	2.91E-05	7.71E-05	1.45E-04	1.37E-11
MANCHE / MER DU NORD	7.66E-07	1.44E-06	5.17E-06	2.67E-05	4.79E-05	4.61E-10
MASSIF CENTRAL	9.64E-07	2.41E-06	8.08E-06	2.74E-05	5.64E-05	4.27E-11
MEDITERRANEE	3.89E-06	7.19E-06	2.00E-05	5.20E-05	8.77E-05	1.42E-06
PLATEFORME OCCIDENTAL	1.87E-07	5.01E-07	1.78E-06	5.64E-06	1.32E-05	2.89E-12
PYRENEES	3.85E-06	9.06E-06	2.56E-05	7.10E-05	1.24E-04	1.21E-08
FRANCE CONTINENTALE	2.33E-06	5.45E-06	1.51E-05	4.13E-05	7.86E-05	1.77E-07
VULNERABILITY CLASS C	D4					
Faccioli & Cauzzi (2006)	V12-0.05	V12-0.16	V12-0.50	V12-0.84	V12-0.95	Historical
ALPES + BALE	9.28E-06	2.40E-05	6.55E-05	1.67E-04	3.46E-04	1.10E-06
BLOC ARMORICAIN	4.65E-07	1.24E-06	4.04E-06	1.17E-05	2.21E-05	3.72E-08
GRABEN DU RHIN	3.13E-06	7.91E-06	2.12E-05	5.90E-05	1.19E-04	1.37E-11
MANCHE / MER DU NORD	4.87E-07	9.67E-07	3.84E-06	2.27E-05	4.11E-05	4.61E-10
MASSIF CENTRAL	5.82E-07	1.61E-06	5.73E-06	2.15E-05	4.68E-05	4.27E-11
MEDITERRANEE	2.68E-06	5.20E-06	1.54E-05	4.22E-05	7.44E-05	1.42E-06
PLATEFORME OCCIDENTAL	1.14E-07	3.32E-07	1.27E-06	4.38E-06	1.06E-05	2.89E-12
PYRENEES	2.21E-06	6.04E-06	1.79E-05	5.24E-05	9.73E-05	1.21E-08
FRANCE CONTINENTALE	1.51E-06	3.83E-06	1.12E-05	3.24E-05	6.46E-05	1.77E-07

APPENDIX 6

Seismic risk for each point – ESHM20

Seismic risk for each point – ESHM20 – 50% percentile
Vulnerability Class B and C - Damage grades D2 – D3 – D4
Fragility curves: Lagomarsino & Cattari (2014)
Conversion equations: Murphy & O'Brien (1977), Faccioli & Cauzzi (2006)

Point nb.	Domain number	Murphy & O'Brien						Faccioli & Cauzzi						
		Class B			Class C			Class B			Class C			
		D2	D3	D4	D2	D3	D4	D2	D3	D4	D2	D3	D4	
1	1	2.70E-03	1.20E-03	4.91E-04	1.18E-03	4.57E-04	1.64E-04	1.88E-03	8.45E-04	3.66E-04	8.29E-04	3.41E-04	1.31E-04	
2		1.39E-03	5.69E-04	2.04E-04	5.59E-04	1.87E-04	5.41E-05	9.23E-04	3.77E-04	1.41E-04	3.70E-04	1.28E-04	3.88E-05	
3		1.28E-03	4.98E-04	1.97E-04	4.91E-04	1.83E-04	6.57E-05	7.91E-04	3.38E-04	1.46E-04	3.32E-04	1.37E-04	5.28E-05	
4		1.16E-03	4.06E-04	1.35E-04	4.00E-04	1.22E-04	3.53E-05	6.87E-04	2.51E-04	9.04E-05	2.45E-04	8.22E-05	2.55E-05	
5		1.52E-03	5.80E-04	2.12E-04	5.70E-04	1.95E-04	6.35E-05	9.47E-04	3.78E-04	1.51E-04	3.71E-04	1.39E-04	4.88E-05	
6		1.08E-03	5.22E-04	2.38E-04	5.13E-04	2.25E-04	8.76E-05	7.71E-04	3.90E-04	1.87E-04	3.84E-04	1.77E-04	7.23E-05	
7		2.67E-03	1.20E-03	4.83E-04	1.18E-03	4.50E-04	1.54E-04	1.86E-03	8.42E-04	3.57E-04	8.27E-04	3.32E-04	1.20E-04	
8		1.33E-03	5.31E-04	1.87E-04	5.22E-04	1.71E-04	4.86E-05	8.68E-04	3.48E-04	1.28E-04	3.41E-04	1.16E-04	3.45E-05	
9	2	1.78E-04	6.44E-05	2.16E-05	6.33E-05	1.96E-05	5.46E-06	1.08E-04	4.05E-05	1.45E-05	3.96E-05	1.32E-05	3.84E-06	
10		2.02E-04	7.22E-05	2.40E-05	7.10E-05	2.18E-05	5.99E-06	1.21E-04	4.51E-05	1.60E-05	4.41E-05	1.45E-05	4.19E-06	
11		1.52E-04	5.63E-05	1.95E-05	5.54E-05	1.78E-05	5.17E-06	9.35E-05	3.60E-05	1.33E-05	3.52E-05	1.22E-05	3.73E-06	
12		1.33E-04	4.35E-05	1.34E-05	4.28E-05	1.20E-05	3.27E-06	7.58E-05	2.55E-05	8.60E-06	2.49E-05	7.73E-06	2.31E-06	
13		1.71E-04	6.01E-05	1.99E-05	5.92E-05	1.80E-05	5.02E-06	1.02E-04	3.72E-05	1.33E-05	3.64E-05	1.20E-05	3.54E-06	
14		2.08E-04	8.02E-05	2.90E-05	7.88E-05	2.66E-05	7.86E-06	1.30E-04	5.28E-05	2.02E-05	5.17E-05	1.86E-05	5.70E-06	
15		2.22E-04	8.14E-05	2.65E-05	8.00E-05	2.39E-05	6.20E-06	1.37E-04	5.09E-05	1.72E-05	4.97E-05	1.55E-05	4.17E-06	
16		1.80E-04	6.22E-05	2.05E-05	6.12E-05	1.86E-05	5.23E-06	1.05E-04	3.83E-05	1.37E-05	3.74E-05	1.25E-05	3.72E-06	
17		2.54E-04	9.55E-05	3.25E-05	9.39E-05	2.95E-05	8.44E-06	1.59E-04	6.07E-05	2.19E-05	5.93E-05	1.99E-05	6.07E-06	
18		2.46E-04	9.28E-05	3.24E-05	9.12E-05	2.96E-05	8.70E-06	1.53E-04	5.98E-05	2.22E-05	5.85E-05	2.03E-05	6.33E-06	
19		1.07E-04	3.49E-05	1.03E-05	3.43E-05	9.16E-06	2.32E-06	6.15E-05	2.00E-05	6.38E-06	1.95E-05	5.68E-06	1.57E-06	
20		2.04E-04	7.05E-05	2.30E-05	6.94E-05	2.08E-05	5.82E-06	1.20E-04	4.31E-05	1.53E-05	4.22E-05	1.39E-05	4.14E-06	
21		2.24E-04	7.90E-05	2.61E-05	7.77E-05	2.37E-05	6.56E-06	1.33E-04	4.89E-05	1.74E-05	4.78E-05	1.58E-05	4.61E-06	
22		1.81E-04	7.03E-05	2.52E-05	6.91E-05	2.31E-05	7.06E-06	1.15E-04	4.59E-05	1.76E-05	4.50E-05	1.61E-05	5.24E-06	
23		1.75E-04	6.84E-05	2.46E-05	6.72E-05	2.26E-05	6.88E-06	1.12E-04	4.48E-05	1.72E-05	4.39E-05	1.57E-05	5.11E-06	
24		1.26E-04	4.27E-05	1.40E-05	4.21E-05	1.27E-05	3.64E-06	7.28E-05	2.61E-05	9.35E-06	2.55E-05	8.50E-06	2.63E-06	
25		1.94E-04	7.49E-05	2.66E-05	7.37E-05	2.44E-05	7.37E-06	1.23E-04	4.86E-05	1.84E-05	4.76E-05	1.69E-05	5.45E-06	
26		1.01E-04	3.30E-05	1.05E-05	3.25E-05	9.46E-06	2.66E-06	5.68E-05	1.97E-05	6.89E-06	1.92E-05	6.23E-06	1.91E-06	
27	1.07E-04	3.79E-05	1.28E-05	3.73E-05	1.16E-05	3.43E-06	6.37E-05	2.36E-05	8.68E-06	2.31E-05	7.92E-06	2.51E-06		
28	3	1.10E-03	4.31E-04	1.51E-04	4.23E-04	1.38E-04	4.04E-05	7.09E-04	2.79E-04	1.03E-04	2.73E-04	9.43E-05	2.93E-05	
29		3.22E-04	1.08E-04	3.57E-05	1.06E-04	3.24E-05	9.54E-06	1.83E-04	6.58E-05	2.40E-05	6.44E-05	2.19E-05	7.00E-06	
30		1.53E-03	6.13E-04	2.21E-04	6.02E-04	2.02E-04	5.96E-05	9.97E-04	4.05E-04	1.53E-04	3.96E-04	1.40E-04	4.31E-05	
31		2.11E-04	7.25E-05	2.51E-05	7.14E-05	2.29E-05	7.02E-06	1.21E-04	4.55E-05	1.74E-05	4.46E-05	1.59E-05	5.24E-06	
32		4	1.01E-04	3.85E-05	1.35E-05	3.78E-05	1.23E-05	3.68E-06	6.36E-05	2.48E-05	9.30E-06	2.42E-05	8.51E-06	2.70E-06
33			1.34E-04	5.36E-05	2.01E-05	5.27E-05	1.85E-05	6.08E-06	8.64E-05	3.57E-05	1.44E-05	3.50E-05	1.33E-05	4.69E-06
34			9.83E-05	3.80E-05	1.39E-05	3.73E-05	1.27E-05	4.00E-06	6.18E-05	2.49E-05	9.78E-06	2.44E-05	9.00E-06	3.01E-06
35			1.18E-04	4.00E-05	1.28E-05	3.94E-05	1.15E-05	3.16E-06	6.86E-05	2.42E-05	8.34E-06	2.36E-05	7.53E-06	2.22E-06
36			2.62E-04	9.36E-05	3.26E-05	9.21E-05	2.98E-05	8.94E-06	1.55E-04	5.94E-05	2.25E-05	5.82E-05	2.06E-05	6.58E-06

Seismic risk for each point – ESHM20 – 50% percentile
Vulnerability Class B and C - Damage grades D2 – D3 – D4
Fragility curves: Lagomarsino & Cattari (2014)
Conversion equations: Murphy & O'Brien (1977), Faccioli & Cauzzi (2006)

Point nb.	Domain number	Murphy & O'Brien						Faccioli & Cauzzi					
		Class B			Class-C			Class B			Class C		
		D2	D3	D4	D2	D3	D4	D2	D3	D4	D2	D3	D4
37	5	2.77E-04	9.71E-05	3.43E-05	9.57E-05	3.14E-05	9.85E-06	1.61E-04	6.18E-05	2.40E-05	6.05E-05	2.21E-05	7.44E-06
38		1.03E-04	3.57E-05	1.22E-05	3.51E-05	1.11E-05	3.40E-06	5.98E-05	2.23E-05	8.40E-06	2.18E-05	7.70E-06	2.54E-06
39		3.87E-04	1.31E-04	4.17E-05	1.29E-04	3.76E-05	1.07E-05	2.25E-04	7.82E-05	2.74E-05	7.63E-05	2.48E-05	7.80E-06
40		2.80E-04	1.04E-04	3.43E-05	1.02E-04	3.11E-05	8.63E-06	1.75E-04	6.47E-05	2.27E-05	6.32E-05	2.05E-05	6.11E-06
41		1.81E-04	6.82E-05	2.42E-05	6.71E-05	2.22E-05	6.72E-06	1.12E-04	4.42E-05	1.68E-05	4.32E-05	1.54E-05	4.97E-06
42		4.15E-04	1.44E-04	4.45E-05	1.41E-04	3.99E-05	1.00E-05	2.47E-04	8.63E-05	2.82E-05	8.42E-05	2.51E-05	6.62E-06
43		1.20E-03	4.70E-04	1.62E-04	4.61E-04	1.48E-04	4.27E-05	7.78E-04	3.02E-04	1.10E-04	2.96E-04	1.00E-04	3.08E-05
44		8.49E-05	2.80E-05	8.51E-06	2.76E-05	7.61E-06	2.00E-06	4.89E-05	1.64E-05	5.39E-06	1.60E-05	4.82E-06	1.38E-06
45		8.97E-05	3.21E-05	1.06E-05	3.16E-05	9.62E-06	2.71E-06	5.42E-05	1.99E-05	7.05E-06	1.95E-05	6.38E-06	1.93E-06
46		2.80E-04	1.04E-04	3.46E-05	1.02E-04	3.13E-05	8.70E-06	1.76E-04	6.53E-05	2.29E-05	6.38E-05	2.07E-05	6.15E-06
47		2.30E-04	7.66E-05	2.51E-05	7.55E-05	2.28E-05	6.55E-06	1.30E-04	4.66E-05	1.68E-05	4.56E-05	1.53E-05	4.74E-06
48		6.48E-05	2.26E-05	7.30E-06	2.22E-05	6.59E-06	1.81E-06	3.85E-05	1.38E-05	4.79E-06	1.35E-05	4.32E-06	1.28E-06
49		2.35E-04	8.96E-05	3.05E-05	8.80E-05	2.77E-05	7.84E-06	1.49E-04	5.70E-05	2.05E-05	5.58E-05	1.86E-05	5.58E-06
50		2.12E-04	7.74E-05	2.67E-05	7.61E-05	2.44E-05	7.23E-06	1.29E-04	4.91E-05	1.83E-05	4.80E-05	1.67E-05	5.30E-06
51		7.14E-04	2.52E-04	7.72E-05	2.47E-04	6.89E-05	1.67E-05	4.34E-04	1.51E-04	4.82E-05	1.47E-04	4.28E-05	1.08E-05
52		6.31E-05	2.24E-05	7.40E-06	2.20E-05	6.71E-06	1.91E-06	3.78E-05	1.38E-05	4.93E-06	1.35E-05	4.47E-06	1.37E-06
53		1.50E-04	5.63E-05	1.86E-05	5.53E-05	1.69E-05	4.65E-06	9.47E-05	3.52E-05	1.23E-05	3.44E-05	1.11E-05	3.27E-06
54		1.65E-04	6.05E-05	1.99E-05	5.94E-05	1.79E-05	4.85E-06	1.02E-04	3.77E-05	1.30E-05	3.68E-05	1.17E-05	3.37E-06
55		1.23E-04	4.33E-05	1.36E-05	4.25E-05	1.22E-05	3.23E-06	7.42E-05	2.62E-05	8.74E-06	2.55E-05	7.84E-06	2.22E-06
56		1.26E-04	4.67E-05	1.62E-05	4.59E-05	1.47E-05	4.31E-06	7.75E-05	2.98E-05	1.10E-05	2.91E-05	1.01E-05	3.12E-06
57	2.07E-04	7.09E-05	2.20E-05	6.98E-05	1.97E-05	5.20E-06	1.23E-04	4.24E-05	1.40E-05	4.13E-05	1.26E-05	3.59E-06	
58	6	4.85E-04	2.09E-04	8.19E-05	2.05E-04	7.60E-05	2.47E-05	3.28E-04	1.45E-04	5.95E-05	1.42E-04	5.51E-05	1.88E-05
59		6.50E-04	2.34E-04	8.02E-05	2.30E-04	7.30E-05	2.31E-05	3.95E-04	1.46E-04	5.50E-05	1.43E-04	5.04E-05	1.77E-05
60		6.25E-04	2.57E-04	9.78E-05	2.53E-04	9.03E-05	2.94E-05	4.11E-04	1.74E-04	7.03E-05	1.70E-04	6.50E-05	2.25E-05
61		3.53E-04	1.29E-04	4.30E-05	1.27E-04	3.89E-05	1.10E-05	2.18E-04	8.05E-05	2.86E-05	7.87E-05	2.59E-05	7.81E-06
62		6.23E-04	2.94E-04	1.28E-04	2.89E-04	1.20E-04	4.38E-05	4.43E-04	2.15E-04	9.79E-05	2.12E-04	9.20E-05	3.52E-05
63		3.21E-04	1.21E-04	4.26E-05	1.19E-04	3.89E-05	1.15E-05	2.00E-04	7.83E-05	2.93E-05	7.66E-05	2.68E-05	8.36E-06
64		2.65E-04	9.99E-05	3.57E-05	9.83E-05	3.27E-05	1.04E-05	1.65E-04	6.44E-05	2.50E-05	6.31E-05	2.30E-05	7.96E-06
65		4.65E-04	1.72E-04	6.10E-05	1.69E-04	5.59E-05	1.78E-05	2.83E-04	1.10E-04	4.26E-05	1.08E-04	3.92E-05	1.35E-05
66		2.53E-04	9.48E-05	3.25E-05	9.32E-05	2.96E-05	8.66E-06	1.58E-04	6.02E-05	2.21E-05	5.89E-05	2.01E-05	6.30E-06

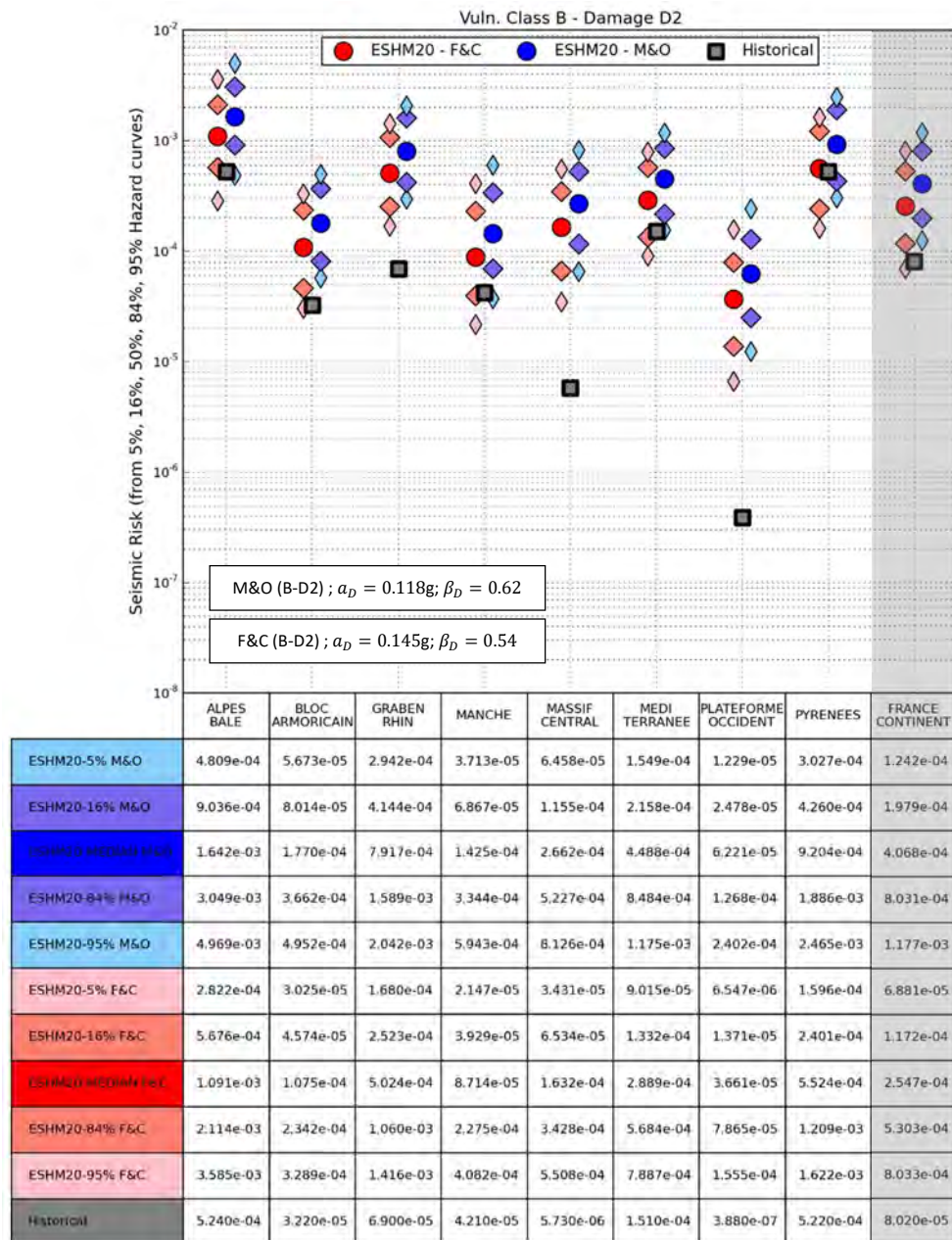
Seismic risk for each point – ESHM20 – 50% percentile
Vulnerability Class B and C - Damage grades D2 – D3 – D4
Fragility curves: Lagomarsino & Cattari (2014)
Conversion equations: Murphy & O'Brien (1977), Faccioli & Cauzzi (2006)

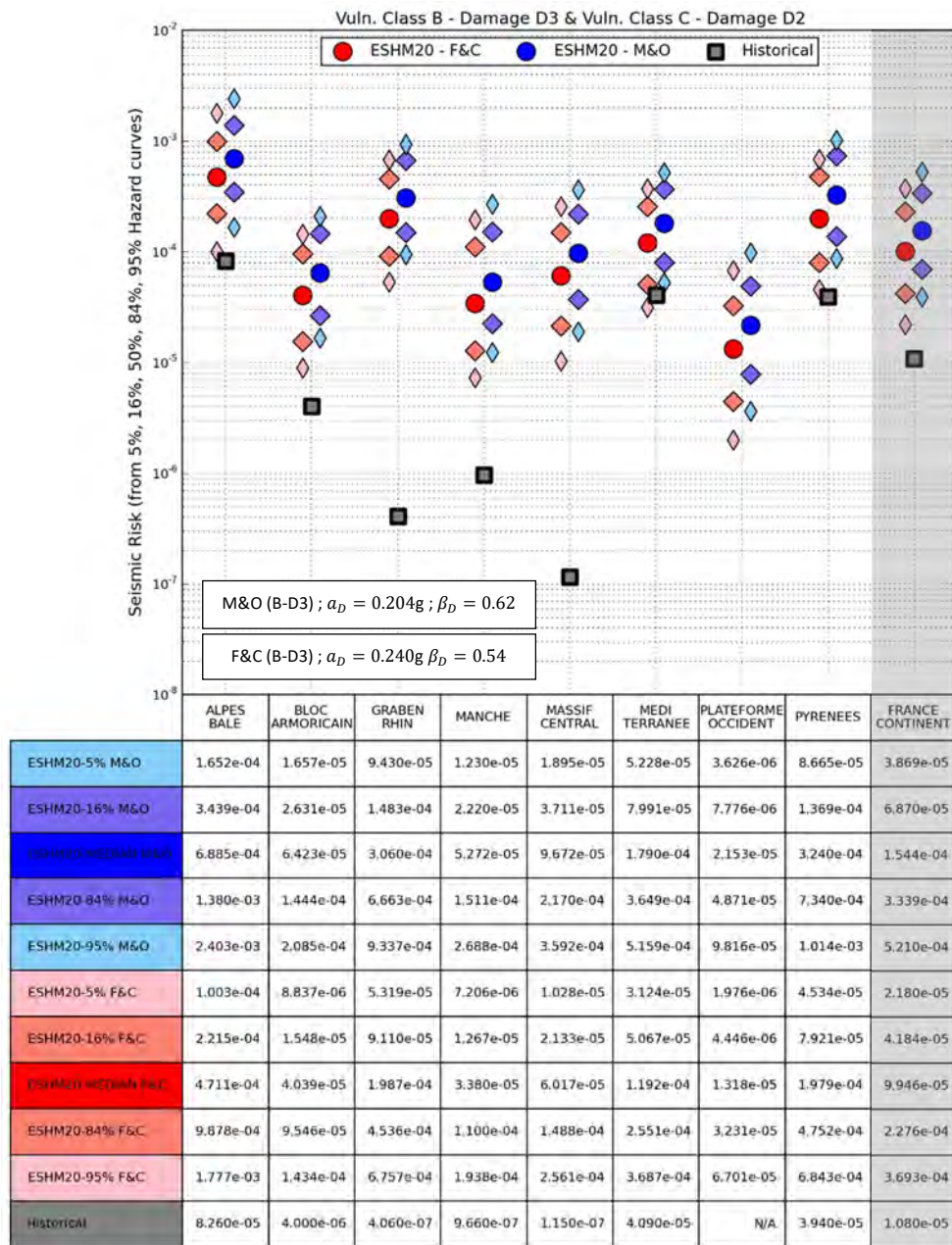
Point nb.	Domain number	Murphy & O'Brien						Faccioli & Cauzzi					
		Class B			Class C			Class B			Class C		
		D2	D3	D4	D2	D3	D4	D2	D3	D4	D2	D3	D4
67	7	5.97E-05	2.16E-05	7.19E-06	2.12E-05	6.52E-06	1.83E-06	3.63E-05	1.35E-05	4.79E-06	1.32E-05	4.34E-06	1.30E-06
68		5.30E-05	2.00E-05	6.82E-06	1.97E-05	6.20E-06	1.74E-06	3.33E-05	1.28E-05	4.58E-06	1.25E-05	4.15E-06	1.23E-06
69		5.62E-05	2.08E-05	6.96E-06	2.04E-05	6.31E-06	1.77E-06	3.48E-05	1.30E-05	4.64E-06	1.28E-05	4.21E-06	1.25E-06
70		7.14E-05	2.52E-05	8.33E-06	2.48E-05	7.54E-06	2.11E-06	4.25E-05	1.56E-05	5.53E-06	1.53E-05	5.01E-06	1.49E-06
71		8.91E-05	3.08E-05	1.04E-05	3.03E-05	9.44E-06	2.76E-06	5.18E-05	1.92E-05	7.03E-06	1.88E-05	6.40E-06	2.01E-06
72		7.87E-05	2.61E-05	8.15E-06	2.57E-05	7.32E-06	1.97E-06	4.52E-05	1.55E-05	5.25E-06	1.51E-05	4.72E-06	1.38E-06
73		5.19E-05	1.97E-05	6.64E-06	1.93E-05	6.03E-06	1.67E-06	3.28E-05	1.25E-05	4.43E-06	1.22E-05	4.01E-06	1.17E-06
74		3.69E-05	1.33E-05	4.38E-06	1.31E-05	3.96E-06	1.11E-06	2.25E-05	8.24E-06	2.90E-06	8.06E-06	2.62E-06	7.88E-07
75		2.73E-05	9.71E-06	3.23E-06	9.55E-06	2.93E-06	8.38E-07	1.64E-05	6.03E-06	2.16E-06	5.90E-06	1.96E-06	6.03E-07
76		3.54E-05	1.27E-05	4.29E-06	1.25E-05	3.90E-06	1.14E-06	2.12E-05	7.94E-06	2.90E-06	7.77E-06	2.64E-06	8.25E-07
77		5.28E-05	1.99E-05	6.65E-06	1.95E-05	6.03E-06	1.65E-06	3.32E-05	1.26E-05	4.41E-06	1.23E-05	3.99E-06	1.15E-06
78		3.62E-05	1.39E-05	4.88E-06	1.36E-05	4.46E-06	1.30E-06	2.29E-05	8.97E-06	3.35E-06	8.78E-06	3.06E-06	9.40E-07
79		1.73E-05	6.53E-06	2.24E-06	6.42E-06	2.03E-06	5.73E-07	1.08E-05	4.17E-06	1.51E-06	4.08E-06	1.37E-06	4.05E-07
80		1.53E-05	5.64E-06	1.94E-06	5.55E-06	1.76E-06	5.09E-07	9.39E-06	3.58E-06	1.32E-06	3.50E-06	1.20E-06	3.66E-07
81		4.66E-05	1.35E-05	4.15E-06	1.33E-05	3.72E-06	1.04E-06	2.35E-05	7.76E-06	2.70E-06	7.58E-06	2.44E-06	7.45E-07
82		5.50E-05	2.03E-05	6.74E-06	1.99E-05	6.11E-06	1.68E-06	3.40E-05	1.27E-05	4.46E-06	1.24E-05	4.03E-06	1.17E-06
83		4.64E-05	1.75E-05	5.99E-06	1.72E-05	5.45E-06	1.53E-06	2.92E-05	1.12E-05	4.03E-06	1.09E-05	3.66E-06	1.08E-06
84		1.67E-05	6.18E-06	2.11E-06	6.08E-06	1.92E-06	5.46E-07	1.03E-05	3.92E-06	1.43E-06	3.84E-06	1.30E-06	3.89E-07
85		1.58E-05	5.68E-06	1.94E-06	5.58E-06	1.77E-06	5.12E-07	9.47E-06	3.58E-06	1.32E-06	3.50E-06	1.20E-06	3.70E-07
86		3.38E-05	1.02E-05	3.07E-06	1.01E-05	2.74E-06	7.38E-07	1.80E-05	5.83E-06	1.96E-06	5.69E-06	1.76E-06	5.17E-07
87		6.85E-05	2.36E-05	7.55E-06	2.32E-05	6.81E-06	1.87E-06	4.03E-05	1.43E-05	4.93E-06	1.40E-05	4.45E-06	1.31E-06
88		3.78E-05	1.28E-05	4.07E-06	1.26E-05	3.66E-06	9.80E-07	2.21E-05	7.74E-06	2.63E-06	7.55E-06	2.37E-06	6.80E-07
89		3.12E-05	1.00E-05	3.13E-06	9.86E-06	2.81E-06	7.73E-07	1.73E-05	5.91E-06	2.03E-06	5.77E-06	1.83E-06	5.46E-07
90		1.02E-04	3.74E-05	1.34E-05	3.68E-05	1.23E-05	3.81E-06	6.14E-05	2.42E-05	9.37E-06	2.37E-05	8.62E-06	2.86E-06
91		9.24E-05	3.51E-05	1.24E-05	3.45E-05	1.14E-05	3.42E-06	5.77E-05	2.27E-05	8.60E-06	2.23E-05	7.87E-06	2.52E-06
92		8.12E-05	3.15E-05	1.10E-05	3.10E-05	1.00E-05	2.87E-06	5.19E-05	2.04E-05	7.48E-06	1.99E-05	6.81E-06	2.06E-06
93		1.01E-04	3.64E-05	1.23E-05	3.58E-05	1.12E-05	3.28E-06	6.13E-05	2.27E-05	8.30E-06	2.22E-05	7.56E-06	2.40E-06
94		4.92E-05	1.52E-05	4.58E-06	1.50E-05	4.09E-06	1.13E-06	2.68E-05	8.69E-06	2.92E-06	8.48E-06	2.63E-06	8.11E-07
95		8.48E-05	3.15E-05	1.11E-05	3.10E-05	1.02E-05	3.09E-06	5.19E-05	2.03E-05	7.70E-06	1.98E-05	7.06E-06	2.29E-06
96		9.97E-05	3.57E-05	1.18E-05	3.51E-05	1.07E-05	3.07E-06	6.05E-05	2.21E-05	7.84E-06	2.16E-05	7.11E-06	2.23E-06
97		1.89E-04	5.16E-05	1.27E-05	5.09E-05	1.10E-05	2.36E-06	9.64E-05	2.60E-05	6.97E-06	2.52E-05	6.00E-06	1.47E-06
98		1.00E-04	3.61E-05	1.21E-05	3.55E-05	1.09E-05	3.20E-06	6.09E-05	2.24E-05	8.09E-06	2.19E-05	7.35E-06	2.34E-06
99		1.19E-04	3.44E-05	9.45E-06	3.39E-05	8.30E-06	1.93E-06	6.18E-05	1.88E-05	5.57E-06	1.83E-05	4.88E-06	1.24E-06
100	8	3.52E-04	1.28E-04	4.44E-05	1.26E-04	4.05E-05	1.22E-05	2.14E-04	8.13E-05	3.05E-05	7.96E-05	2.79E-05	9.05E-06
101		5.24E-04	1.90E-04	6.29E-05	1.87E-04	5.70E-05	1.60E-05	3.21E-04	1.18E-04	4.18E-05	1.15E-04	3.79E-05	1.14E-05
102		9.95E-04	3.28E-04	9.55E-05	3.23E-04	8.47E-05	2.04E-05	5.79E-04	1.88E-04	5.81E-05	1.84E-04	5.13E-05	1.33E-05
103		5.57E-04	1.86E-04	5.97E-05	1.83E-04	5.38E-05	1.49E-05	3.19E-04	1.12E-04	3.93E-05	1.09E-04	3.56E-05	1.05E-05
104		9.21E-04	3.07E-04	9.40E-05	3.02E-04	8.41E-05	2.13E-05	5.33E-04	1.82E-04	5.94E-05	1.77E-04	5.31E-05	1.42E-05
105		1.72E-03	5.98E-04	1.86E-04	5.88E-04	1.67E-04	4.28E-05	1.03E-03	3.58E-04	1.19E-04	3.50E-04	1.06E-04	2.88E-05
106		2.02E-03	7.41E-04	2.46E-04	7.29E-04	2.23E-04	6.15E-05	1.25E-03	4.63E-04	1.64E-04	4.53E-04	1.48E-04	4.30E-05
107		8.07E-04	2.31E-04	6.39E-05	2.28E-04	5.63E-05	1.41E-05	4.20E-04	1.24E-04	3.86E-05	1.21E-04	3.42E-05	9.55E-06
108		1.52E-03	5.35E-04	1.63E-04	5.26E-04	1.45E-04	3.51E-05	9.23E-04	3.21E-04	1.01E-04	3.13E-04	8.94E-05	2.27E-05
109		1.31E-03	4.68E-04	1.48E-04	4.60E-04	1.33E-04	3.44E-05	8.00E-04	2.85E-04	9.47E-05	2.78E-04	8.48E-05	2.33E-05
110		5.65E-04	1.93E-04	6.44E-05	1.91E-04	5.84E-05	1.70E-05	3.27E-04	1.19E-04	4.34E-05	1.16E-04	3.95E-05	1.24E-05
111		7.86E-04	2.81E-04	9.50E-05	2.76E-04	8.64E-05	2.52E-05	4.71E-04	1.76E-04	6.43E-05	1.72E-04	5.86E-05	1.83E-05
112		5.13E-04	1.80E-04	6.10E-05	1.77E-04	5.55E-05	1.65E-05	3.02E-04	1.12E-04	4.16E-05	1.09E-04	3.80E-05	1.22E-05
113		6.98E-04	2.61E-04	8.76E-05	2.57E-04	7.94E-05	2.22E-05	4.38E-04	1.65E-04	5.83E-05	1.61E-04	5.28E-05	1.57E-05
114		7.47E-04	2.74E-04	9.00E-05	2.69E-04	8.14E-05	2.18E-05	4.61E-04	1.70E-04	5.92E-05	1.67E-04	5.35E-05	1.50E-05
115	7.01E-04	2.83E-04	1.10E-04	2.79E-04	1.02E-04	3.41E-05	4.52E-04	1.92E-04	8.02E-05	1.88E-04	7.45E-05	2.64E-05	
France		4.07E-04	1.54E-04	5.45E-05	1.52E-04	4.98E-05	1.51E-05	2.55E-04	9.95E-05	3.76E-05	9.74E-05	3.45E-05	1.12E-05

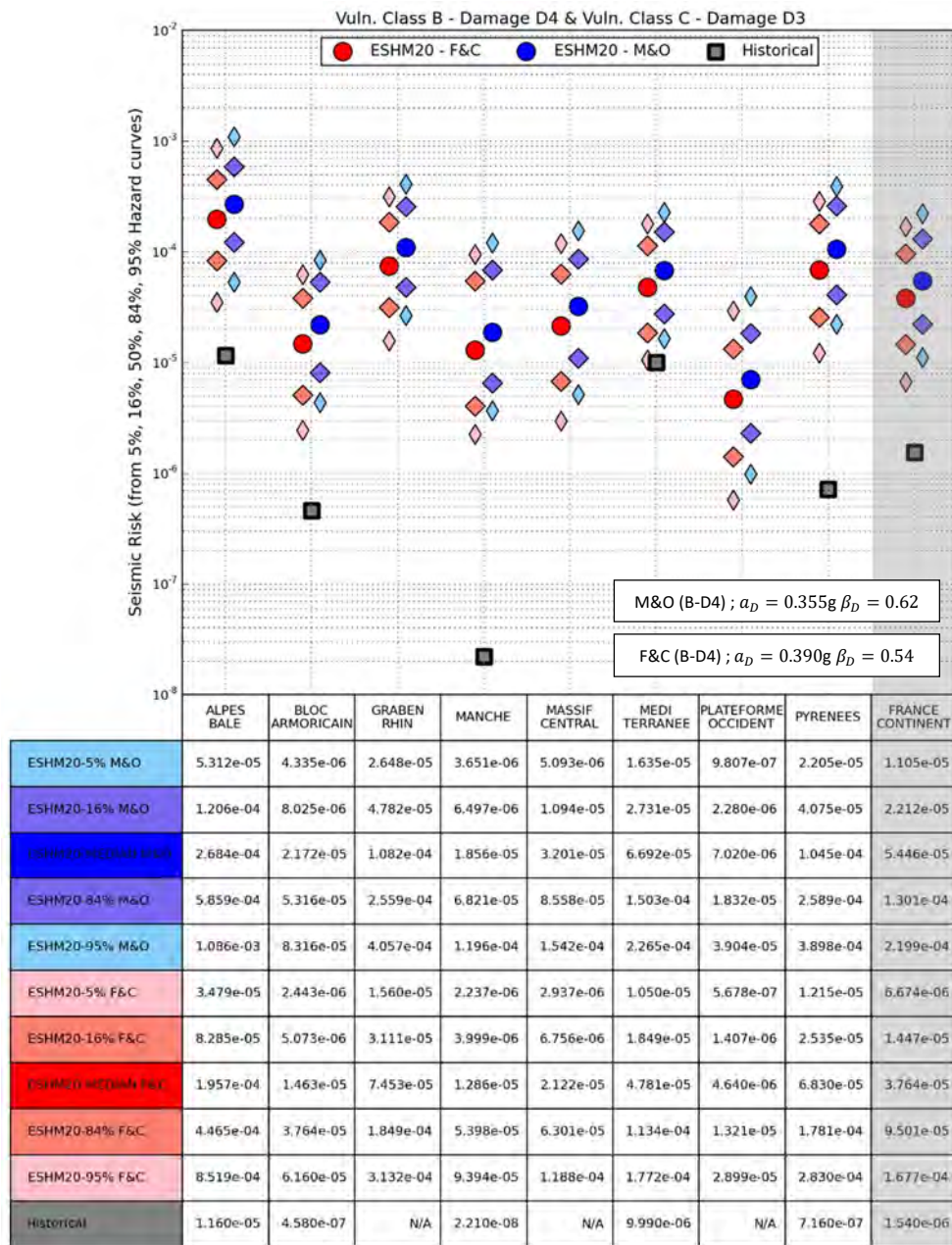
APPENDIX 7

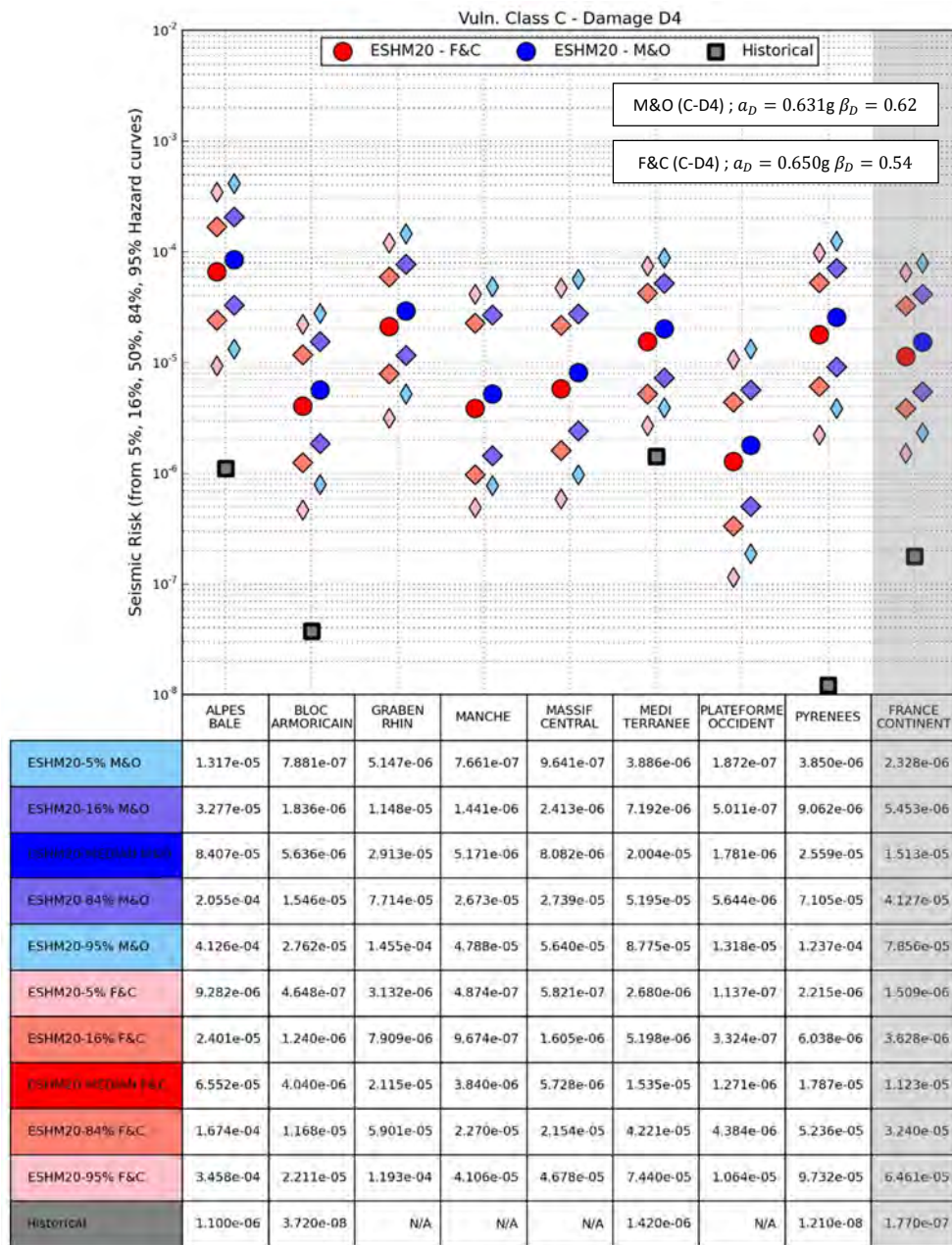
Seismic risk for conversion equations M&O (1977) vs. F&C (2006)

Results by geographic domain, for each percentile (5%, 16%, 50%, 84%, 95%) of hazard curves ESHM20. Results corresponding to Faccioli & Cauzzi conversion equations are presented in magenta dots. Blue dots correspond to the results using Murphy & O'Brien conversion equations.



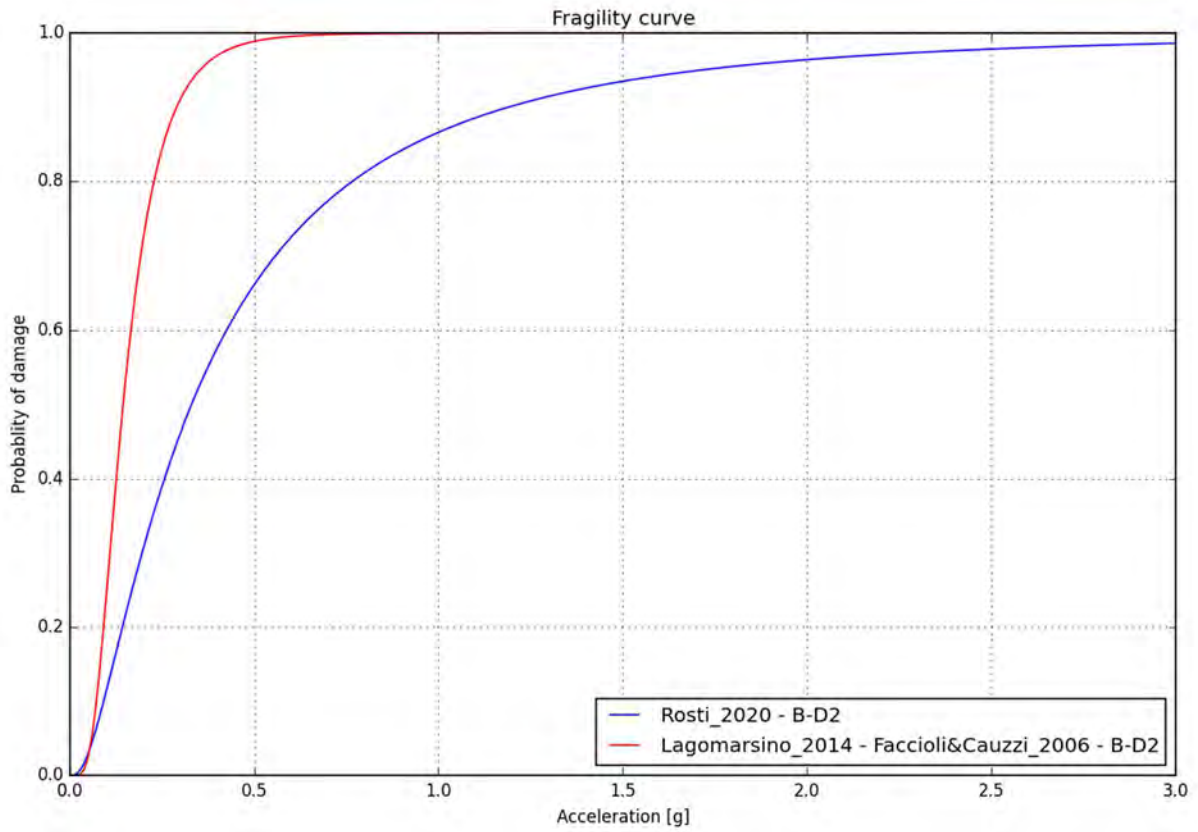


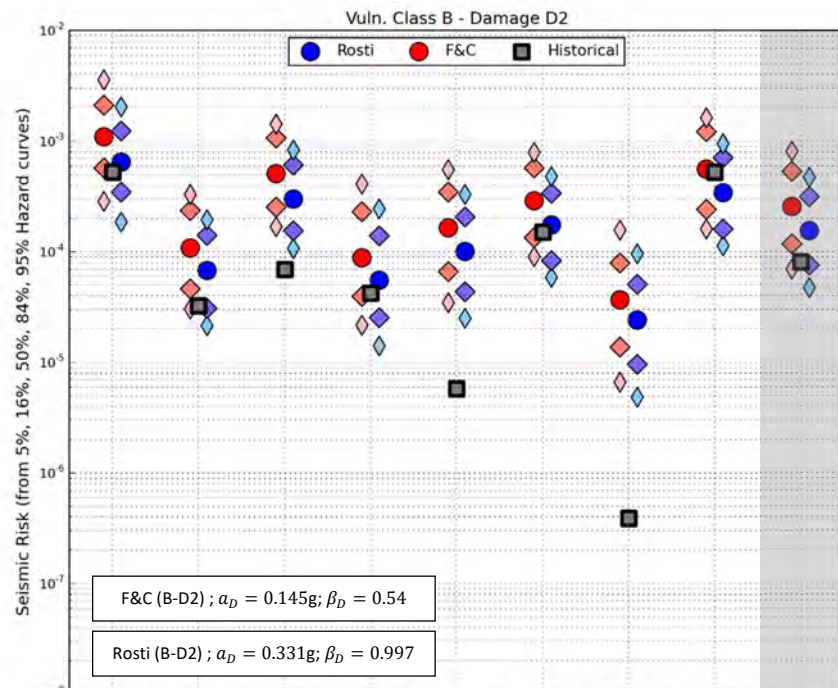




APPENDIX 8

Seismic risk for fragility curves from Rosti et al. (2020)





	ALPES BALE	BLOC ARMORICAIN	GRABEN RHIN	MANCHE	MASSIF CENTRAL	MEDI TERRANEE	PLATEFORME OCCIDENT	PYRENEES	FRANCE CONTINENT
ESHM20 - F&C - 5%	2.822e-04	3.025e-05	1.680e-04	2.147e-05	3.431e-05	9.015e-05	6.547e-06	1.596e-04	6.881e-05
ESHM20 - F&C - 16%	5.676e-04	4.574e-05	2.523e-04	3.929e-05	6.534e-05	1.332e-04	1.371e-05	2.401e-04	1.172e-04
ESHM20 - F&C - 50% (Rosti)	1.091e-03	1.075e-04	5.024e-04	8.714e-05	1.632e-04	2.889e-04	3.661e-05	5.524e-04	2.547e-04
ESHM20 - F&C - 84%	2.114e-03	2.342e-04	1.060e-03	2.275e-04	3.428e-04	5.684e-04	7.865e-05	1.209e-03	5.303e-04
ESHM20 - F&C - 95%	3.585e-03	3.289e-04	1.416e-03	4.082e-04	5.508e-04	7.887e-04	1.555e-04	1.622e-03	8.033e-04
ESHM20 - Rosti - 5%	1.833e-04	2.127e-05	1.068e-04	1.405e-05	2.474e-05	5.838e-05	4.805e-06	1.126e-04	4.673e-05
ESHM20 - Rosti - 16%	3.428e-04	3.042e-05	1.539e-04	2.530e-05	4.331e-05	8.229e-05	9.549e-06	1.605e-04	7.475e-05
ESHM20 - Rosti - 50% (Rosti)	6.389e-04	6.726e-05	2.988e-04	5.481e-05	9.977e-05	1.732e-04	2.398e-05	3.418e-04	1.545e-04
ESHM20 - Rosti - 84%	1.220e-03	1.401e-04	6.077e-04	1.387e-04	2.057e-04	3.366e-04	5.036e-05	7.050e-04	3.116e-04
ESHM20 - Rosti - 95%	2.030e-03	1.936e-04	8.259e-04	2.424e-04	3.280e-04	4.767e-04	9.507e-05	9.454e-04	4.685e-04
Historical	5.240e-04	3.220e-05	6.900e-05	4.210e-05	5.730e-06	1.510e-04	3.880e-07	5.220e-04	8.020e-05